

# The Effectiveness of Mangroves in Attenuating Cyclone- induced Waves



*A Master's Thesis report submitted in partial fulfillment of the requirements for the MSc CoMEM degree by*

**SIDDHARTH NARAYAN**

Delft University of Technology

Department of Civil Engineering and Geosciences

Section of Hydraulic Engineering, Coastal Engineering

June 2009

*Graduation Committee:*

Prof. M.J.F. Stive	Hydraulic Engineering Section, TU Delft
ir. Henk Jan Verhagen	Hydraulic Engineering Section, TU Delft
Tomohiro Suzuki, M. Eng	Hydraulic Engineering Section, TU Delft
Dr. Roshanka Ranasinghe	UNESCO-IHE and Hydraulic Engineering Section, TU Delft
Dr. W.N.J. Ursem	Botanische Tuin, TU Delft



## **Acknowledgements**

First and foremost I would like to thank the members of my committee – Prof. Marcel Stive, ir. Henk Jan Verhagen, Dr. Roshanka Ranasinghe, Tomohiro Suzuki and Dr. W.N.J Ursem for their valuable inputs into this work, for supporting me and helping me stay on the right track. I express my deep gratitude especially to Tomohiro for being so patient with me during all those discussions and meetings and even more so for his interest in my work and progress. My thanks to the CoMEM girls – Lenie, Madelon, Mariette and Inge for always being there and helping take care of the small details that are an essential part of any undertaking and to Wanda Kunz for trying her best to fit me into Dr. Ursem’s agenda. My sincere thanks to Ali Dastgheib and the staff at UNESCO-IHE, Addie Ritter and Jaap de Lange of the TU Library, Nalin Wikramanayake of the Open University of Sri Lanka and Dr. Peter Cowell for their help during the initial stages. I am grateful to the people at the Service Point for their prompt help with my requests for software. I would also like to acknowledge Dr. Marcel Zijlema for his help with doubts I had with the SWAN model. I thank my parents, grandmothers, aunts and uncles for their continuous support and blessings. I am grateful to my teachers, cousins and friends from across the seas and in Europe for their wishes and interest in my work. I’d like to take this chance to thank my CoMEM batch mates across four countries who have given me a wonderful and unforgettable two years in Europe. My regards and thanks to Maggie, Chris, Egon, Nicolas, Lesly, Chiara, Roger, Loek, Wouter and Bart for all our fun times and coffee breaks during my thesis and without whom it would have been quite a dreary five months. My thanks to Saravanan for having helped me sort out my issues in Southampton amongst all his other work. I’d also like to express my gratitude to Reinoud, Tada, Casper, Akiko, Mamiko, Hiroko and all the other members and guests of SGI with whom I have spent some truly memorable days and had very nice discussions. Finally, I would like to thank Badri and Saleh for putting me up for my first two weeks here and the rest of the CoMEM 2010 batch for their constant support and many pleasant parties, dinners and lunch sessions at the Aula.

## **Abstract**

A study of the effectiveness of mangroves in attenuating cyclone- induced waves was done using the SWAN 40.55MOD numerical model. Hydraulic parameters during extreme events and local mangrove vegetation parameters were estimated for the Kanika Sands mangrove island near the upcoming Dhamra Port in Orissa, India. Simplified generic analyses were first conducted to obtain insights into the characteristics and behaviour of the model and the system. These were used to select relevant scenarios for simulations of actual conditions at the case-study site. The mangroves were found to be effective in reducing wave heights at the port behind the island though the effectiveness is limited by its geometry and distance from the port. The presence of vegetation has a marked effect though the effect of a variation in vegetation density is limited. An optimum cross-shore width range for maximum protection was quantified. The required size of the mangrove patch for maximum wave attenuation under all conditions is 300 to 800 m in the cross-shore direction and around 6 km in the alongshore direction. At present the vegetation is 1.5 km cross-shore by a 4 km alongshore at a maximum with a shape that is slightly different from the optimum. Given the conditions of the area northward expansion is considered more relevant. Vegetation strips around the island seem to be an effective option though the effects of density reductions become important in this case. Model characteristics such as the sensitivity trend of hydraulic parameters and the comparative effects of emergent and submergent vegetation were also investigated. Conclusions regarding model and system characteristics observed during the study are also presented. Based on the work done recommendations were made regarding mangrove management options for the port and directions for future research in case of further numerical modeling, physical modeling and field studies.

## Table of Contents

<b>Acknowledgements</b> .....	<b>ii</b>
<b>Abstract</b> .....	<b>iii</b>
<b>List of Figures</b> .....	<b>vi</b>
<b>List of Tables</b> .....	<b>viii</b>
<b>List of Symbols and Abbreviations</b> .....	<b>ix</b>
<b>1 Introduction</b> .....	<b>1</b>
1.1. Problem Description .....	1
1.2. Problem Statement .....	1
1.3. Study Objectives.....	2
1.4. Study Methodology .....	2
<b>2 Literature Review</b> .....	<b>5</b>
2.1. Tropical Cyclones.....	5
2.1.1. Basics .....	5
2.1.2. Cyclones in the Bay of Bengal .....	5
2.1.3. Cyclones in Orissa .....	6
2.2. Mangroves.....	8
2.2.1. Basics and Distribution .....	8
2.2.2. Mangroves and Extreme Events.....	9
2.2.3. Mangroves and Waves .....	10
2.3. The SWAN Model for Vegetation .....	12
2.3.1. SWAN - Basics .....	12
2.3.2. Vegetation Dissipation in SWAN .....	12
2.3.3. Model Considerations.....	13
2.4. The Case Study Site.....	15
2.4.1. Location and Environmental Conditions .....	15
2.4.2. Morphology and Hydrology.....	16
2.4.3. Site Vegetation Characteristics.....	18
<b>3 Determination of Model Boundary Conditions</b> .....	<b>20</b>
3.1. Extreme Event Data Analysis .....	20
3.1.1. Introduction.....	20
3.1.2. Assumptions .....	21
3.1.3. Estimation of Cyclone Parameters .....	21
3.1.4. Estimation of Offshore Wave Parameters.....	24
3.1.5. Near-shore Surge Levels and Offshore Wave Parameters for Desired Return Periods .....	26
3.1.6. Conclusions.....	27
3.1.7. Verification of Results.....	28
3.2. Offshore Bathymetry .....	30
3.3. Hydraulic Boundary Conditions for 2-D Models .....	31
3.3.1. Wave Transformation.....	31
3.3.2. Determination of Water Level at Near-shore Boundary.....	33
3.3.3. Conclusions.....	33

3.4.	Vegetation Parameter Analysis.....	35
<b>4</b>	<b>Generic Modeling Studies.....</b>	<b>37</b>
4.1.	Model Considerations for Parameter Formulation .....	37
4.2.	2-D Generic Model Setup.....	39
4.3.	General Process for Sensitivity Analyses.....	40
4.3.1.	<i>Modeling Parameter Combinations.....</i>	<i>40</i>
4.3.2.	<i>Analysis of Resultant Outputs.....</i>	<i>41</i>
4.4.	Preliminary Sensitivity Analysis.....	42
4.4.1.	<i>Parameter Formulation .....</i>	<i>42</i>
4.4.2.	<i>Results and Conclusions .....</i>	<i>47</i>
4.5.	Secondary Sensitivity Analyses .....	54
4.5.1.	<i>Sensitivity Trend of Hydraulic Parameters.....</i>	<i>54</i>
4.5.2.	<i>Distinction between Emergent and Submergent Vegetation.....</i>	<i>57</i>
<b>5</b>	<b>Case Study – Kanika Sands .....</b>	<b>59</b>
5.1.	2D Model Setup .....	59
5.2.	Parameter Formulation .....	62
5.3.	Results and Conclusions .....	64
5.3.1.	<i>Effectiveness of Mangrove Vegetation.....</i>	<i>65</i>
5.3.2.	<i>Model Characteristics.....</i>	<i>70</i>
5.4.	Horizontal Variation Studies .....	73
5.4.1.	<i>Alongshore Extensions.....</i>	<i>73</i>
5.4.2.	<i>Density Variations .....</i>	<i>76</i>
5.4.3.	<i>Vegetation Strip Plantations.....</i>	<i>77</i>
<b>6</b>	<b>Conclusions.....</b>	<b>80</b>
6.1.	Process Summary and Assumptions .....	80
6.2.	Conclusions .....	80
6.2.1.	<i>Mangroves and the Port.....</i>	<i>80</i>
6.2.2.	<i>Model and Vegetation Characteristics .....</i>	<i>81</i>
<b>7</b>	<b>Recommendations .....</b>	<b>83</b>
7.1.	Mangroves and the Port.....	83
7.2.	Numerical Model.....	84
7.3.	Physical Modeling and Field Work.....	85
7.4.	Detail and Accuracy .....	87
<b>8</b>	<b>References.....</b>	<b>88</b>
<b>9</b>	<b>Appendices.....</b>	<b>93</b>

## List of Figures

Figure 1: Flowchart – Study Methodology	4
Figure 2: Global distribution of tropical storm tracks with local names (Abbot, 2006 from Fritz H.M. & Blount C, 2007)	5
Figure 3: Detailed map of Orissa and its location within India with the Bhadrak district circled	6
Figure 4: Districts of Orissa state affected by the 1999 super cyclone with current area of interest circled	7
Figure 5: Typical structures of three distinct mangrove species	8
Figure 6: World-wide extent and distribution of mangroves (FAO Forestry paper 153, 2007)	9
Figure 7: Table from Das S (2007) showing the protective effect of mangroves in present scenario and projected effect if previously existing mangroves had been protected	10
Figure 8: Mangrove tree height schematization followed in SWAN 40.55MOD (Burger, 2005)	13
Figure 9: Map of the rivers and coast of Orissa with the five designated coastal management zones (Mohanty P.K. et al., 2008)	15
Figure 10: Map of Kanika Sands Island, Dhamra port and other features of the case-study site (Dhamra port website, 2008)	16
Figure 11: Google Earth Image of Case Study Site (c. 2006)	17
Figure 12: Survey of India Toposheets showing the shifting morphology of the region (Forest Survey of India, State of Forest Report, 2003)	17
Figure 13: Species Zonation based on Tides (Giesen W. et al., 2007)	19
Figure 14: Root systems of three mangrove families (from De Vos, 2004)	19
Figure 15: Comparisons of $\Delta P$ values for the chosen events with the three different methods; the 50 year event is circled in red	23
Figure 16: Comparison of wave heights for all events for the five methods examined	25
Figure 17: Offshore wave periods for different events for the control method and two different cases of average values - one across methods 1, 3, 4 and 5 and the other across methods 3, 4 and 5	26
Figure 18: Offshore wave heights and wave periods for selected return periods of 5, 10, 25, 50 and 100 years calculated based on data from Murthy et al. (2007)	27
Figure 19: Storm Surges for different return periods from Jayanti et al., (1986) (from Murthy et al., 2007) used as basis for return period analysis	27
Figure 20: Maximum storm surge levels along the Orissa coast for a 50 year return period with the current area of interest circled (from Chittibabu et al., 2004)	29
Figure 21: Interpolated 1-D Bathymetry for deep to shallow water wave transformation calculations	30
Figure 22: Historic cyclone tracks (Chittibabu et al. 2004) with predominant wave direction during normal conditions indicated in red	32
Figure 23: Water depth and wave height transformation from deep to shallow water	32
Figure 24: Graph of significant wave heights and wave periods at -11 m contour vs. the return period in years under storm surge conditions	33
Figure 25: Details of calculated bathymetry, EIWLs ( measured with respect to CD) and schematized vegetation heights	35
Figure 26: Vegetation and water levels schematised based on the Dalrymple formulation (Myrhaug, et al., 2009)	38
Figure 27: Bathymetry (left) and Vegetation Density (right) grids for Generic Modeling Studies with angle of wave attack indicated	39
Figure 28: Relation between $C_d$ and Reynold's Number (Battjes, 1999 from Burger B., 2005)	43
Figure 29: Bathymetry (left) and Vegetation Density (right) grids for Generic Modeling Studies with angle of wave attack indicated	47
Figure 30: Transmitted wave heights across forest width for varying vegetation density values and fixed hydraulic parameters ( $h=9.6m$ , $H_s=2.5m$ , $T_p=15s$ )	48
Figure 31: Transmitted wave heights at 200 m forest width for different vegetation factor values and different input wave heights for increasing return periods (constant $h = 9.6 m$ and $T_p = 15 s$ )	48
Figure 32: Transmitted wave heights across the forest for different input wave heights at constant (MEDIUM) vegetation factor values (constant $h = 9.6 m$ and $T_p = 15 s$ )	49
Figure 33: Reduction factor ( $r$ ) ratios vs. forest width for $h 4.1 m / h 9.6 m$ for increasing vegetation densities (constant $H_s = 2.5 m$ and $T_p = 15 s$ )	50

Figure 34: Transmitted wave heights across forest width at constant (LOW) vegetation factor values for different wave periods (constant $h = 7$ m and $H_s = 3.74$ m)	51
Figure 35: Transmitted wave heights at 200 m forest width for different values of $H_s$ , $h$ and $T_p$ for return periods of 100, 25 and 5 years and different (LOW and HIGH) vegetation factors	51
Figure 36: Variation in reduction factor ( $r$ ) across forest width for different vegetation factor values at constant hydraulic parameter values	52
Figure 37: Reduction Factor ( $r$ ) ratios for water depth ( $h$ ), wave height ( $H_s$ ) and wave period ( $T_p$ ) variations across mangrove forest width for constant vegetation factors	56
Figure 38: Variation in reduction factor for an increase in hydraulic parameter values ( $H_s$ , $h$ and $T_p$ ) by a factor of 1.5 across forest width	56
Figure 39: Transmitted wave heights across forest width for emergent and submergent vegetation with identical depth averaged vegetation factors for a 25 year event	57
Figure 40: Ratio of reduction factors for emergent vegetation and submergent vegetation (Right-hand axis) along the mangrove forest width for constant depth-averaged vegetation factors	58
Figure 41: Interpolated near-shore bathymetry for 2-D models with CD indicated	59
Figure 42: Isometric view of assumed island bathymetry with vertical northern and southern sides (heights measured relative to CD)	60
Figure 43: Bathymetry (left) and Vegetation Density grids (right) for case study with modeled region indicated in actual bathymetry map (from Map Room, Delft University of Technology) on top	61
Figure 44: Graph showing transmitted wave heights across an island with high vegetation density with and without diffraction computations	63
Figure 45: Bathymetry grid (left), vegetation density grid (middle) and transmitted wave heights (right) for an island with a 'high' vegetation density and an event of a return period of 25 years. The two analysis sections X-X (cross-shore) and Y-Y (alongshore) are indicated on the transmitted wave heights grid.	64
Figure 46: Transmitted wave heights from offshore (right) along Section X-X (cross-shore) for different vegetation factors compared with the 'no veg. and no island' case for a 25 year event	65
Figure 47: Transmitted wave from offshore (right) along Section X-X (cross-shore) for different vegetation factors for return periods of 100 years (TOP) and 5 years (BOTTOM)	65
Figure 48: Transmitted wave heights along Section X-X within the vegetation and between the vegetation and the port for a 25 year event	66
Figure 49: Difference in transmitted wave heights between 'LOW' and 'HIGH' cases at different alongshore sections between the island and the port versus forest width at that point	67
Figure 50: Transmitted wave heights along Section Y-Y (alongshore) at the port for varying angles of wave attack and constant vegetation and hydraulic parameters corresponding to a 25 year event	68
Figure 51: Wave heights at the port at a point directly behind the mangroves versus return periods for different cases of vegetation	69
Figure 52: Transmitted wave heights for cases of an island and no island both with vegetation of varying densities for a 25 year event	70
Figure 53: Magnified view of transmitted wave heights around the mangrove island for a 25 year event and high vegetation factors	71
Figure 54: Transmitted wave heights along Section Y-Y at the port with and without diffraction approximations for a 25 year event and high vegetation factors	72
Figure 55: Vegetation grids for Case 1 (Left) and Case 2 (Right)	74
Figure 56: Wave heights at port for original mangroves and the two extension cases at 22.5 deg wave attack angles for a 25 year event with the port region indicated	75
Figure 57: Vegetation density grid for the case with a value of 0.5 m for a 200 m width all around the island	76
Figure 58: Transmitted wave heights at 2000 m forest width (TOP) and 600 m forest width (BOTTOM) for the three density variation cases for a 25 year event	77
Figure 59: Vegetation Density grid with a 300 m mangrove strip of density 1 (Case 2) all around and no mangrove in between for a 100 year event.	78
Figure 60: Transmitted wave heights for three vegetation strip cases and the normal case for a 100 year event	79
Figure 61: Wind-speed Surface pressure correlation (from Pidwirny - Physicalgeography.net)	96
Figure 62: Transmitted wave height chart for a flat bathymetry and no vegetation illustrating the energy leakage effect	102
Figure 63: SWAN 40.55MOD input file for a case study scenario with high density plants and 25 year return period hydraulic conditions	103

## List of Tables

<i>Table 1: Species Zonation based on Tides</i>	18
<i>Table 2: <math>H_s</math>, <math>T_p</math> and storm surge for various return periods</i>	28
<i>Table 3: Wave statistics and water levels at -11 m depth contour for different return periods</i>	34
<i>Table 4: Boundary Wave Conditions for Generic 2-D Model (+3 m contour)</i>	34
<i>Table 5: Species – S. alba (Fig 2: Extreme right; Fig 3: Extreme Left) (compiled from Sun Q, et al., 2004, Hossein M.K. et al., 2003, Aluka Webpage (online), 2006-2008, Azote 2008 (online), Flowers of India (online), n.d., Dr. W.N.J. Ursem, 2009)</i>	36
<i>Table 6: Species – R. mucronata (Fig 2: middle; Fig 3: extreme right) (compiled from Hossein M.K. et al., 2003, Aluka Webpage (online), 2006-2008, Azote 2008 (online), Duke N.C., 2006, Dr. W.N.J. Ursem, 2009)</i>	36
<i>Table 7: Parameters varied for Generic Model Runs</i>	40
<i>Table 8: Range of realistic vegetation parameter values (lowest VFR value corresponding to stem layer in bold)</i>	44
<i>Table 9: Modeled Vegetation Factor Values for ‘LOW’, ‘MEDIUM’ and ‘HIGH’ scenarios</i>	45
<i>Table 10: Modeled Vegetation Height values for emergent and submergent scenarios</i>	45
<i>Table 11: Modeled Hydraulic Parameter Values for Primary Sensitivity Analysis (varied values in bold)</i>	46
<i>Table 12: Modeled Hydraulic Parameter Values for Secondary Sensitivity Analysis (varied values in bold)</i>	55
<i>Table 13: Simplified vegetation parameter variation for emergent and submergent cases</i>	57
<i>Table 14: Vegetation and Hydraulic scenarios for Case Study (constant angle of wave attack)</i>	62
<i>Table 15: Angle of wave attack scenarios for Case Study (for a 25 year event)</i>	62
<i>Table 16: Vegetation parameter values for Case Study</i>	63
<i>Table 17: Hydraulic parameter values for Case Study (constant angle of wave attack)</i>	63

## List of Symbols and Abbreviations

$\alpha$	Ratio of vegetation height to water depth
$\varepsilon_v$	Time-averaged rate of energy dissipation
$\Omega$	Latitude (angle) of location
$\rho$	Density of fluid (sea-water in this study, assumed as a constant)
$\sigma$	Wave frequency
$b_v$	Vegetation area per unit height of vegetation for each stand perpendicular to $u$
$c_g$	Group velocity
$f$	Coriolis' parameter ( $f = 2\Omega \sin(\Omega)$ ) (rad/s)
$g$	Acceleration due to gravity
$h$	Water depth
$k$	Wave number
$r$	Wave reduction factor
$u$	Water particle velocity in the x – direction
$z$	Water particle velocity in the z – direction
$CD$	Chart Datum
$C_D$	Depth-averaged drag coefficient
$E$	Wave energy
$EIWL$	Extreme Instantaneous Water Level
$F_{x(z)}$	Force acting on the vegetation per unit volume in the x (z) - direction
$H$	Wave height (m)
$H_{in}$	Wave – height at first grid point
$H_o$	Maximum significant wave height (also referred to as $H_s$ (max))
$H_{rms}$	Root mean square wave height
$H_{trans}$	Wave – height at second grid point
$N$	Number of vegetation stands per unit horizontal area
$P_n$	Peripheral pressure
$P_o$	Central pressure

$R$	Radius to maximum wind
$R'$	Effective radius to maximum wind
$SLR$	Sea-level Rise
$SS$	Storm Surge Level
$T_p$	Peak wave period
$U_{\max}$	The maximum gradient wind speed at 10 metres above the mean surface
$U_r$	The maximum sustained wind speed at 10 metres above the mean surface (from measurements)
$V_{fm}$	Velocity of forward movement
VFR	Vegetation Factor Ratio
WL	Water Level (measured with respect to $CD$ )

# **1 Introduction**

## **1.1. Problem Description**

Tropical coastlines are under great pressure due to a rapid increase in population and infrastructure. Large-scale mismanagement of these coastlines and the inability to cope with events such as cyclones can have devastating long and short term effects especially in developing countries. It is a well-established fact that mangroves help protect the hinterland by attenuating waves during extreme events and reduce long term coastal erosion by trapping sediment (UNEP-WCMC 2006). Mangroves are a coastal inter-tidal ecosystem consisting of salt-tolerant plants that occurs in inter-tidal regions of tropical and sub-tropical coasts. While there is an increasing emphasis on protecting and preserving mangrove eco-systems little is still understood of these systems, especially on how they respond to changes in their environment. In recent times, numerical models have been created that give a fairly good representation of the hydrological and sedimentary processes within a mangrove ecosystem. The SWAN 40.55MOD model (Tomohiro Suzuki, Personal Communication), developed at the Delft University of Technology is one such model that attempts to calculate wave dissipation in a mangrove vegetation patch. Given the high rate of destruction of mangroves world-wide (UNEP-WCMC 2006) it is essential that this understanding be used to establish the value of these ecosystems. Also, it is necessary to go one step further and combine this understanding with effective management techniques to prevent long term misuse of such ecosystems.

## **1.2. Problem Statement**

With increasing population pressure, demand for development on tropical coastlines and the world-wide necessity for environmental protection it is urgent and essential to establish the usefulness of mangroves in protecting ports or other coastal developments from the effects of a tropical cyclone. This study looks at the wave dissipation process in mangroves with regard to various controlling hydraulic and vegetation parameters using the SWAN40.55MOD numerical model and attempts to establish, as a case-study, the protection offered during tropical cyclones by a mangrove inhabited island in the Bay of Bengal to an upcoming Indian port behind it. The location of this island in the vicinity of

an important coastal development, the region's susceptibility to some of India's most severe cyclones and most of all the prevalence of mangroves on the island were thought to make this island a highly suitable choice for the case study.

### 1.3. Study Objectives

The main objectives of this study are as follows:

1. To determine, under extreme conditions, the manner in which various controlling hydraulic and vegetation parameters influence the process of wave attenuation in mangroves.
2. To determine the parameter combination scenarios relevant for studying the effect of mangrove vegetation on a leeward structure under extreme conditions.
3. To determine as a case-study the effectiveness of the mangrove island of Kanika Sands in protecting the Dhamra port in terms of wave attenuation under extreme conditions and to come up with recommendations regarding the same.

### 1.4. Study Methodology

The SWAN 40.55MOD numerical model was used to study the effectiveness and extent of wave attenuation in a mangrove vegetation patch under extreme water level and wave parameter conditions. An island in the Bay of Bengal, in Orissa, India was chosen for this purpose due to the high frequency of severe cyclones and a considerable presence of mangrove habitats along the coast. An extensive literature review was conducted to establish the nature of the cyclones and mangrove vegetation characteristics in the region. Statistical data on cyclones in Orissa were used to approximate offshore cyclone parameters corresponding to events of selected return periods between 100 and 5 years.

The offshore wave parameters corresponding to these cyclone parameters were estimated based on different regional and global empirical relationships and the final values taken as the average of methods with comparable results. The offshore bathymetry in the region was roughly approximated from low scale hydrographic charts. This was used in the SWAN 1Dv numerical model to estimate wave height transformation from deep to shallow water for the chosen return periods. Extreme near-shore storm surges were calculated from available statistical studies based on past observations. These were added

to estimates of high tide and sea-level rise to obtain the extreme instantaneous water levels for the chosen return periods. Vegetation characteristics such as heights, diameters and densities were approximated with information about general regional vegetation characteristics from the literature review. The calculated wave parameters, water levels and vegetation parameters were used as the inputs for the near-shore vegetation dissipation analyses.

First a generic analysis was conducted to obtain insights into the characteristics and behaviour of the model and the system. For this a flat bathymetry was used with the simplified vegetation parameters and calculated wave and water level conditions. Various scenarios were simulated based on different possible combinations of hydraulic and vegetation parameter values. From the results conclusions were drawn regarding the model and system characteristics. These were used to select a reduced number of relevant combination scenarios for the case–study which would involve more realistic bathymetry and vegetation parameters. Also, some secondary generic analyses were done to examine in detail certain trends observed in the preliminary analyses.

A case–study was done for the site of Kanika Sands, a mangrove inhabited island 3.5 km off the Orissa coast between the channels of the Dhamra River. Located at roughly 20° 47' N and 86° 59' E the island lies directly offshore of the upcoming Dhamra Port. The case study used the selected scenarios to assess the effectiveness of the mangroves in protecting the port against extreme cyclone events and to determine what would be needed to enhance the same. Finally conclusions were drawn regarding the effectiveness of the mangroves in protecting the port and the range of cross-shore and alongshore sizes of the vegetation patch necessary to provide a minimum level of protection. Also, some secondary conclusions were drawn regarding the model characteristics and the direction of future improvements in numerical models, physical experiments and field work in this field. Figure 1 on the next page has a flowchart illustrating the steps in this process.

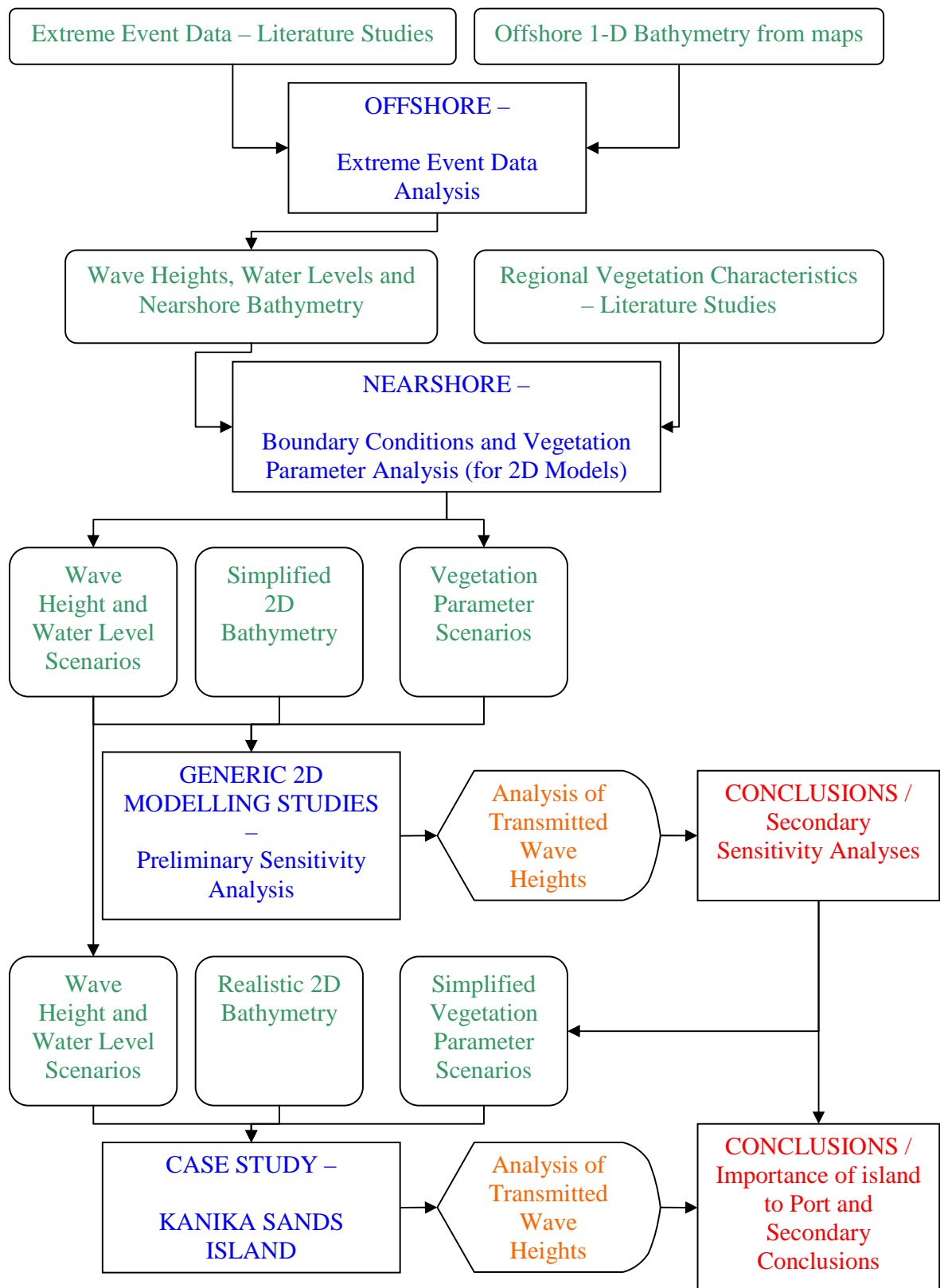


Figure 1: Flowchart – Study Methodology

## 2 Literature Review

### 2.1. Tropical Cyclones

#### 2.1.1. Basics

In tropical regions at a sufficient distance from the equator where the effect of the Coriolis' force is appreciable, cloud clusters may form leading to an organized closed circulation of air. When this circulation develops to a point where the maximum sustained wind speed exceeds 121 km / hr the cluster is termed a *cyclone*, *typhoon* or *hurricane* depending on whether it occurs in the Indian Ocean, the Western Pacific Ocean or the Atlantic and Eastern Pacific Oceans respectively. A cyclone is said to have made landfall when its trajectory takes it over a landmass. The distribution of tropical storms is illustrated below in Figure 2 (Fritz H.M. & Blount C, 2007).

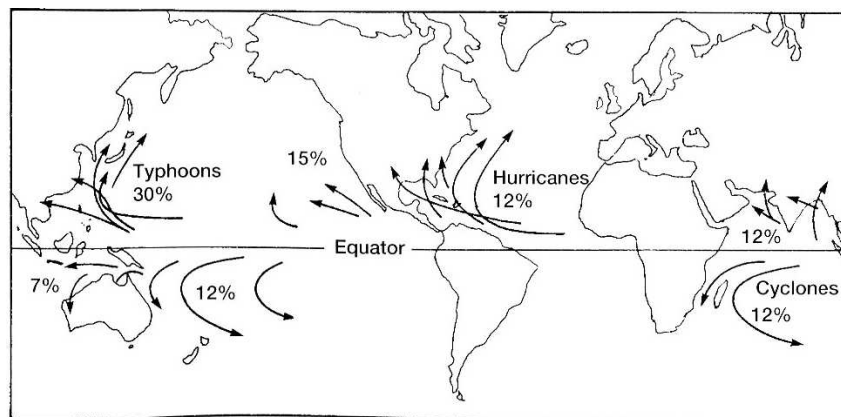


Figure 2: Global distribution of tropical storm tracks with local names (Abbot, 2006 from Fritz H.M. & Blount C, 2007)

#### 2.1.2. Cyclones in the Bay of Bengal

The Bay of Bengal is a huge, shallow extension of the Indian Ocean bordered on three sides by India, Bangladesh, Burma and Thailand. It experiences two monsoon seasons – a South-West Monsoon season from June to October and a milder North-East Monsoon season from November to February. Since it is climatologically favourable for the development of a cyclone most Bay of Bengal cyclones are formed in the monsoon trough – a low pressure trough whose location depends on seasonal conditions. Sometimes cyclones are also formed immediately before or after the monsoon seasons.

Studies have shown that the frequency of cyclone formation in the Bay of Bengal is very high, almost 6 to 7 times higher than in its western counterpart, the Arabian Sea (Aggarwal & Lal 2000). Due to the large scale destruction caused by cyclones several vulnerability studies of coastal regions in India have been conducted with regard to cyclones. One such study found that the most affected region in eastern India is the northern section of the east coast (Alam M et al., 2003). The study showed that in the period 1974 – 1999 two-thirds of the cyclones that crossed the east coast of India within the monsoon period made landfall in this region. It has been observed that almost 90% of the damage associated with a cyclone is caused by flooding with the remaining 10% being attributed to wind related damage (Gonert et al., 2001 in Chittibabu et al., 2004). While the most damaging effect of a cyclone in a coastal town is the flooding due to the storm surge, high tide and rainfall (Chittibabu et al., 2004), increasing development of parts of the coastline with ineffective protection has resulted in an increased exposure to extremely high cyclone waves. This work focused on a region in the coastal district of Bhadrak (circled in Figure 3) in the Indian state of Orissa, bordering the northern Bay of Bengal.



**Figure 3: Detailed map of Orissa and its location within India with the Bhadrak district circled**

### ***2.1.3. Cyclones in Orissa***

The state of Orissa has suffered severe damage almost every year from cyclones originating in the Bay of Bengal. Statistical studies indicate that for the months of October and November Orissa has the highest probability (56 %) among the states on the east coast of India that at least one cyclone makes landfall every year (Mascarenhas A., 2004). One study by Dube et al. in 2000 used a numerical model developed by the Indian Institute of Technology - Delhi to simulate storm surges due to six cyclones that made

landfall on the Orissa coast. This study was based on data from records of the India Meteorological Department (IMD). A later, more comprehensive study by Chittibabu et al. in 2004 used this model to assess the effect of climate change on storm surges along the Orissa coast. Chittibabu et al., 2004 brought together two databases for cyclones in Orissa – one from the IMD with data from 1877 to 2000 and the other from various records including the British East India Company, the IMD and state government records with data from 1804 to 2000. 16 cyclone events were selected in this study for which cyclone parameter values were estimated by various empirical means when data was not available. These 16 events were modeled using the storm surge model described in Dube et al. (2000) and the obtained values were verified with available data. In July – October 1999 a super cyclone with winds exceeding 250 km / hr made landfall near the port city of Paradip in Orissa claiming approximately 10,000 lives and causing extensive damage to property. The study showed that this cyclone has a return period of roughly 50 years indicating that such extreme events are quite common in the region. Figure 4 shows the parts of Orissa directly affected by the super cyclone of 1999 (Chittibabu et al., 2004) with the present area of interest indicated.

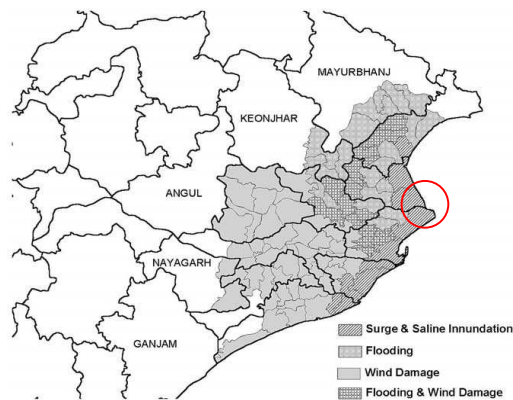


**Figure 4: Districts of Orissa state affected by the 1999 super cyclone with current area of interest circled**

## 2.2. Mangroves

### 2.2.1. Basics and Distribution

*Mangroves* or *mangal* refer to a coastal inter-tidal ecosystem of halophytic wooded plants that occur in inter-tidal regions of tropical and sub-tropical coasts. A unique feature of mangrove vegetation is their emergent root system that allows the trees to breathe in saturated soils or even under partially submerged conditions. Mangroves generally occur between mean sea level and the highest spring tidal level. They very often exhibit a distinct shore-parallel zonation thought to depend on a number of factors including species competition, topography and tidal range, soil type and chemistry and nutrient content (Alongi, 2002). A single mangrove patch may consist of a variety of different species all of which adapt in different ways to survive in a typically harsh environment. A true mangrove plant usually consists of small or large roots above ground level, a single stem and a large canopy as shown in Figure 5.



**Figure 5: Typical structures of three distinct mangrove species**

Studies conducted by the Food and Agricultural Organisation (FAO Forestry Paper 153, 2007) in the last decade showed that mangrove systems were most extensively distributed in Asia, followed by Africa and South America. As of 2005, India was estimated to have 3% of the world's mangroves corresponding to nearly 500,000 hectares of mangrove forest. Figure 6 below indicates the world-wide distribution of mangroves

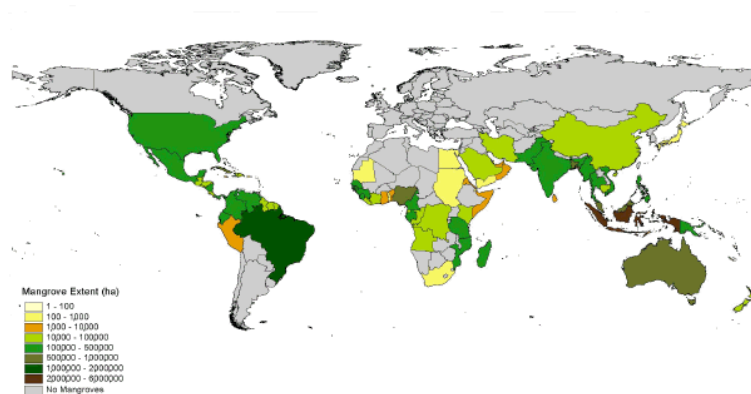


**Figure 6: World-wide extent and distribution of mangroves (FAO Forestry paper 153, 2007)**

India's extensive coastline is dotted with several small and large mangrove patches. The largest single block of halophytic mangroves in the world, the Sunderbans occur within the Ganges-Brahmaputra Delta straddling the border between India and Bangladesh. Other major mangrove systems include river deltas on the east coast in the states of Orissa, Andhra and Tamil Nadu, the Gulf of Kutch on the west coast in the state of Gujarat, adjacent to Pakistan and systems within the Andaman and Nicobar islands near the Indonesian archipelago. Despite the knowledge that mangroves serve to protect the hinterland large-scale destruction of these habitats is being witnessed across parts of the country.

### ***2.2.2. Mangroves and Extreme Events***

The role of mangroves as coastal protection is crucial in India especially along the east coast which is subject almost annually to severe cyclonic events. It has been well established from observations and socio-economic studies that mangroves play a major role in protecting the hinterland from the destructive effects of hurricanes, cyclones and to an extent, even tsunamis. A socio-economic study conducted in Orissa (Das S., 2007) investigating the effect of a devastating super-cyclone in July 1999 established that coastal villages situated behind mangroves escaped with much less damage compared to villages that did not enjoy their protection. Das S. (2007) also concluded that one hectare of mangroves can be nearly two times as valuable economically as the 'cleared' land that exists in its stead in many coastal areas in the region. It is therefore of great interest for public and private authorities to focus on mangrove management since mangroves can

provide considerable economic value if properly managed. Figure 7 from this study shows the extent to which mangroves have protected the hinterland in this region.

Actual deaths during 1999 super cyclone	392
Predicted deaths if there were no Mangroves	603
Predicted deaths if current mangroves were at 1950 level	31
Predicted deaths if current mangroves were at 1950 level and villages established after clearing the mangrove forest were not located there	17

**Figure 7: Table from Das S (2007) showing the protective effect of mangroves in present scenario and projected effect if previously existing mangroves had been protected**

Due to the complexity of the hydrodynamics and sediment regimes in mangrove systems and the relative lack of data there is a gap in current understanding about the processes by which mangroves offer protection against extreme events and therefore on how they can be optimally managed. While on the one hand the very nature of such events makes measurements extremely difficult, if not impossible, there is a need to understand and quantify the effects of mangrove systems in the event of a cyclone or a storm, especially in light of the perceived effects of climate change.

### ***2.2.3. Mangroves and Waves***

Studies have been conducted in some places on the physical processes involved in attenuation of waves by mangroves under normal conditions. Due to the high complexity of these processes, their dependence on the vegetation characteristics and hydrodynamic regime and the high regional variability in all these factors, most of these studies are highly region specific. Wave attenuation in vegetation depends on hydraulic parameters such as wave height and wave period and vegetation characteristics such as geometry, stiffness, density and spatial configuration (Mendez & Losada, 2004). Analytical and numerical wave attenuation models have been proposed that calculate the energy loss in a wave propagating through a vegetation field. Due to the lack of in-depth understanding of the flow within mangroves and since they focus on wave energy dissipation these models restrict themselves to two dimensions, namely, 'x', the axis along the wave front propagation direction and 'z', the vertical axis. All these models assume the linear wave theory to be valid within the vegetation region. The conventional definition for the depth-

integrated time-averaged energy dissipation in a vegetation field per unit horizontal area is given by the expression

$$\varepsilon_v = \overline{\int_{-h}^{-h+\alpha h} Fudz} \quad (1)$$

where the over-bar represents the time averaging in a wave period, and  $F (= F_x u + F_z w)$  is the force acting on the vegetation per unit volume along the vertical and one horizontal axis. It is generally assumed that in an anisotropic dissipative medium like vegetation, the  $F_z w$  term is negligible compared to the  $F_x u$  term which results in the expression

$$\varepsilon_v = \overline{\int_{-h}^{-h+\alpha h} F_x u dz} \quad (2)$$

While an accurate calculation of the  $F_x u$  term would include the effect of swaying motions and both inertial and drag forces many models simply neglect the swaying motions and inertial forces and calculate only the drag forces for purposes of simplicity. In such a case the vegetation induced forces are given by a Morison type equation where the vegetation is assumed as comprising several cylindrical units.

$$F_x = \frac{1}{2} \rho C_D b_V N u |u| \quad (3)$$

Since this non-linear force can include the relative velocity between the plant and the fluid it may be considered valid for rigid as well as flexible plants, with a different bulk drag coefficient being used in case of flexible plants to make up for the lack of more accurate information on plant motion (Dalrymple et al., from Mendez & Losada, 2004). These formulations were presented in an empirical model by Mendez & Losada (2004). The model depends on a parameter similar to drag coefficient which was parameterized as a function of the Keulegan – Carpenter number for a given plant based on laboratory experiments for different plant types (Mendez & Losada, 2004). Based on this work a routine was developed within the SWAN 2dv near-shore wave model by Burger (2005) to calculate wave transformation in vegetation fields.

## 2.3. The SWAN Model for Vegetation

### 2.3.1. SWAN - Basics

SWAN (Simulating WAVes Near-shore) is a third generation wave model based on the wave action balance equation with sources and sinks, developed by a team at the Delft University of Technology in the Netherlands. The model can be used to obtain realistic wave parameter estimates in coastal and near-shore areas given certain wind, current and bottom conditions. It can be used for simulation of random short-crested wind generated waves in deep, intermediate and shallow water depths and can simulate the following physical phenomena:

1. Wave propagation in time and space, shoaling, refraction due to current and depth, frequency shifting due to current and non-stationary depth
2. Wave generation by wind
3. Non-linear wave-wave interaction (quadruplets and triads)
4. White-capping, bottom friction and depth-induced breaking
5. Blocking of waves by current

The model does not explicitly calculate wave diffraction or reflection. SWAN currently employs a phase-decoupled approach to produce the same qualitative behaviour of spatial redistribution and changes in wave direction, as a substitute for more expensive diffraction computations. This approach however is not considered very effective in front of reflecting obstacles (SWAN User Manual, SWAN Cycle III version 40.72A).

### 2.3.2. Vegetation Dissipation in SWAN

Burger (2005) introduced a sub-routine in SWAN to estimate vegetation dissipation by schematizing the vegetation into different layers composed of cylindrical units. The new version of the model was labeled SWAN 40.55. The energy dissipation expression used in this model, given in equation (4), is the one by Dalrymple et al. (1984) which forms the basis of the empirical model developed by Mendez & Losada (2004).

$$\varepsilon_v = \frac{2}{3\pi} \rho C_D b_v N \left( \frac{gk}{2\sigma} \right)^3 \frac{\sinh^3 k\alpha h + 3 \sinh k\alpha h}{3k \cosh^3 kh} H^3 \quad (4)$$

where  $\varepsilon_v$  is the time-averaged rate of energy dissipation per unit area,  $C_D$ ,  $b_v$  and  $N$  are the vegetation drag coefficient, diameter and spatial density (number of stands per unit

area),  $k$  is the wave number,  $\sigma$  the wave frequency,  $\alpha$  the ratio of plant height to water depth,  $h$  the water depth and  $H$  the wave height at that point. This formula was subsequently improved upon with some corrections and alterations and was renamed SWAN 40.55MOD (Tomohiro Suzuki, Personal Communication) though the basic concept remained the same. The SWAN 40.55MOD model uses the Morison's equation to calculate wave attenuation in cylinders. It however neglects the effect of swaying motion and inertial forces and calculates only the drag force on the cylinder. The horizontal orbital velocities are calculated using the linear wave theory. These are then used to calculate the drag force at each point and their product is integrated along the cylinder's height to obtain the total drag force. Finally the total drag force is equated to the time-averaged energy dissipation per horizontal unit over the vegetation height as given by Dalrymple et al. (1984). The mathematics behind the model is described in Appendix A.

### 2.3.3. Model Considerations

The SWAN 40.55MOD model assumes the mangrove vegetation to consist of cylindrical units. This assumption is an accepted simplification that allows a fairly reasonable simulation of the processes within the vegetation. The important factors in such a case are the diameter and density of each cylinder. Most mangrove trees exhibit a structure with three distinct layers – roots, stem and canopy, with regard to the projected surface though not all mangrove vegetation necessarily follows this behaviour. The schematization of a mangrove tree into three layers, shown in Figure 8 below, is considered sufficiently representative of actual field conditions.

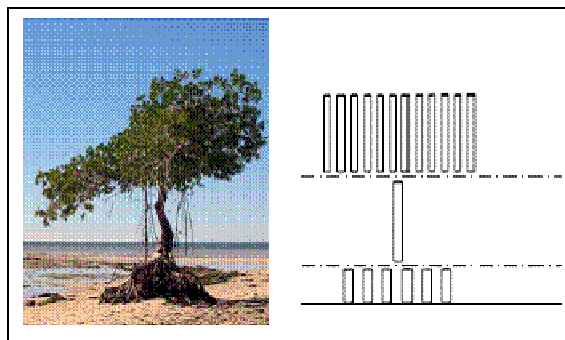


**Figure 8: Mangrove tree height schematization followed in SWAN 40.55MOD (Burger, 2005)**

The SWAN 40.55MOD model neglects swaying motions. This is thought to be acceptable due to the typical rigidity of a mangrove plant. Even though the canopy region is less rigid and may show appreciable swaying motion, its effect was considered negligible for the purposes of this study. Since the force is time-averaged the net contribution of the inertial force which is out of phase with the velocity is zero (National Research Council, National Academy of Sciences, Washington D.C., 1977). Inertial forces are therefore neglected in the Dalrymple formulation. While this is an accepted practice in most models attempting to reproduce wave dissipation processes it may affect the results in some cases. The model performs a depth-averaging of the vegetation parameters before applying the Dalrymple formulation at each grid point. While this limits the model's sensitivity to parameter variations to an extent it still provides a good representation of the wave dissipation mechanism. The manner in which these considerations affected the selection of parameter values and scenarios in this study is described in detail in Section 4.1. Since this study focused on wave attenuation current-induced effects were not included in the computations.

## 2.4. The Case Study Site

### 2.4.1. Location and Environmental Conditions

The coast of Orissa is mostly depositional in nature, its formation being mainly influenced by the Mahanadi and Brahmani – Baitarani river deltas. In 1974, the Government of Orissa divided its coast into five cyclone zones for the purpose of coastal zone management (Mohanty P.K. et al., 2008). These five zones are illustrated along with the river drainage systems in Figure 9 below.

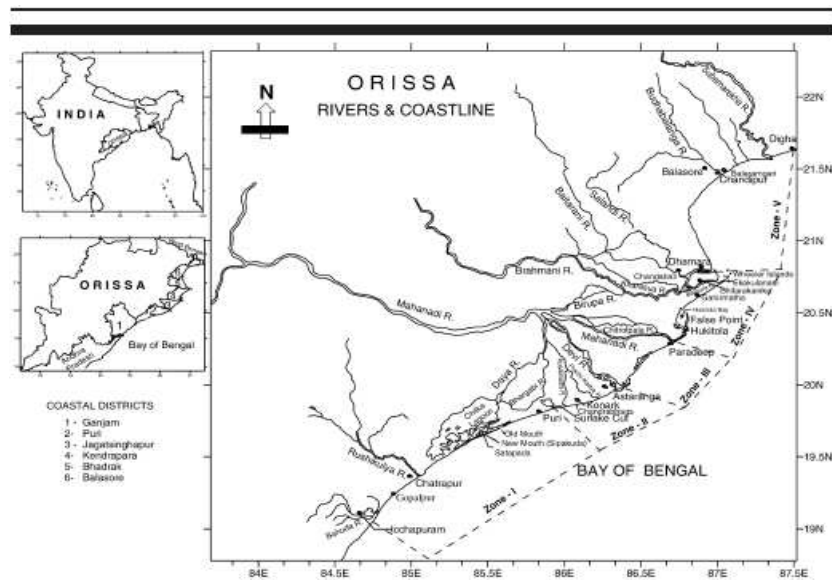


**Figure 9: Map of the rivers and coast of Orissa with the five designated coastal management zones (Mohanty P.K. et al., 2008)**

The site chosen for the case study is the site of a deep water port being built for the import and export of coal and mineral ore. The port is located at roughly  $20^{\circ}47'N$  and  $86^{\circ}58'E$  on the coast to the north of the Dhamra river mouth, which is formed by the confluence of the Baitarani and Brahmani rivers. This region lies at the northern boundary of Zone IV in Figure 9 above. The region is extremely flat and highly susceptible to cyclonic storm surges. The area is heavily forested with mangroves. Immediately south of this region lies the Bhitarkanika wildlife sanctuary which encompasses the second largest block of halophytic mangroves in India. A sandy beach and a fairly long spit are present immediately south of the river mouth. Though relatively protected by the extended sand spit immediately to the south, due to the propagation of storm surges along the coast the area often feels the effect of several nearby cyclones.

Being located at the outer tip of a westward bend in the coastline the case study site has been directly in the path of several cyclones that have occurred in the region. It also feels the heavy winds, waves and surges caused by the outer bands of cyclones that frequently pass parallel to this section of coast along a N – S axis. However, the port and the coastline possibly benefit from the existence of the offshore island of Kanika Sands – a mangrove inhabited island that could help protect the port from the fury of extreme events. As mentioned earlier, the location of the island in front of an important port, the area's susceptibility to some of India's most severe cyclones and the prevalent mangrove vegetation on the island were thought to make the island of Kanika Sands a highly suitable choice for the case study. Figure 10 below shows the island, port and other features of the case-study site.

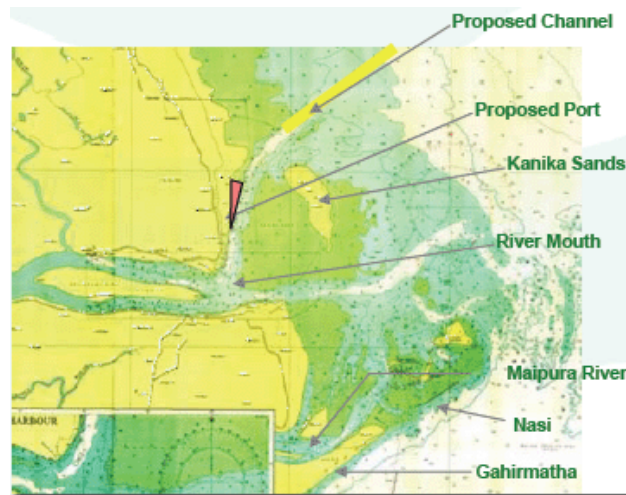


**Figure 10: Map of Kanika Sands Island, Dhamra port and other features of the case-study site (Dhamra port website, 2008)**

#### ***2.4.2. Morphology and Hydrology***

The newly formed Kanika Sands island, seen more clearly in Figure 11, is oval in shape and is roughly 4 km along the N-S axis and 1.5 km along the E-W axis at a maximum. Largely inhabited by mangroves, with a sandy spit to the north and a small sandy ridge on the south-western side, the island is observed to serve as an obstacle to waves, with waves breaking on the windward side and a calm shadow region being developed on the leeward side. A study of the island using Google Earth images showed some mangrove colonization on an arm extending southwards. The island is at a distance of around 3.5 km from the port.



**Figure 11: Google Earth Image of Case Study Site (c. 2006)**

The island is observed to have formed recently as seen from a comparison of Survey of India toposheets from 1972 and 1998. Also evident is the instability of the morphology of the region from the appearance and disappearance of islands over the past few decades as seen in Figure 12. From this and other evidence it was concluded that the morphology in the region is highly unstable though showing a tendency for progradation.

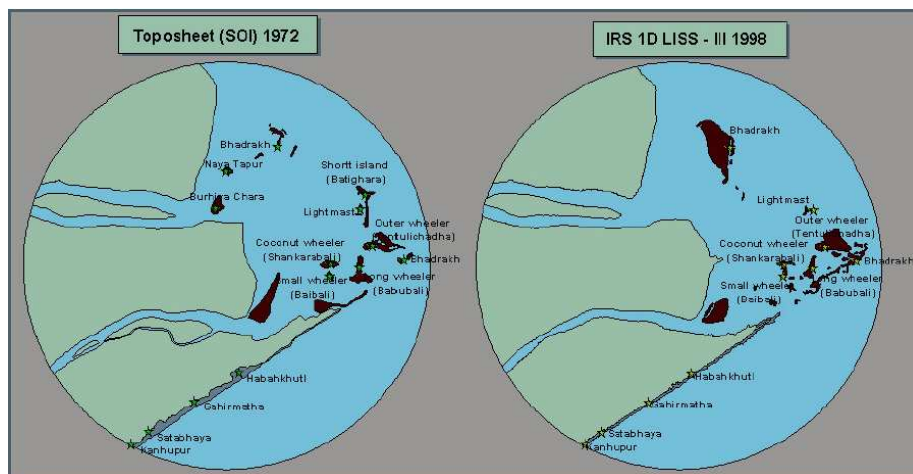


**Figure 12: Survey of India Toposheets showing the shifting morphology of the region (Forest Survey of India, State of Forest Report, 2003)**

The island of Kanika Sands lies within the ebb-tidal delta of the Dhamra river and acts as a barrier separating the northern tidal channel from the southern riverine channel. The tide in the region is mostly semi-diurnal with an amplitude of around 4.5 m at the mouth of the estuary and 2.8 m within the estuary (Selvam V, 2003).

### 2.4.3. Site Vegetation Characteristics

The island of Kanika Sands is inhabited nearly completely by mangrove species. The mangroves and other coastal vegetation on the island were found to consist mainly of *Avicennia marina*, *Avicennia alba*, *Sonneratia alba*, *Rhizophora mucronata* and *Phoenix paludosa* and were found to attain a height of 10m or more (Johnston & Santillo, 2007). The nine vegetation parameters – three for each of the three layers that had to be estimated or measured based on the requirements of the SWAN 40.55MOD model are the diameters, densities and heights of the roots (pneumatophores in the case of *S. alba*), stem and canopy. Before this however, the type of vegetation and its distribution relative to the site topography would have to be determined to enable a more accurate selection of parameter values later on. For this purpose a literature study was done of the mangrove species in the region. Many studies observe that mangrove zonation is strongly influenced by inundation depths which in turn are decided by the land topography in relation to tidal levels as illustrated in Table 1 and Figure 13. Due to the absence of data assumptions were made regarding the topography of the island as described in Section 3.4. By putting together these assumptions with tidal levels obtained from literature (Chittibabu et al., 2004), estimates of the mangrove species, their relevant properties and their relative zonation at the site were made. These estimates were partially verified by checking the occurrence, properties and zonation of mangrove trees in locations with similar geophysical and ecological environments.

**Table 1: Species Zonation based on Tides**

Species	Elevation	Reference
1. <i>E. agallocha</i> (surface roots)	At or just above high-tide mark	Lovelock C., 1993, Field Guide to the Mangroves of Queensland, AIMS Queensland
2. <i>H. fomes</i> (pneumatophores)	Spring tide inundation of only 4 to 5 days	RNGR Tropical Tree Seed Manual (Hossain & Nizam, 2003)
3. <i>A. marina</i> (pneumatophores)	Entire inter-tidal range above MSL	Protabase (web database on useful plants of tropical Africa)
4. <i>S. alba</i> (pneumatophores)	Seaward most fringe along with <i>A. marina</i>	From Giesen W. et al. 2007
5. <i>R. mucronata</i> (stilt roots)	Inter-tidal zone, 0-6m	Duke, 2006 Species Profiles for Pacific Island Agroforestry

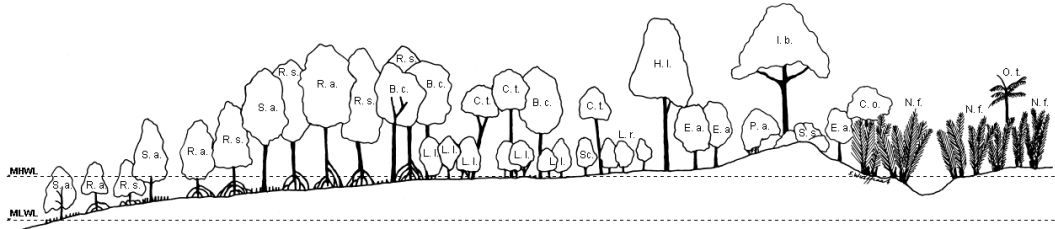


**Figure 13: Species Zonation based on Tides (Giesen W. et al., 2007)**  
**Elevations at site: 0-3 m; MSL – 1.66 m; MHWL – 3.3 m**

Based on the above-mentioned factors it was decided to generalise the species existing on the island into two main families – *Rhizophora mucronata* and *Sonneratia alba*. Most mangrove species are distinguished based on their root systems. For instance trees of the species *Sonneratia* are seen to have small roots appearing out of the ground around the base of the stem. These roots may vary in height up to a maximum of less than a metre. A species like *Rhizophora* however exhibits stand roots that come out of the main stem and have been observed to go up to heights of more than 8 – 10 m. Based on the root systems of the two species shown in Figure 14 and their zonation with regard to water levels it was assumed that *R. mucronata* would occur on the low-lying fringes of the island from elevations of 0 to 2.5 m while *S. alba* would occur in the higher hinterland from elevations of about 2.5 to 3 m. These species were also chosen since it was felt that the difference in their root systems might make a difference to the wave attenuation process.

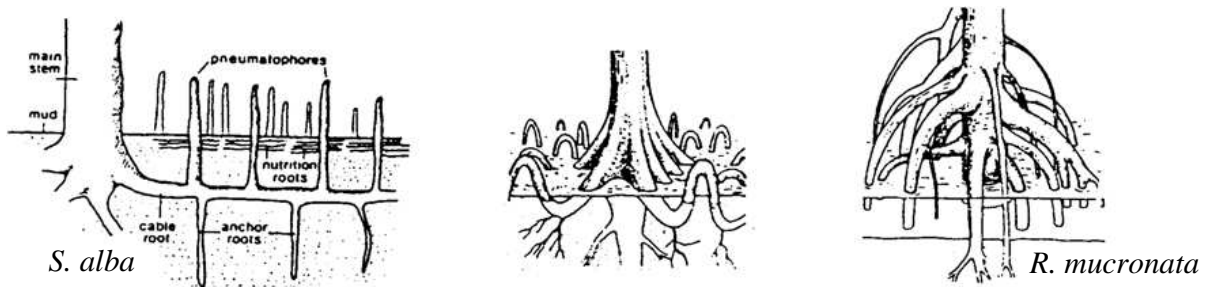


**Figure 14: Root systems of three mangrove families (from De Vos, 2004)**

## 3 Determination of Model Boundary Conditions

### 3.1. Extreme Event Data Analysis

#### 3.1.1. Introduction

The main cyclone parameters that influence wave characteristics in deep water are as follows (Chittibabu et al., 2004):

1. The intensity of the cyclone as expressed by the pressure drop from the periphery of the cyclone to its inner core,  $\Delta P$  (hPa)
2. The maximum wind speed sustained by the cyclone (usually for a duration of 1 minute),  $U_r$  (m/s)
3. The radius to maximum wind of the cyclone,  $R$  (km) from its centre
4. The velocity of forward movement of the cyclone,  $V_{fm}$  (m/s)

Estimation of cyclone parameters and cyclone waves at present is done using state of the art ocean models and satellite data. In the absence of such data however, there exist several empirical models developed in the past that give a fairly good approximation of these values. All these methods suggest relations between cyclone parameters and the waves generated by its heavy winds. A mix of such methods, both global and regional was used in this study to ensure accuracy. Being the most comprehensive study found, statistics from Chittibabu et al. (2004) were used as the basis for this section. Of the 16 cyclone events occurring between 1971 and 2000 listed in Chittibabu et al. (2004) 13 events were chosen based on the availability of  $\Delta P$  and the other necessary values. In the first stage the cyclone parameters necessary for calculation of the wave characteristics – namely, pressure drop  $\Delta P$  and the maximum gradient wind-speed  $U_{max}$  were estimated. The term gradient wind speed refers to a theoretical wind-speed in a cyclone vortex used to parameterize a cyclone that can be estimated from actual wind speed measurements. Three commonly used methods were examined in this stage. One method was used as a control for the estimated values. Averaged values that were in sufficient agreement with the control values were chosen for the next step. The second stage was the determination of the maximum significant wave height,  $H_o$  and peak wave period,  $T_p$  for each event. Due to the highly empirical nature of the procedures a comparison was made between

five commonly used studies and as in stage 1, averaged values that fell within an acceptable range were used in the final stage. The final stage was the determination of offshore wave parameters  $H_o$  and  $T_p$  and near-shore water levels for specific return periods. Statistical studies correlating regional cyclone intensities and near-shore storm surges with return periods were used as the basis for this step.

### ***3.1.2. Assumptions***

The following basic assumptions were made in the calculations based on relevant data and literature studies:

1. The radius of maximum wind speed,  $R$  was assumed to be a constant 45 km (Kumar et al. 2003) Where  $\Delta P$  values were available values for  $R$  were assumed based on Bell's distribution of cyclone diameters in relation to the central pressure,  $P_o$  for the North-west Pacific (Sinha & Mandal, 1999) since typhoons and cyclones have similar basic characteristics.
2. The peripheral pressure for the Bay of Bengal was assumed as a constant 1012 hPa. (Varkey, 1985 in Kumar et al., 2003, p.2241)
3. The velocity of forward movement for all the cyclones,  $V_{fm}$  was assumed as a standard 6 m/s based on literature from the region (Kumar et al., 2003). Further, for calculations based on USACE methods this value was assumed to indicate a cyclone moving slow enough for application of the formulae. The value of the empirical constant for speed  $-\alpha$ , was therefore taken as 1 in the determination of  $H_o$  and  $T_p$  (SPM, 1984 in Hsu et al., 2000, p. 825).
4. The return period correlations were assumed to hold for the calculated average return periods, maximum wave heights, wave periods (Chittibabu et al., 2004) and the predicted storm surges (Murthy, 2007).

### ***3.1.3. Estimation of Cyclone Parameters***

#### **3.1.3.1. Methods Examined**

The cyclone parameters needed for calculation of the wave characteristics were  $\Delta P$  and  $U_{max}$ . These were either taken directly from previously measured or estimated values or

calculated based on available  $U_r$  values. The estimation of  $\Delta P$  and  $U_{\max}$  values for the 16 selected events were based on three methods:

1. The USACE's empirical method outlined in the Shore Protection Manual (1984) as described in Hsu, et al. (2000)
2. The empirical method described by Kumar, et al. (2003) for the Bay of Bengal region using the  $\Delta P$  values from Chittibabu et al. (2004)
3. The commonly assumed linear relationship between cyclone wind speed and sea surface pressure as outlined by Pidwirny (2006).

The first is a commonly used empirical method that relates the value of R of a slow – moving cyclone to its  $\Delta P$  and uses these to estimate the generated wave characteristics. This method has been validated in the study by Hsu et al. (2000). Based on this method, Hsu et al. (2000) proposed a simplified relation for quicker estimates. The third method is also a quick – estimation technique based on a very simple and widely observed linear correlation between the sea-surface pressure during a cyclone and the wind speed. The region-specific method by Kumar et al. (2003), based on the Young's parametric model has been validated for the southern Bay of Bengal. It was therefore decided to use this to verify the values from methods (1) and (3). Even though the study was for the southern Bay of Bengal these results would serve as an effective control due to the similar nature of cyclones in the southern and northern Bay of Bengal. The final values were taken as the averages of the methods chosen from the ones examined. The choosing of methods is detailed in the following section. Details of each method are given in Appendix B.

### **3.1.3.2. Methods Chosen**

It was observed from calculations that while values from method (1) show a high degree of correlation with the values of  $\Delta P$  and  $U_{\max}$  from the control method there is a tendency for over-estimation of the higher values and under-estimation of the lower values. This over and under-estimation of values by the USACE method was thought to be due to the error in the assumption that a hurricane or cyclone with a forward velocity of 6 m/s would classify as a slow-moving hurricane. However, the linear regression relation of method (3) results in a smoothing of the values compared to method (1). Though this method shows a lower degree of overall correlation with the control method as compared to method (1) it shows a better estimation of the general value trend and the

peak values. These trends, which are common for  $\Delta P$  and  $U_{\max}$ , are illustrated for  $\Delta P$  in Figure 15 below.

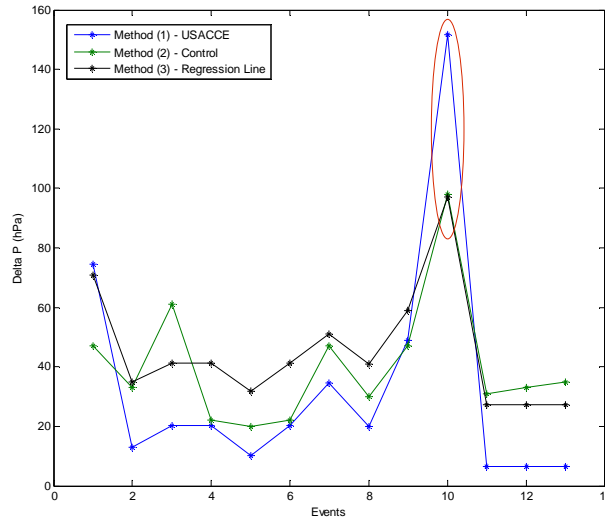


**Figure 15: Comparisons of  $\Delta P$  values for the chosen events with the three different methods; the 50 year event is circled in red**

Though a detailed statistical analysis was difficult for such few data points a decision on which methods to use for the calculation of  $\Delta P$  and  $U_{\max}$  was taken based on these comparisons. From the findings presented above and due to the relative importance of the peak values and behaviour trends during a severe cyclone it was decided to use the average of the values from methods (2) and (3) – the control method and the linear regression analysis – for the next step. Also, average values across all three methods were compared with average values from methods (2) and (3) alone. The comparison was done by correlating the two datasets with the  $\Delta P$  values from Chittibabu et al. (2004) and the  $U_{\max}$  values from Kumar et al. (2004). The correlation coefficient for the averages across methods (2) and (3) alone were seen to be higher than the correlation coefficient for all three methods for both  $\Delta P$  and  $U_{\max}$ .

### ***3.1.4. Estimation of Offshore Wave Parameters***

#### **3.1.4.1. Methods Examined**

The offshore wave characteristics were calculated using the average values for  $\Delta P$  and  $U_{\max}$  obtained from stage 1. Similar to stage 1 values of  $H_o$  and  $T_p$  were estimated using five different studies.

1. Empirical method outlined by the USACE in the Shore Protection Manual (1984) as described in Hsu et al. 2000
2. Simplified relationships for wave heights and wave periods suggested by Hsu et al. 2000.
3. Empirical method for the southern Bay of Bengal obtained from multiple regression analyses by Kumar, et al. (2003) based on the Young's parametric hurricane prediction model (Young, 1988). This was the control method for this step.
4. Simplified empirical method proposed by Kumar et al. (2003) that was validated for 32 cyclones along the entire Indian coast.
5. The three-step method proposed by Young in his parametric hurricane prediction model (Young, 1988).

Here again the empirical method proposed by Kumar et al. (2003) was chosen as the control since it has been validated in the Bay of Bengal. Methods (1) and (2) were chosen as globally accepted and validated methods for wave parameter estimation. Method (5) is another globally accepted method, developed for a simplified numerical model, that uses the fetch-limited JONSWAP spectrum to provide a simple but flexible and reasonably accurate prediction of cyclone wave characteristics in deep water (from Young, 1988). Method (4) was chosen since it was a locally validated method based on the control method. All the methods were examined and the averages of all values that showed a reasonably accurate prediction of the trends were used for the final step. Methods that were seen to deviate considerably from the control values were not used in the final analysis. The five methods examined are described in detail in Appendix C.

### 3.1.4.2. Methods Chosen

The predicted wave heights by the five methods were compared to determine which methods would finally be applied. The control method in this case was method (3), the empirical method proposed by Kumar et al. (2003). It was seen that of the five methods the simplified method proposed by Hsu et al., method (2), results in appreciable over-estimation of the wave height for the cyclone of 1999. This method was therefore not considered in the calculation of averages. The USACE method shows a consistent over-prediction of wave height values by a factor of around 1.3 except for the cyclone of 1999 compared to the control values. This may be due to the error in the assumption that cyclones with a forward velocity of 6 m/s were ‘slow-moving cyclones’. The values from method (4) show very good agreement with the control value with the exception of an under-prediction of wave height for the cyclone of 1999. Values from method (5) are also seen to agree very well with the control values. It was seen that the averages of wave heights using methods (1), (3), (4) and (5) and the averages using only methods (3), (4) and (5) show very good agreement with the control method and with each other. The wave heights from the five methods are compared in Figure 16.

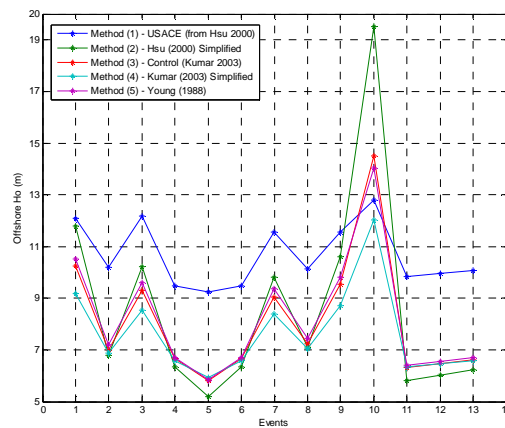


**Figure 16: Comparison of wave heights for all events for the five methods examined**

To decide whether to include method (1) in the final step an analysis of the wave periods was carried out. As shown in Figure 17 below the averaged values of wave periods do not agree as well with the control values when method (1) is included.

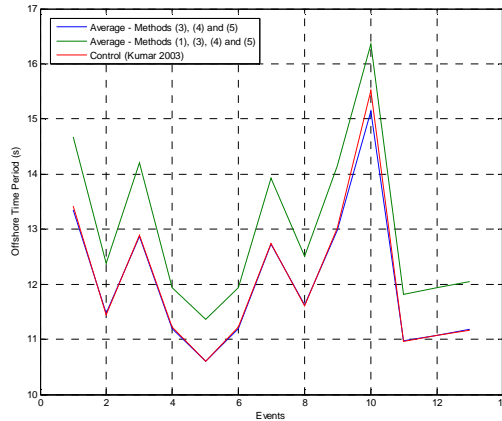


**Figure 17: Offshore wave periods for different events for the control method and two different cases of average values - one across methods 1, 3, 4 and 5 and the other across methods 3, 4 and 5**

A decision was therefore made to use the average wave height and wave period values from methods (3), (4) and (5) only. It was however also felt that these differences were too small to have a significant impact on the final wave characteristics at the 2-D model boundary.

### ***3.1.5. Near-shore Surge Levels and Offshore Wave Parameters for Desired Return Periods***

From statistical studies conducted by Chittibabu et al. (2004) for the state of Orissa, a regression relation was obtained between the  $\Delta P$  value of a cyclone event and its approximate return period. This relation was used to determine the return periods of the selected 16 events, using the average  $\Delta P$  values for each obtained in sub-section 3.1.3. Next, graphs were plotted between the events'  $H_o$  and  $T_p$  values from sub-section 3.1.4 and their return periods. A regression equation for best fit was estimated. This equation was used to extrapolate  $H_o$  and  $T_p$  values for the desired return periods of 100, 50, 25, 10 and 5 years. Figure 18 shows the wave heights and wave periods calculated for selected return periods as described above.

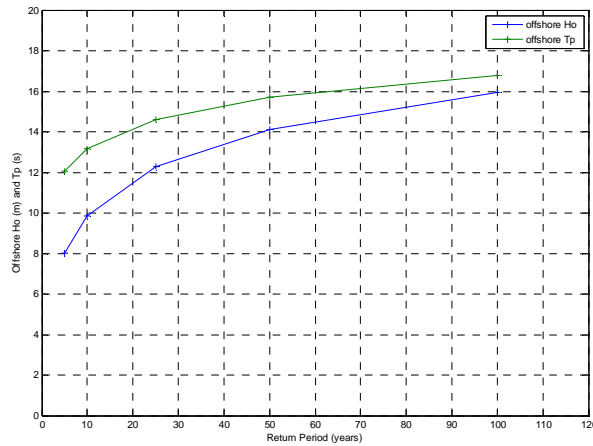


**Figure 18: Offshore wave heights and wave periods for selected return periods of 5, 10, 25, 50 and 100 years calculated based on data from Murthy et al. (2007)**

Near-shore storm surge levels for the northern Bay of Bengal for different return periods were used (Jayanti, N, 1986 in Murthy, et al., 2007). These levels were obtained based on cyclone data from 1890 to 1984. Using these results the near-shore storm surge heights for the chosen return periods were calculated in a manner similar to the one described above. The storm surge – return period correlation based on the data from Jayanti (1986) that was used to extrapolate the values in this study is shown in Figure 19.

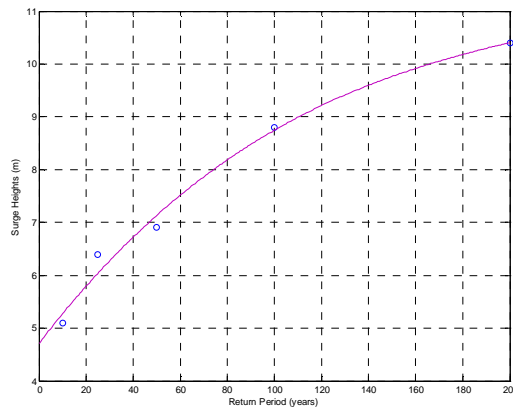


**Figure 19: Storm Surges for different return periods from Jayanti et al., (1986) (from Murthy et al., 2007) used as basis for return period analysis**

### 3.1.6. Conclusions

The final computed values of  $H_o$  and  $T_p$  in deep water and near-shore storm surge heights for various return periods as calculated in sub-section 3.1.5 are shown in Table 2

below. These values would be used in SWAN 1-D to estimate the shallow water boundary conditions for the 2-D model.

**Table 2:  $H_s$ ,  $T_p$  and storm surge for various return periods**

Desired Return Period (yrs)	Offshore ( $H_o$ ) (m)	$T_p$ (s)	Near-shore Storm Surge (m)
100	16	17	8.9
50	14	16	7.6
25	12	15	6.3
10	10	13	4.7
5	8	12	3.4

### ***3.1.7. Verification of Results***

Cyclone events are usually marked by a lack of measured wave data due to their extreme nature. However in this case a single deep water wave height instance was found that was recorded during the super-cyclone of 1999 that made landfall near Paradip, Orissa. A significant wave height of 8.44 m was recorded by a deep water buoy during the event on 28th of October 1999 (Rajesh et al., 2005). Using a relation defined by Kumar et al., (2005) it has been estimated that the maximum significant wave height for that event was 13.93 m (Rajesh et al., 2005). Further, statistical studies by Chittibabu et al., (2004) based on cyclone intensities and frequencies in the region showed that this event has a return period of approximately 47 years. Combining the two studies it is seen that the calculated maximum significant wave height of 14 m (refer Table 2) for a return period of 50 years is in very good agreement with the value of  $H_o$  from observations. The near-shore storm surge levels calculated based on statistical studies by Jayanti et al. (1986) were compared with modeled near-shore storm surge levels from Dube et al. (2000) and Chittibabu et al. (2004). The studies from Dube et al. (2000) showed a maximum near-shore storm surge of 7.8 m at the point of landfall for a cyclone similar to the cyclone of July 1999. Later modeling studies by Chittibabu et al. (2004) showed the storm surge level in the region of interest as being in the range of 7 to 8 m for a return period of 50 years. These values were thought to agree well with the calculated near-shore storm surge level of 7.6 m (refer Table 2) used in this study. Figure 20 below shows the maximum storm-surge

values for a 50 year return period along the coast of Orissa from Chittibabu et al. (2004) with the region of interest circled.

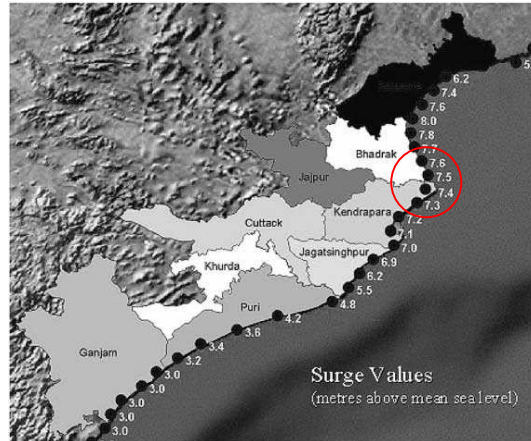


**Figure 20: Maximum storm surge levels along the Orissa coast for a 50 year return period with the current area of interest circled (from Chittibabu et al., 2004)**

## 3.2. Offshore Bathymetry

The bathymetry was estimated using satellite images and hydrographic charts. Two basic bathymetry estimations were carried out – a 1D estimation from deep to shallow water and a 2-D estimation in near-shore waters. The mean sea level (MSL) and Mean High Water Springs (MHWS) were assumed from literature as being approximately 2 m and 3.3 m above the Chart Datum (CD) respectively (Chittibabu et al., 2004).

### *1-D Bathymetry Estimation*

The 1-D cross-shore bathymetry was estimated using low spatial scale (1 in 200000) hydrographic maps from the Map Room of the TU Delft. This was used in the program SWAN 1-D to convert offshore cyclone generated wind waves into near-shore waves and thereby obtain the wave characteristics at the boundary of the 2D model. Eight depth contours from 10 to 1000 m (extending up to 23 km offshore) were digitised manually from the maps. Intermediate contours were piece-wise cubic interpolated using a simple Matlab script to create a more or less representative one-dimensional bathymetry grid with a resolution of 100m in the 'x' direction. During the process it was assumed that the depth contours run parallel to the section of coast being studied and are more or less monotonic in nature. The interpolated bathymetry is shown in Figure 21.

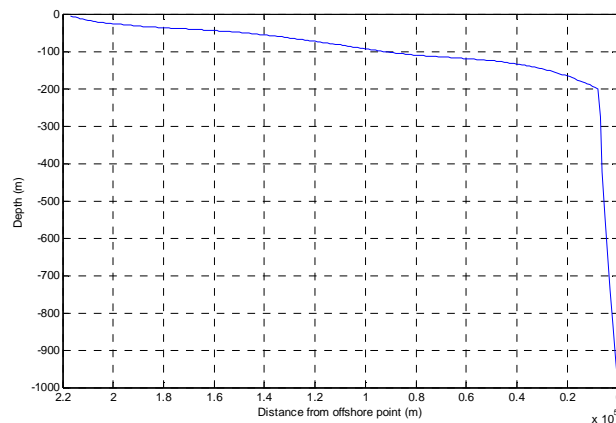


**Figure 21: Interpolated 1-D Bathymetry for deep to shallow water wave transformation calculations**

### 3.3. Hydraulic Boundary Conditions for 2-D Models

The calculated offshore wave characteristics, the assumed water levels and the digitized 1-D depth contours were used in SWAN 1-D for different angles of wave approach to calculate the near-shore wave conditions at the boundary of a smaller 2-D grid for the case study. The SWAN 1-D model was instructed to use the default JONSWAP spectrum which was considered sufficiently accurate. The waves at the boundary of the 2-D grid were propagated further inland to calculate the wave heights at the boundary for the generic model which lay closer to the shore. Two cases were investigated in terms of water depths. In the first case, wave transformations were computed for the given offshore wave heights for a normal high tide of 3.3 m and a wind speed of 10 m/s. However, the worst case scenario in case of cyclones would be the occurrence of a storm surge along with high tide. Due to the inability of SWAN 1-D to predict water level setup due to wind, another case was used where a constant water depth equal to the sum of the near-shore storm surge and high tide was assumed throughout. Wave characteristics were then calculated for these depths. It was decided to use the results from the second case as they are more realistic.

#### ***3.3.1. Wave Transformation***

Cyclones in the region show an anti-clockwise circulation pattern due to Coriolis' forces that is in keeping with the expected circulation pattern in the Northern Hemisphere. Also statistics showed that most cyclones in the region have either a south – north or southwest – northeast orientation, seen in Figure 22. For the former, the majority of the highest waves could be expected from an angle of about  $90^\circ$  while for the latter, the angle of attack of the highest waves could be anywhere within a sector  $22.5^\circ$  to  $157.5^\circ$  to the coast depending on whether the cyclone track crosses the island to the north or south. The predominant angle of wave attack under normal conditions was seen to be at angles greater than  $45^\circ$  to the coast in the offshore regions.

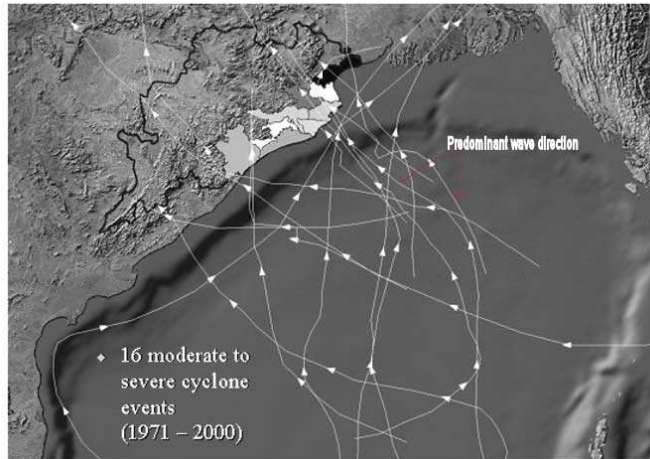


**Figure 22: Historic cyclone tracks (Chittibabu et al. 2004) with predominant wave direction during normal conditions indicated in red**

Wave height transformations were calculated for five different return periods – 100, 50, 25, 10 and 5 years using the SWAN 1-D model. Due to the symmetry of the supposed bathymetry it was observed that the wave heights for  $22.5^\circ$  and  $157.5^\circ$  and similarly for  $45^\circ$  and  $135^\circ$  were nearly the same. Wave conditions were therefore calculated for the angles –  $22.5^\circ$ ,  $45^\circ$  and  $90^\circ$  and the average of the wave heights for these angles, at the desired depth contour, was used as the boundary condition all along the eastern (seaward) boundary of the 2-D grid. The averaged wave height value for the three angles and the depth for a return period of 50 years are shown in Figure 23 below. This figure illustrates the manner of wave transformation from deep to shallow water in the region.

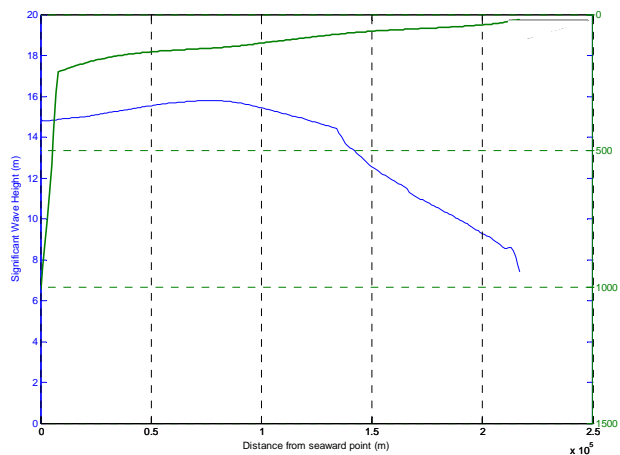


**Figure 23: Water depth and wave height transformation from deep to shallow water (for RP = 50 years,  $H_o = 8.4$  m,  $T_p = 18$  s and storm surge = 10 m)**

### 3.3.2. Determination of Water Level at Near-shore Boundary

The total water level at the boundaries of the 2-D models, designated Extreme Instantaneous Water Level (EIWL) for a particular return period was determined using the formula,

$$EIWL = Storm\ Surge + Tide\ (above\ CD) + SLR \quad (5)$$

An average spring high tide of 3.3 m above *CD* (Chittibabu et al., 2004) was used for the calculation of the EIWLs. Storm surge values for the near-shore region were taken from sub-section 3.1.5. Sea Level Rise was assumed as an average 5 mm / year (Aggarwal & Lal, 2000) and calculated for a total of 80 years for all cases.

### 3.3.3. Conclusions

The final average wave characteristics and water depths relative to *CD* calculated at the -11 m contour are shown for two cases – one with only high tide and the other with storm surge and SLR – in Table 3. A graph of the variation of wave heights and wave periods at the -11 m contour with return periods for the second case is shown in Figure 24.

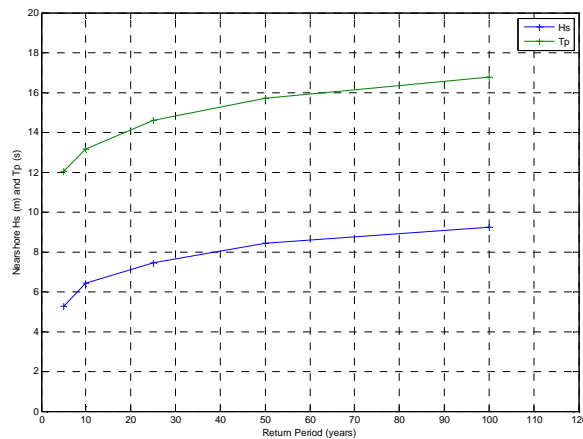


**Figure 24: Graph of significant wave heights and wave periods at -11 m contour vs. the return period in years under storm surge conditions**

Since the focus of the study is on wave attenuations during extreme events and due to the incapability of SWAN to predict water level setup due to wind, the wave heights used in the 2-D models were the ones calculated using the predicted storm surge levels. The boundary wave heights for the generic 2-D model at the +3 m contour, for the various return periods were calculated based on the conditions obtained at the -11 m contour

using a similar procedure. These results are shown in Table 4. The wave periods and water levels were assumed to be the same as at the -11 m contour.

**Table 3: Wave statistics and water levels at -11 m depth (relative to CD) for different return periods**

Return Period (years)	Original Depth (m)	With only tide		With Storm Surge, Tide and SLR		Wave Period ( $T_p$ )
		Average $H_s$ (m)	Average Depth (m)	Average $H_s$ with SS (m)	Average Depth with SS (m)	
100	11.0	6.51	14.4	9.25	23.6	17
50	11.0	5.95	14.4	8.42	22.3	16
25	11.0	5.37	14.3	7.44	21.0	15
10	11.0	4.88	14.3	6.43	19.4	13
5	11.0	4.03	14.3	5.28	18.1	12

**Table 4: Boundary Wave Conditions for Generic 2-D Model (+3 m contour relative to CD)**

S. No	Return Period (yrs)	Significant Wave Height, $H_s$ (m)	Peak Period, $T_p$ (s)
1.	100	4.76	17
2.	50	4.27	16
3.	25	3.74	15
4.	10	3.05	13
5.	5	2.50	12

### 3.4. Vegetation Parameter Analysis

For the vegetation species decided upon in sub-section 2.4.3 the value range and control values of vegetation parameters were determined based on literature as well as communication with experts in the field (Dr. W.N.J Ursem). The control values for all parameters were taken as the average of the given value range with some exceptions. The height ranges for both *R. mucronata* and *S. alba* were chosen within realistic values such that they were distributed across the different EIWLs calculated in sub-section 3.3.3. The stem heights for both species were assumed to vary between 6 and 7 m. This assumption was checked with the fact that the canopy of a mangrove tree usually remains above MHWL under normal conditions (Mazda et al., 2007). The heights of the *S. alba* pneumatophores are controlled mainly by tidal levels. Therefore these were calculated based on the average depth of spring tidal inundation. Thus, with an assumed topography of 3 m and an average spring tidal height of 3.3 m, the range of pneumatophore heights was assumed as 0.3 to 0.8 m with a control value of 0.5 m. Further, due to the increased strength of its root system it was assumed that *R. mucronata* would occur on the fringes of the island. Details of the calculated EIWLs and the assumed vegetation heights are given in Figure 25. Finally due to lack of data, values for the canopies were assumed arbitrarily based on the characteristics of a typical mangrove tree. The selected parameters are shown in Table 5 and Table 6 for the species *Sonneratia alba* and *Rhizophora mucronata* respectively.

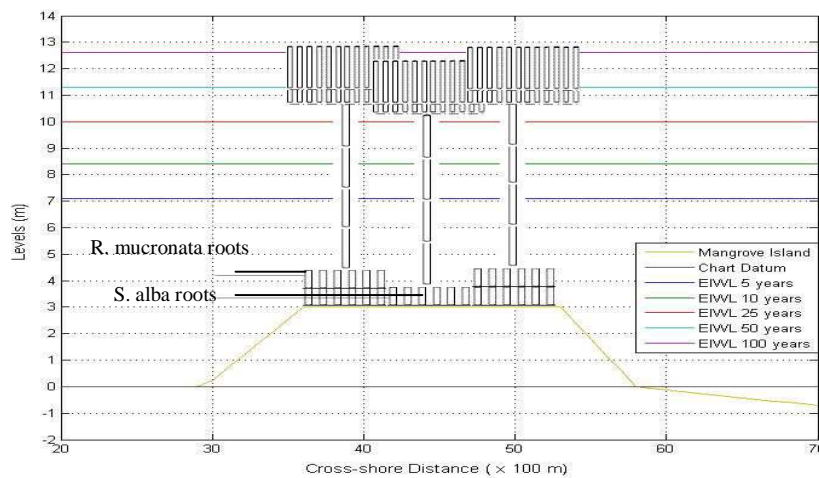


**Figure 25: Details of calculated bathymetry, EIWLs ( measured with respect to CD) and schematized vegetation heights**

**Table 5: Species – *S. alba* (Fig 2: Extreme right; Fig 3: Extreme Left) (compiled from Sun Q, et al., 2004, Hossein M.K. et al., 2003, Aluka Webpage (online), 2006-2008, Azote 2008 (online), Flowers of India (online), n.d., Dr. W.N.J. Ursem, 2009)**

Parameter	Value Range	Control Value
1. Stem Diameter (DBH)	0.2 – 0.5 m	0.3 m
2. Pneumatophore Diameter	0 – 0.04 m	0.02 m
3. Canopy Diameter	0.02 – 1 m	0.5 m
4. Stem Density	0.5 – 1.7 m <sup>-2</sup> *	0.7 m <sup>-2</sup>
5. Pneumatophore Density	4 – 100 m <sup>-2</sup>	50 m <sup>-2</sup>
6. Canopy Density	1 – 100 m <sup>-2</sup>	100 m <sup>-2</sup>
7. Stem Height	3 – 15 m	6 m <sup>+</sup>
8. Pneumatophore Height	0.3 – 0.8 m	0.5 m
9. Canopy Height	0.2 – 3 m	2 m

\* Estimated from overall density of species in nearby forest block (from Mishra P.K. et al., 2005)

**Table 6: Species – *R. mucronata* (Fig 2: middle; Fig 3: extreme right) (compiled from Hossein M.K. et al., 2003, Aluka Webpage (online), 2006-2008, Azote 2008 (online), Duke N.C., 2006, Dr. W.N.J. Ursem, 2009)**

Parameter	Value Range	Control Value
1. Stem Diameter (DBH)	0.15 – 0.4 m	0.25 m
2. Root Diameter	0.05 – 0.1 m	0.075 m
3. Canopy Diameter	0.02 – 1 m	0.5 m
4. Stem Density	0.5 – 1.7	0.7
5. Root Density	1 – 130 m <sup>-2</sup>	60 m <sup>-2</sup>
6. Canopy Density	1 – 100 m <sup>-2</sup>	100 m <sup>-2</sup>
7. Stem Height	5 – 8 m	6 m <sup>+</sup>
8. Root Height	0 – 1 m	0.8 m
9. Canopy Height	0.2 – 3 m	2 m

## 4 Generic Modeling Studies

### 4.1. Model Considerations for Parameter Formulation

The SWAN 40.55MOD model is used in this study. This is an improved version of SWAN 40.55 which in turn was a product of modifications by Burger (2005) that enable calculation of wave dissipation due to rigid vegetation. A detailed description of the model formulations is given in Appendix A. In summary, the time averaged rate of energy dissipation per horizontal area due to vegetation in SWAN 40.55MOD is first obtained by integrating the drag force over the height of a cylindrical vegetation unit using the basic Dalrymple formulation. This is linearised in terms of the wave energy,  $E$  so that it can be implemented as a dissipation term in the model. This is done by recasting the wave height term in the original Dalrymple formulation as a function of the spectral energy (refer Appendix A) (Tomohiro Suzuki, Personal Communication and Burger, 2005).

$$\varepsilon_v = \frac{2}{3\pi} \rho C_D b_v N \left( \frac{gk}{2\sigma} \right)^3 \frac{\sinh^3 k\alpha h + 3 \sinh k\alpha h}{3k \cosh^3 kh} H^3 \quad (6)$$

In the SWAN 40.55MOD version the vegetation parameters,  $C_D$ ,  $b_v$  and  $N$  are lumped together for modeling purposes into a single ‘vegetation factor’ (VF) for each layer. These vegetation factors are then averaged, weighted based on the height of each layer. The final depth averaged vegetation factor is then used in the Dalrymple formulation to calculate the rate of vegetation induced energy dissipation. Also, the parameter  $\alpha h$  is calculated using the total height of the vegetation. Therefore the effect of individual vegetation layer properties is limited to the calculation of the depth-averaged vegetation factor. The lumped vegetation factor values are multiplied by values specified in a vegetation density file at each grid point. This enables horizontal variation of the vegetation densities if necessary, though only as relative factors. The basic schematization in the Dalrymple formulation is shown in Figure 26 below. The effect of the variable hydraulic parameters as seen from Equation (6) is determined by the behaviour of the parameters  $k$ ,  $\sigma$ ,  $h$  and  $H$ .

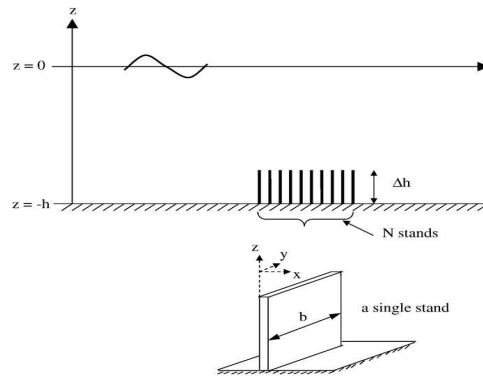


**Figure 26: Vegetation and water levels schematised based on the Dalrymple formulation (Myrhaug, et al., 2009)**

It was felt that for the generic modeling studies a simplification of the bathymetry and parameters was needed to allow comparative analyses and in-depth studies. On the other hand, due to the intrinsic lumping of parameters by the model too much simplification of the variable parameters would not serve the purpose of this study. Since the primary interest lay in studying the behaviour of a real mangrove system to extreme situations it was decided to use moderately simplified bathymetry and parameters for the preliminary generic analysis. In case the preliminary sensitivity analysis revealed certain aspects of the system or the model that warranted more in-depth examination the parameters could be simplified further on a case-by-case basis. From the preliminary analysis conclusions would also be reached on the desirable extent of simplification and the specific parameter values to be used in the case study. Parameter formulation for the preliminary analysis is described in detail in sub-section 4.4.1 while the formulation of parameters for the secondary analyses and the case study are dealt with in sections 4.5 and 5.2 respectively.

## 4.2. 2-D Generic Model Setup

The wave heights and water levels at the boundary of the generic grid for different return periods were estimated as described in Section 3.1. The island was assumed to be flat throughout to reduce the number of variables in the model, enabling a more effective study of the influence of vegetation. However it was given a constant height of 3 m based on the actual bathymetry in the region to allow the use of realistic boundary conditions. This resulted in effective water depths ( $h$ ) 3 metres lower than the calculated water levels. The grid was stretched lengthwise and given an aspect ratio of 1:7 to eliminate the 'spreading effect' across the central band of interest (refer Appendix D). The modeled grid is therefore 40 km by 6 km as shown in Figure 27. Finally the mangrove patch was introduced in the centre of the island as a square of 4 km by 4 km. The cross-shore width of the island was increased for the generic studies so that the effect of mangroves on wave attenuation could be studied over a larger distance. A gap of 2 km was provided between the vegetation boundary and the grid's seaward boundary to allow the model to adjust to local conditions before encountering vegetation. The input and computational grids were given a resolution of 100 m by 100 m which was felt to provide an appropriate balance between computational accuracy and computing time.

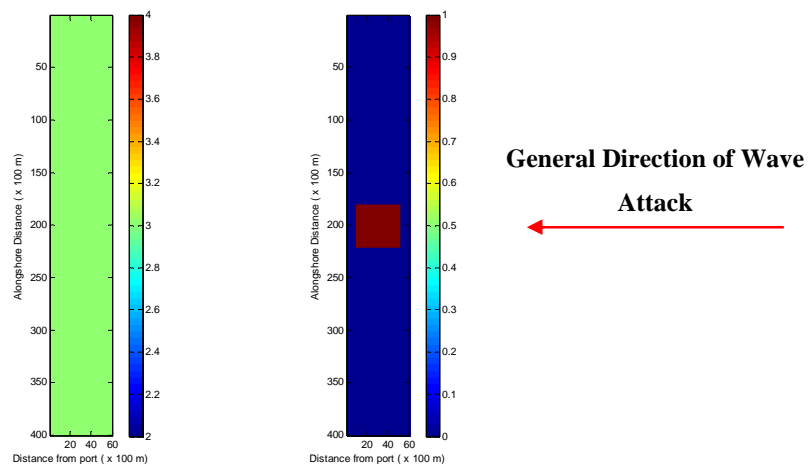


**Figure 27: Bathymetry (left) and Vegetation Density (right) grids for Generic Modeling Studies with angle of wave attack indicated**

### 4.3. General Process for Sensitivity Analyses

The generic sensitivity analysis was divided into two parts, both involving modeling different combinations of the chosen parameters in the SWAN 40.55MOD model and analyzing the resultant outputs.

A preliminary sensitivity analysis was first carried out with parameters that were as close to the actual situation as possible. The parameters to be varied in this study included three vegetation factor cases, two vegetation height cases and three cases each of three hydraulic parameters – wave heights ( $H_s$ ), effective water depths ( $h$ ) and wave periods ( $T_p$ ). The scenarios are shown in Table 7 below. The aims of this analysis were to understand the behaviour of the system and the manner in which it was modeled by the program and also to help reduce the number of parameters for the case study. Additionally, simplified secondary analyses were carried out to examine in detail a few interesting phenomena revealed in the preliminary analysis.

**Table 7: Parameters varied for Generic Model Runs**

<b>Vegetation Factors</b>	<b>Vegetation Height</b>	<b>Hydraulic Parameters – <math>H_s, T_p, h</math></b>
Low	Emergent	RP 100
Medium		RP 25
High	Submergent	RP 5

While the main difference between the two analyses lay in the selection of parameters and the manner of their variation (refer Sub-section 4.4.1), the basic process followed was essentially the same – each parameter was varied in turn while keeping the other parameters constant resulting in a number of different scenarios. The basic steps followed in the preliminary analysis are detailed below:

#### ***4.3.1. Modeling Parameter Combinations***

The model was first tested with only the bathymetry to ensure that the grids were setup properly after which the square vegetation patch was introduced in the centre. Three vegetation factor scenarios, two vegetation height scenarios and three hydraulic

parameter values were combined to produce different simulation scenarios. The different scenarios were simulated with the SWAN 40.55MOD program. The program was instructed to use the default JONSWAP spectrum for wave spectrum generation at the seaward boundary. The output was in the form of a resultant significant wave height at each grid point.

#### ***4.3.2. Analysis of Resultant Outputs***

To avoid the spreading effect (refer Appendix D), the transmitted wave heights were analysed along the centre-line of the grid alone. The transmitted wave heights were analysed under different groupings depending on the input parameters being varied. Thus, transmitted wave heights for a given hydraulic parameter were analysed at different vegetation densities and heights and vice versa. The rate of wave attenuation through the mangrove forest was quantified using the wave reduction factor,  $r$ , defined by Burger (2005) shown in Equation (7). This factor was chosen since it is thought to give a good insight into the rate at which wave attenuation varies across the width of the mangrove forest. This in turn could be linked directly to the effectiveness of the forest in attenuating waves.

$$r = (H_{in} - H_{trans}) / H_{in} \quad (7)$$

Wave reduction factors from different cases were compared with each other to give an understanding of the relative importance of different hydraulic and vegetation parameters to the wave attenuation process. All the comparisons were summarised in groups of results described in sub-section 4.4.2.

## 4.4. Preliminary Sensitivity Analysis

### ***4.4.1. Parameter Formulation***

The preliminary analysis was intended as a partially generic study to understand the effect of changes in various parameters on transmitted wave heights for actual extreme conditions and to establish the relative importance, if any, of these parameters. The analysis was conducted in terms of some significant controlling parameters that were chosen based on the behaviour of similar systems in reality and additionally on how this behaviour was modeled in the SWAN 40.55MOD program. These were broadly classified as vegetation and hydraulic parameters, each of them consisting of sub-classes. Each parameter was varied in turn while keeping the others constant at suitable values. The following sections describe in brief the chosen parameters and how they were varied with respect to each other.

During a cyclone it is highly probable that the island stays inundated for more than 24 hours apart from being exposed to severe wave conditions. The species *R. mucronata* is seen to be more resilient to continued inundation and extreme wave conditions compared to *S. alba*. This could be due to the increased height and structural strength of its roots. Based on this reasoning and with the aim of simplifying the generic analyses, a single mangrove species – *R. mucronata* was considered in the calculations. The vegetation was assumed to be uniform all over the island. Since the calculated vegetation factor is multiplied with the value in the vegetation density file for each grid point (refer Section 4.1), it was sufficient to specify actual vegetation density values within the vegetation factor and assume a value of 1 in the vegetation density file at all grid points.

#### **4.4.1.1. Vegetation Parameters**

The vegetation parameters were divided into two sub-classes based on the manner in which they are used by the SWAN model – Vegetation Factors and Vegetation Heights. The manner in which they were formulated is described below.

## Vegetation Factor

Since the model lumps together the products of diameter, density and drag coefficient of each vegetation layer into a single ‘Vegetation Factor’ in its calculations, it was decided to do the same with the parameters. The ‘Vegetation Factor’ is defined as the product of the diameter, density and assumed drag coefficient of the roots, stem and canopy. First the range of vegetation factor values that each layer could take was determined from literature. Ideally field data for the vegetation diameter and density would be obtained for the three layers and this would be used in conjunction with preliminary model runs and further field data to calibrate the drag coefficients. In this study however, in the absence of relevant field measurements, the parameter value ranges were estimated from literature studies as detailed in Section 3.4 and Table 6

The Reynold’s number for water flow within a mangrove vegetation patch is typically of the order of  $1 \times 10^5$  under the given extreme conditions. Though such highly turbulent flow within a mangrove system could affect the results in reality, in this study these factors are not considered for the sake of simplicity. In this case the Reynold’s number lies within the range ‘B’ on the graph shown in Figure 28 below for which the value of the drag coefficient is approximately unity. The drag coefficient was therefore simply assumed to be 1 for all the layers.

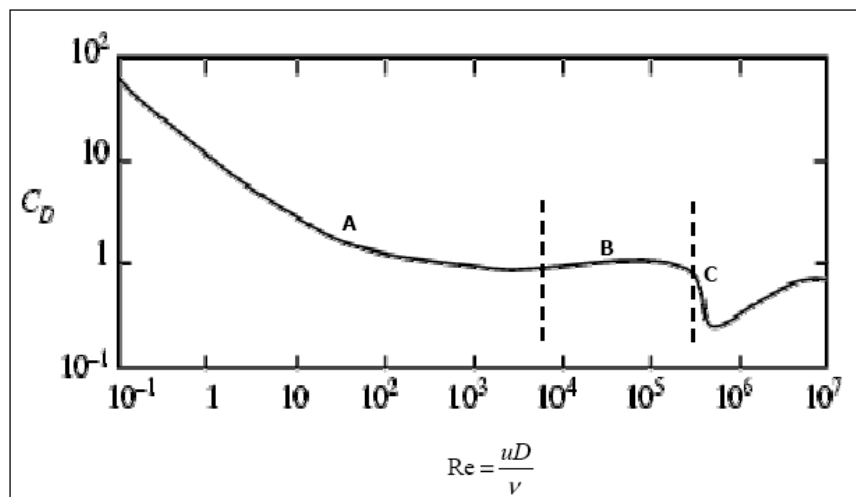


Figure 28: Relation between  $C_d$  and Reynold's Number (Battjes, 1999 from Burger B., 2005)

However, each layer had specific ranges within which its diameter and density could vary (refer Table 6). The manner in which these values could be combined was assumed

arbitrarily based on the nature of a typical mangrove patch. The calculated vegetation factors were thus in the form of low and high values for each layer. However, these ranges are not of the same size. Values of the vegetation factor ratio (VFR) – defined as the ratio between high and low vegetation factors – were calculated to indicate the extent of variation in each layer. This is illustrated in Table 8.

**Table 8: Range of realistic vegetation parameter values (lowest VFR value corresponding to stem layer in bold)**

Layer	Diameter Range (m)	Density Range (n/m <sup>2</sup> )	Drag Coefficient	Approximate Vegetation Factor Range	Vegetation Factor Ratio (VFR)
Roots	0.05 – 1	1 – 130	1	0.05 – 6.5	130
Stem	0.15 – 0.35	0.5 – 1.7	1	0.075 – 0.6	<b>8</b>
Canopy	0.02 – 0.1	1 – 100	1	0.1 – 2	20

For the study, vegetation factors for the three layers were all varied at once, in three scenarios – ‘LOW’, ‘MEDIUM’ and ‘HIGH’. Each scenario therefore assumed a set of values for the vegetation factors of the roots, stem and the canopy. This decision was based on the fact that the program performed a depth averaging of all the layers, weighted based on their heights, before applying the Dalrymple formulation. Therefore, modeling different value combinations between the three layers would not contribute much to the understanding of their sensitivities. To keep the values as realistic as possible the ‘LOW’ factors were assumed directly from literature. To ensure uniformity in variation the ‘LOW’ factors for all three layers were multiplied by two constants – one for the ‘MEDIUM’ and one for the ‘HIGH’ scenario. From Table 8 it is seen that in reality the stem shows the least variation between low and high factors since it has the lowest VFR. To ensure that the ‘HIGH’ factors for the stem do not fall outside the determined realistic range, this VFR value was chosen as the constant for all three layers. The ‘HIGH’ factors for root, stem and canopy were thus obtained by multiplying the respective ‘LOW’ factors by 8. The ‘MEDIUM’ factors, assumed to lie exactly in the middle, were obtained by multiplying the ‘LOW’ factors by 4. The resulting vegetation factors are given in Table 9 below. Extra simulations with different vegetation factors were run whenever highlighting of a particular trend was necessary.

**Table 9: Modeled Vegetation Factor Values for ‘LOW’, ‘MEDIUM’ and ‘HIGH’ scenarios**

<b>Layer</b>	<b>Low</b>	<b>Medium (Low x 4)</b>	<b>High (Low x 8)</b>
Roots	0.05	0.2	0.4
Stem	0.075	0.3	0.6
Canopy	0.1	0.4	0.8

**Vegetation Height**

In reality the height of each vegetation layer would be very important in determining the overall drag induced by that layer. However, since the model considers an overall depth averaged vegetation factor weighted on the basis of the heights of each layer, the vegetation heights were considered simply in the form of two cases – one combination that would render the entire vegetation emergent under all the chosen water depths – called ‘Emergent Vegetation’ and one that would render it submergent under one water depth– called ‘Submergent Vegetation.’ This distinction was made since the difference between emergent and submergent vegetation was thought to be important with regard to the attenuation of incoming waves. The two height cases are shown in Table 10.

**Table 10: Modeled Vegetation Height values for emergent and submergent scenarios**

<b>Layer</b>	<b>Vegetation Height (m)</b>	
	<b>Emergent</b>	<b>Submergent</b>
Roots	1	0.5
Stem	7	5
Canopy	2	0.5

**4.4.1.2. Hydraulic Parameters**

The controlling hydraulic parameters are the wave heights, effective water depths and wave periods. The wave conditions at the boundary of the generic model were determined as described in Section 3.1. For the major part of the analysis each parameter was varied in turn keeping the other parameters constant at suitable values. Since the generic sensitivity analyses were primarily meant to understand the effect of mangroves during extreme events, actual values were used for the hydraulic parameters. To reduce the number of simulations however only the values calculated for return periods of 100,

25 and 5 years were used. Variation in the angle of wave attack was not considered relevant for the generic sensitivity analyses since this part of the study focused on the relationship between linear vegetation width and transmitted wave heights for a variation in parameters. The angle of wave attack was therefore kept constant at 90° for all sensitivity analyses. The constant values were chosen differently for each hydraulic parameter within the realistic range of values calculated in Section 3.2 while taking care to provide the minimum necessary depth to avoid depth-induced breaking during simulation. The constant and variable hydraulic parameter values are given in Table 11. In this table, the actual water levels are presented as water depths, after subtracting the height of the island (3 metres). Though the island has a varying bathymetry, it is to be noted that the entire vegetation was assumed to exist on its surface at a 3 m elevation for simplicity.

**Table 11: Modeled Hydraulic Parameter Values for Primary Sensitivity Analysis (varied values in bold)**

Variation in	Chosen Constant Values of		
	Wave Height (m)	Water Depth (m)	Wave Period (s)
Wave Height	<b>4.76, 3.74, 2.5</b>	9.6	15
Water Level	2.5	<b>9.6, 7, 4.1</b>	12
Wave Period	3.74	7	<b>17, 15, 12</b>

The vegetation and bathymetry grids as described in Section 4.2 with a constant angle of wave attack are indicated below in Figure 29.

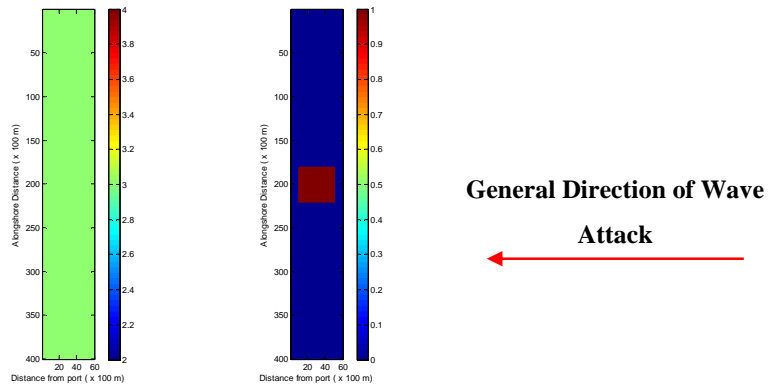


**Figure 29: Bathymetry (left) and Vegetation Density (right) grids for Generic Modeling Studies with angle of wave attack indicated**

#### ***4.4.2. Results and Conclusions***

The SWAN 40.55MOD model was run for various scenarios using the parameter values obtained in Section 4.4 and the obtained transmitted wave heights were analysed in detail as described above in Section 4.3. First some results were obtained that could be divided depending on the parameter being varied. Further, some results observed to be common for a set of parameters were also got that are presented under the title “General Results”. Finally, based on the results conclusions were drawn regarding the system characteristics and the selection of scenarios for further simulations. These results and conclusions are described in detail in the sections below.

##### **4.4.2.1. Modeling Results**

###### **Vegetation Factor Variations**

Some of the results obtained from the variation of vegetation parameters such as vegetation factor and height, for given hydraulic parameters are described below:

1. The model shows an expected overall increase in sharpness of wave attenuation from low density to high density as seen in Figure 30.

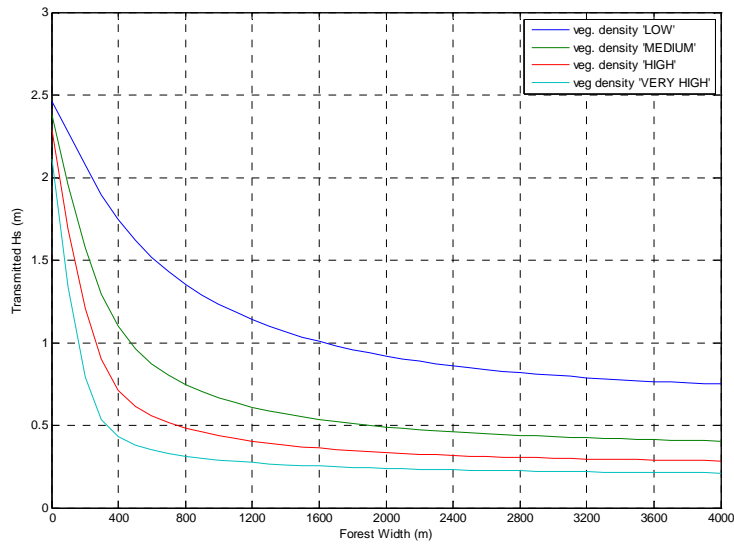


**Figure 30: Transmitted wave heights across forest width for varying vegetation density values and fixed hydraulic parameters ( $h=9.6\text{m}$ ,  $H_s=2.5\text{m}$ ,  $T_p=15\text{s}$ )**

2. Due to the cubic dependence on wave height, the rate of wave attenuation seems to become negligible after some distance.
3. As seen in Figure 31 the difference between the effects of higher and lower input waves at any specific point within the vegetation reduces with an increase in the overall vegetation factor becoming nearly constant for all the input wave heights at very high vegetation factors.

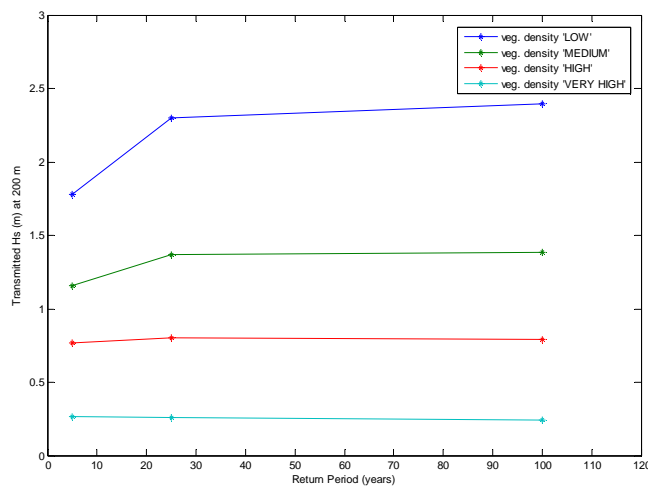


**Figure 31: Transmitted wave heights at 200 m forest width for different vegetation factor values and different input wave heights for increasing return periods (constant  $h = 9.6\text{ m}$  and  $T_p = 15\text{ s}$ )**

- For a given water depth of 7 m, wave height of 2.5 m and peak period of 12 s the wave heights at 4000 m vary between 45 cm and 11 cm for ‘Low,’ and ‘High’ vegetation factors. This corresponds to around 18% to 4% of the initial wave heights.
- An analysis of an extremely high, depth averaged overall vegetation factor of 100 for a water depth of 9.6 m, boundary wave height of 3.74 m and a peak period of 15 s showed a very quick attenuation within 200 m to a value of 4 cm (1%) beyond which there is no reduction throughout.

### Vegetation Height Variations

- This analysis seemed to indicate that a situation with emergent mangroves causes greater wave attenuation.

### Hydraulic Parameter Variations

#### Wave Heights

- Due to the cubic dependency of the Dalrymple formulation on wave heights the expected trend of sharper attenuation with increase in input wave heights was observed though the differences between the transmitted wave heights become very small beyond a point, shown in Figure 32
- The wave heights at 4000 m for varying input wave heights, constant (LOW) vegetation factor values, constant water depth of 9.6 m and a constant peak period of 15 s range between 44 and 23 cm, equal to approximately 10% of the original wave height.

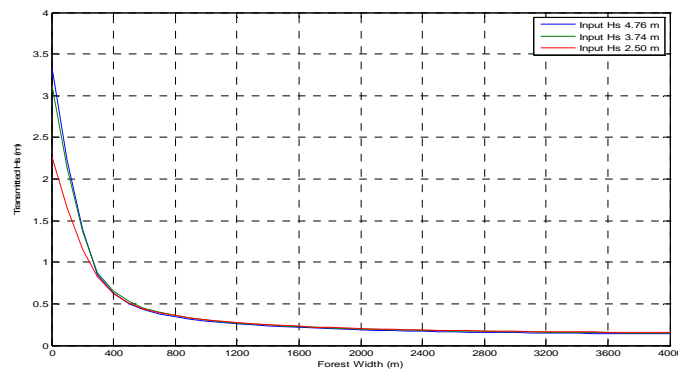


**Figure 32: Transmitted wave heights across the forest for different input wave heights at constant (MEDIUM) vegetation factor values (constant  $h = 9.6$  m and  $T_p = 15$  s)**

### Water Depths

1. Wave attenuation shows an increasing trend with decreasing water depths as expected.
2. The ratio of the wave reduction factors between water depths 4.1 m and 9.6 m shows a slight increasing trend further inland seeming to suggest that at increasing forest widths lower water levels have a relatively higher attenuation effect than higher water levels. This is illustrated in Figure 33. This result however is affected by variations in effective vegetation densities between the two cases.
3. For varying water depths with a constant boundary wave height of 2.5 m and peak period of 12 s the wave heights at 4000 m vary between 75 and 21 cm corresponding to around 30% and 8% respectively of the original wave height.

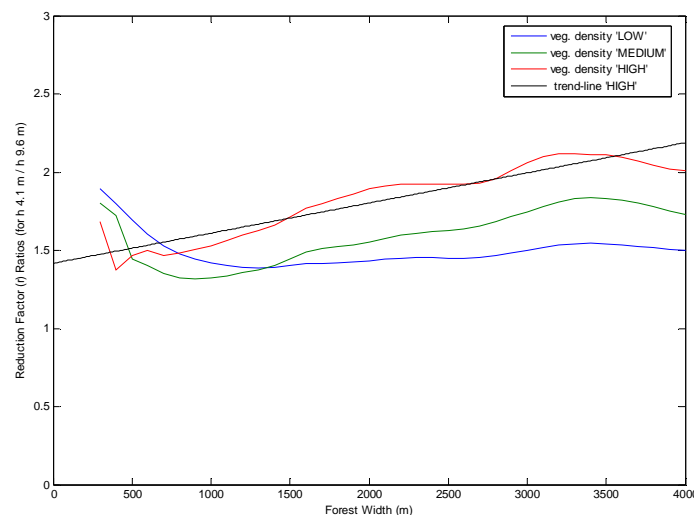


**Figure 33: Reduction factor (r) ratios vs. forest width for h 4.1 m / h 9.6 m for increasing vegetation densities (constant  $H_s = 2.5$  m and  $T_p = 15$  s)**

### Wave Periods

1. Figure 34 shows that longer waves show slightly sharper attenuation than shorter waves for a given vegetation density.
2. The sensitivity to a change in wave period for a given density was observed to be less than that of wave heights or water levels. This can also be seen from Figure 35.

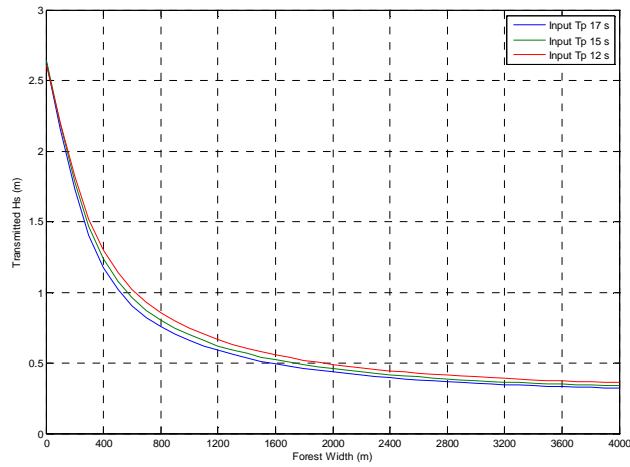


**Figure 34: Transmitted wave heights across forest width at constant (LOW) vegetation factor values for different wave periods (constant  $h = 7$  m and  $H_s = 3.74$  m)**

### Some General Results

1. An increase in vegetation factor values was seen to cause a reduction in sensitivity to hydraulic parameter variations at a particular point within the forest. This is shown in Figure 35.

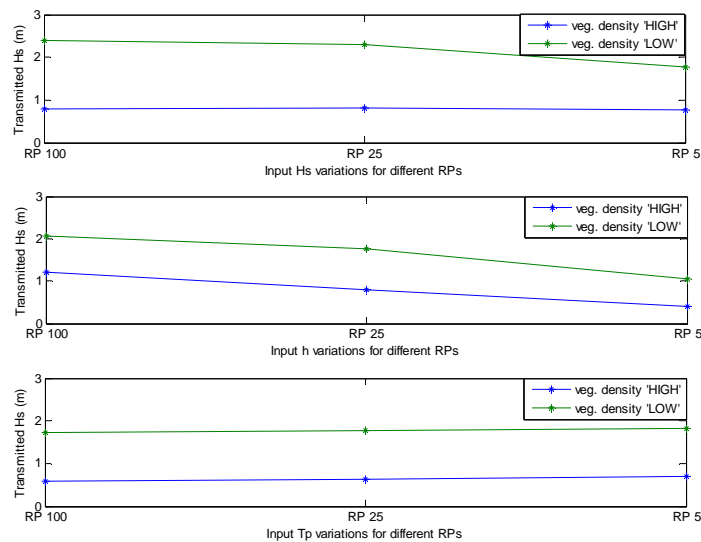


**Figure 35: Transmitted wave heights at 200 m forest width for different values of  $H_s$ ,  $h$  and  $T_p$  for return periods of 100, 25 and 5 years and different (LOW and HIGH) vegetation factors**

2. A sharp peak in the reduction factor was observed between 100 m and 400 m forest widths. The peaks of the reduction factor show a narrowing and a slight

shift inland with an increase in the vegetation factors and/or hydraulic parameters illustrated in Figure 36.

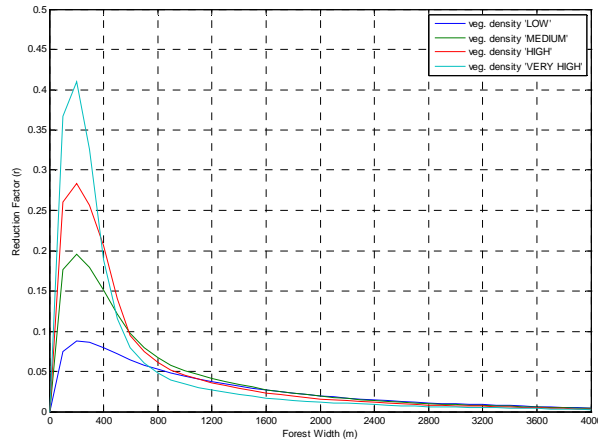


**Figure 36: Variation in reduction factor ( $r$ ) across forest width for different vegetation factor values at constant hydraulic parameter values**

3. Preliminary analysis indicated that the sensitivities of hydraulic parameters in terms of the rate of wave attenuation for constant vegetation parameters show a particular trend. However the values of the constant parameters differed for each hydraulic variation case. Also it was thought that the difference between emergent and submergent vegetation might play a significant role. This result would therefore need to be examined in detail, separating the effect of emergent and submergent vegetation.

#### 4.4.2.2. Conclusions

##### Regarding System Behaviour

1. The peaks in the reduction factors can not be fully explained by the cubic dependency of the formulation on wave heights. This behaviour is similar to that observed in a study on the salt marshes of New Orleans (Vosse, 2008) where it was found that wave reduction is sharper at the edge of the marsh. It is felt that the suddenness of the vegetation's influence and possibly the numerics of the SWAN model both contribute to the formation of the peak between 100 m and 400 m forest widths though this is not an intended feature of this model.

2. The analysis of hydraulic parameters at specific points along the forest width showed that at very high vegetation factors differences in parameter variations become negligible. Also the wave attenuation curve due to medium density vegetation was seen to lie in between the low and high density vegetation curves, as was expected.
3. The difference between emergent and submergent cases, though not very high, was thought to be an important feature of the system's behaviour. A detailed examination with more simplified parameters would be necessary to establish the characteristics of this distinction.
4. The effect of variations in water levels and wave heights were seen to be more important than variations in wave period under the given conditions. Here also an in-depth investigation would be necessary to verify this difference in sensitivities.

#### **4.4.2.3. Regarding Further Simulations**

1. The width range of 100 m to 400 m could be considered as a possible 'critical width' for further simulations under similar conditions. Wave height attenuation within these points could be given special attention.
2. The vegetation factors in the case study could be limited to two scenarios – 'LOW' and 'HIGH'. These could be modified based on the literature studies and vegetation analysis so that the values are more representative of the region.
3. The regularity of behaviour with hydraulic parameters for decreasing return periods validated the decision to use only three of the five return period events calculated. Further simulations could therefore remain limited to 100, 25 and 5 year events. Also, the hydraulic parameters to be varied could be limited to wave heights and water levels.
4. It was decided to ignore the variation between emergent and submergent cases as it was felt that the differences between the two were too small to be of importance in the case study.
5. The chosen grid aspect ratio of 1:7 was seen to provide sufficiently accurate wave heights across the central band of interest.

## 4.5. Secondary Sensitivity Analyses

As described in Section 4.4 above, the preliminary sensitivity analysis indicated a trend in sensitivities to hydraulic parameter variations. However, since the preliminary analysis used different values for the constants in each scenario a further simplified study was needed with common constant values for all scenarios in order to establish this trend. Due to the importance of hydraulic parameters in this particular study it was decided to examine and establish the indicated trend with a simplified secondary sensitivity analysis. Also interesting to note was the difference between emergent and submergent vegetation for constant hydraulic parameters and identical overall vegetation factors. A second simplified analysis was therefore conducted to study this phenomenon in detail. The procedure followed in these analyses was basically the same as that used in the previous analysis. The main differences lay in the number of parameters being varied and the nature of their variation. For both analyses, it was considered important to keep the number of variables to a minimum as this was not feasible in the primary analysis.

Here again the angle of wave attack was kept constant at  $90^\circ$ . Since the wave reduction factor,  $r$ , defined earlier (Section 4.3) was felt to be a convenient and effective tool to study the rate of wave attenuation it was used in these analyses as well. Since all the parameters were varied by a constant factor, the ratio of their reduction factors was also studied to help draw conclusions about the effect of this variation. The following sections describe the selection of parameter values and combinations for the two secondary analyses and the results and conclusions drawn from them.

### ***4.5.1. Sensitivity Trend of Hydraulic Parameters***

#### **4.5.1.1. Parameter Formulation**

Since this analysis focused on hydraulic parameters the vegetation parameters were kept constant. Emergent vegetation of a constant height of 10 m and medium vegetation factors was assumed. The three hydraulic parameters wave height, wave period and water depth were varied once each, by multiplication by a factor of 1.5 with the other two constant. Similar to the previous analyses the values were selected to avoid depth-induced breaking. The parameter variations are detailed in Table 12 below. Here again

the water levels are presented as water depths after subtracting the height of the flat island (3 meters).

**Table 12: Modeled Hydraulic Parameter Values for Secondary Sensitivity Analysis (varied values in bold)**

Variation in	Chosen Constant Values of		
	Wave Height (m)	Water Depth (m)	Wave Period (s)
Wave Height	<b>2, 3</b>	7	12
Water Level	2	<b>7, 10.5</b>	12
Wave Period	2	7	<b>12, 18</b>

#### 4.5.1.2. Conclusions

For purposes of analysis ratios  $R_h$ ,  $R_{H_s}$ , and  $R_{T_p}$  were defined as the ratio of wave reduction factors between high and low values of water depths, wave heights and wave periods respectively. This was thought to be an effective indicator of the behaviour of the parameters since each parameter had been varied by a constant factor. Though the reduction factor values for all parameters remain close to 1 the analysis indicated a higher overall sensitivity to wave height variations. Within the critical width region and slightly beyond there is a sensitivity trend with values of  $R_{H_s} > R_h > R_{T_p}$ . Further within the forest however there seems to be an increase in sensitivity to wave height and wave period variations and a slight decrease in the sensitivity to water depth variations. This is indicated below in Figure 37.

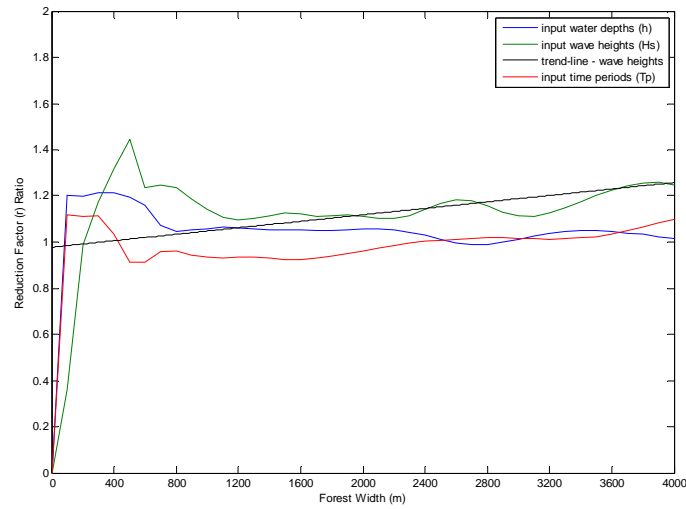


**Figure 37: Reduction Factor (r) ratios for water depth (h), wave height ( $H_s$ ) and wave period ( $T_p$ ) variations across mangrove forest width for constant vegetation factors**

Additionally, a lateral shifting tendency in the peaks of the reduction factor ratios was observed. This tendency follows the same trend as above, being most sensitive to wave height variations followed by water depth variations with a negligible effect due to variations in wave period. This is illustrated in Figure 38 below.

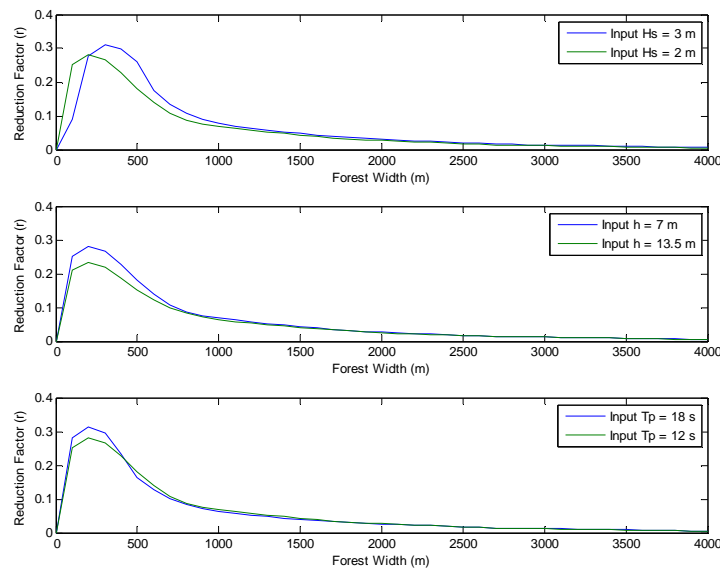


**Figure 38: Variation in reduction factor for an increase in hydraulic parameter values ( $H_s$ , h and  $T_p$ ) by a factor of 1.5 across forest width**

## 4.5.2. Distinction between Emergent and Submergent Vegetation

### 4.5.2.1. Parameter Formulation

For the analysis of the distinction between emergent and submergent vegetation, the hydraulic parameters were kept constant corresponding to a 25 year event. The vegetation parameters were varied to provide one emergent case and one submergent case, both with identical depth averaged vegetation factors. The matching of the vegetation factors was done to reduce the number of variables. Table 13 gives the vegetation parameters for the emergent and submergent vegetation.

**Table 13: Simplified vegetation parameter variation for emergent and submergent cases**

Layer	Emergent Vegetation		Submergent Vegetation	
	Vegetation Factor	Height (m)	Vegetation Factor	Height (m)
Roots	0.1	1	0.2	0.5
Stem	0.25	5	0.25	5
Canopy	0.2	1	0.4	0.5
<b>Identical Depth Averaged Vegetation Factor = 0.22</b>				

### 4.5.2.2. Conclusions

A difference was observed between emergent and submergent vegetation even with an identical depth-averaged vegetation factor as shown in Figure 39 below.

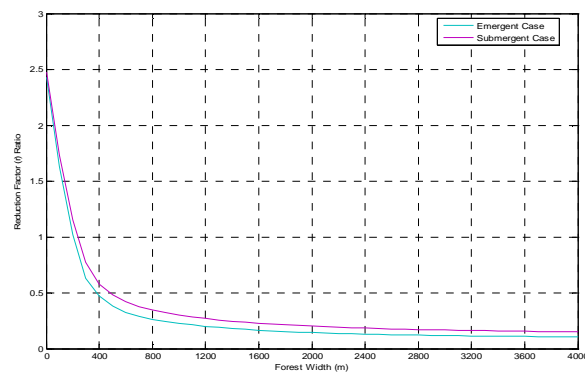


**Figure 39: Transmitted wave heights across forest width for emergent and submergent vegetation with identical depth averaged vegetation factors for a 25 year event**

The ratio of the reduction factor for emergent vegetation to the factor for submergent vegetation does not show any clear trend within the critical width region. However it was clear that emergent vegetation is more effective in wave attenuation since the ratio of reduction factors is greater than 1. Also observed was an overall reduction in the ratio to a value of one for greater forest widths. This suggests a decrease in the difference between emergent and submergent vegetation with increasing forest widths and decreasing transmitted wave heights. These trends and results are shown in Figure 40.

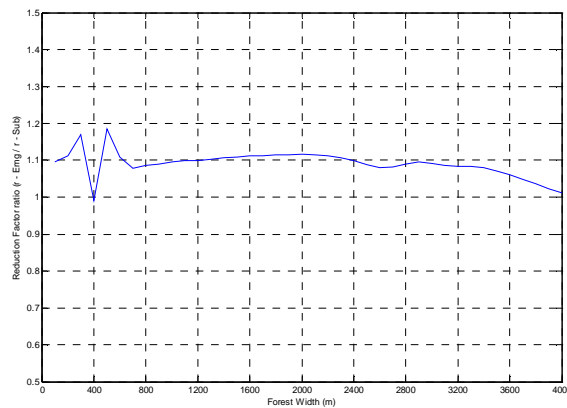


**Figure 40: Ratio of reduction factors for emergent vegetation and submergent vegetation (Right-hand axis) along the mangrove forest width for constant depth-averaged vegetation factors**

## 5 Case Study – Kanika Sands

A case study was performed using simplified scenarios based on the findings from the preliminary sensitivity analysis. From the case study it was hoped that conclusions could be drawn regarding the importance of the Kanika Sands mangrove vegetation patch, specifically in terms of wave attenuation, as a protective system for the nearby port against cyclones. The basic procedure was the same as in the previous analyses. Here too the transmitted wave heights along the central line were chosen for the analysis. The following sections describe the conditions of the case study and the results and conclusions obtained.

### 5.1. 2D Model Setup

The hydraulic boundary conditions used in the case study were the boundary conditions at the -11 m depth contour calculated in Section 3.3. A 2D bathymetry, shown in Figure 41 below was simulated based on a realistic linear bathymetry profile obtained from 1 in 50000 scale navigation maps. The island of Kanika Sands was however not indicated explicitly on these maps. Therefore a simplified bathymetric profile was simulated for the island based on information from Google Earth and literature from the region. The vegetation was assumed to be on the island is at a distance of approximately 3.5 km from the coast and the port.

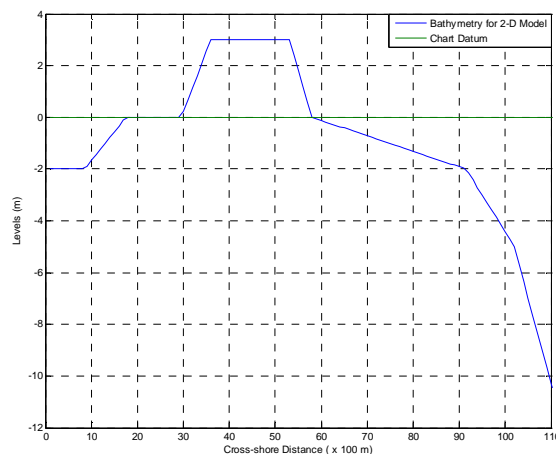


**Figure 41: Interpolated near-shore bathymetry for 2-D models with CD indicated**

The grid shown in Figure 43 was elongated along the ordinate (y) axis to provide an aspect ratio of 1 in 7. This ratio was chosen based on observations from the generic analyses (Sub-section 4.4.2) as being sufficient for avoiding spreading effects in SWAN 2D across the central band of interest. The grid extends seaward up to the -11 m depth contour which translates to a distance of around 11 km. The final size of the bathymetry grid is therefore 77 km by 11 km. Grid resolutions for input, computational and output grids were kept constant at 100 m similar to the grids used in the generic analyses.

The windward and seaward sides of the island were assumed to have a slope of around 1 in 200 partly based on the adjacent bathymetry. Sedimentation by mangroves would generally give much flatter slopes in case of an old island. Since Kanika Sands is a relatively new island and is influenced by other large-scale morphological drivers in the region (refer sub-section 2.4.1) this assumption was thought to be acceptable. The northern and southern boundaries were assumed to be straight for simplicity. This assumption would have an effect on the wave patterns immediately next to and behind the island, at the two boundaries, but this was not considered relevant to this study. Figure 42 below shows an isometric view of the island bathymetry.

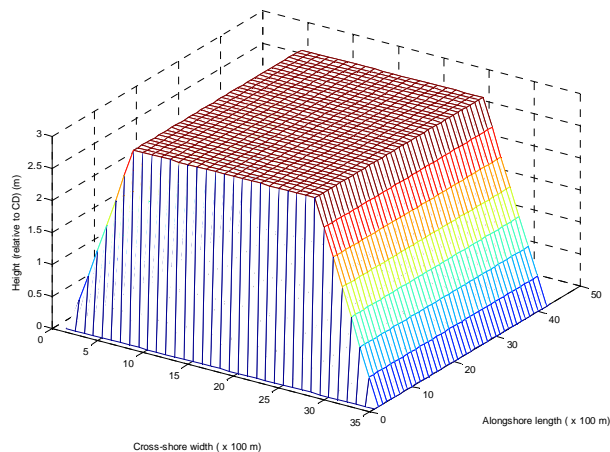


**Figure 42: Isometric view of assumed island bathymetry with vertical northern and southern sides (heights measured relative to CD)**

The spatial vegetation density file for input into the SWAN 40.55MOD model was created based on an approximation of the actual shape of the mangrove patch as observed in Google Earth images and literature. The roughly oval shape of the mangrove patch with two extended arms on the northern and southern sides was approximated as shown

in Figure 43 (right) below. The coordinates of the mangrove patch were also decided based on available images and photographs due to the lack of accurate data. From the generic analyses it was concluded that the model allows a limited representation of the spatial variation of mangrove species in terms of multiple values of a base vegetation density. Some authors consider the effect of the mangroves' roots to be important in the wave attenuation process (Schierreck & Booij, 1995 and Vosse, 2008), with their influence increasing at lower water depths. However the effect of variations in the root systems is thought to be less, both in the model due to the lumping of parameters as well as in reality. The high water depths used in this study also limit the sensitivity of the results to such variations. Finally, a review of the vegetation characteristics in the region indicated that the two species assumed predominant in this region *S. alba* and *R. mucronata* have nearly similar depth-averaged vegetation densities. Based on these considerations a single species *R. mucronata* was used and the spatial vegetation density file was given a uniform value of 1 throughout except in case of the horizontal variation studies (section 5.4).

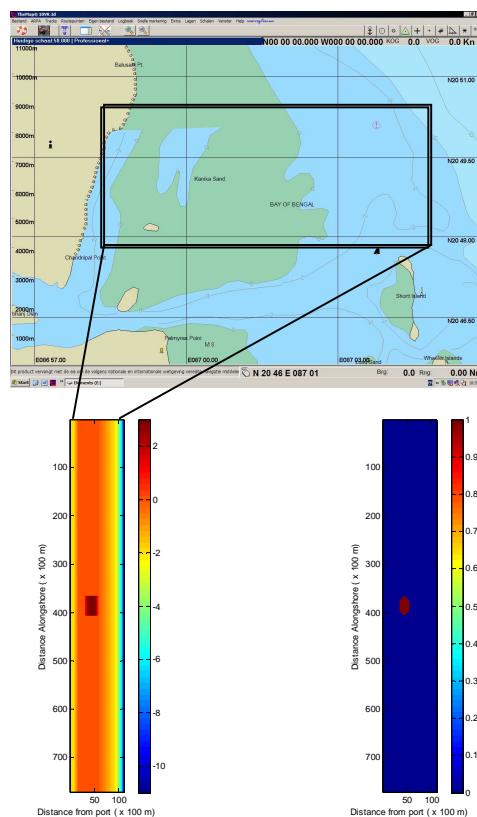


**Figure 43: Bathymetry (left) and Vegetation Density grids (right) for case study with modeled region indicated in actual bathymetry map (from Map Room, Delft University of Technology) on top**

## 5.2. Parameter Formulation

Based on the findings from the preliminary sensitivity analysis the scenarios for the case study were limited to three hydraulic scenarios corresponding to 100, 25 and 5 year events and three vegetation scenarios corresponding to ‘HIGH’ ‘LOW’ and ‘ZERO’ vegetation factors. The parameter values for vegetation and hydraulic characteristics were chosen based on actual values from the literature studies and data analysis (sections 2.4 and 3.2). The angles of attack for these scenarios were kept constant at 90°. Additionally three simulations with varying angles of wave attack – 22.5°, 45° and 90° were run for different vegetation cases. Since it was felt that the variation between the three wave angle cases would follow a regular trend for all events a single hydraulic scenario corresponding to a 25 year event was used. Table 14 and Table 15 below list the various scenarios simulated. Table 16 and Table 17 list the parameter values chosen for each scenario. Finally a scenario with no island and no vegetation and a 90° angle of attack was simulated to serve as a control case for comparisons. The water levels here are presented as the actual water levels measured with respect to the *CD*.

**Table 14: Vegetation and Hydraulic scenarios for Case Study (constant angle of wave attack)**

Vegetation Factors	Hydraulic Parameters – H <sub>s</sub> , T <sub>p</sub> , WL
HIGH	RP 100
LOW	RP 25
ZERO	RP 5

**Table 15: Angle of wave attack scenarios for Case Study (for a 25 year event)**

Vegetation Factors	Angle of Wave Attack, Alpha (deg)
HIGH	22.5
LOW	45
ZERO	90

**Table 16: Vegetation parameter values for Case Study**

Layer	Vegetation Factor		Height (m)
	Case 'LOW'	Case 'HIGH'	
Roots	0.05	6.5	0.5
Stem	0.075	0.6	5
Canopy	0.1	2	0.5

**Table 17: Hydraulic parameter values for Case Study (constant angle of wave attack)**

Return Period (years)	Wave Height (m)	Water Level (m)	Wave Period (s)
100	9.25	12.6	17
25	7.44	10.0	15
5	5.28	7.1	12

Due to the presence of an island and vegetation of a high density, diffraction effects were thought to be a possibility. The SWAN 40.55MOD by default does not compute diffraction effects. Therefore a simulation was carried out with diffraction computations included for an island with high density vegetation. The results from the simulations with and without diffraction indicated that apart from an apparent smoothing of the values the model is relatively insensitive to the inclusion of diffraction computations under the given conditions. The results of the two simulations are shown in Figure 44 below. It must be kept in mind that the SWAN model used is not meant for precise diffraction computations and makes only a rough approximation of the diffraction effect.

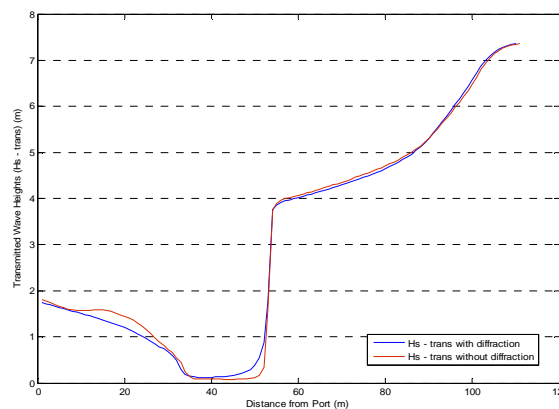


**Figure 44: Graph showing transmitted wave heights across an island with high vegetation density with and without diffraction computations**

### 5.3. Results and Conclusions

Wave analysis was done along two sections – one in the cross-shore direction across the centre of the island (Section X-X) and one in the alongshore direction at the port (Section Y-Y). Figure 45 below shows an illustrative case of transmitted wave height values along with the two sections indicated. Conclusions regarding the effectiveness of the mangrove vegetation on the island to the port in terms of wave attenuation are presented below. Also, a few conclusions regarding the model characteristics based on observations during the entire process are described.

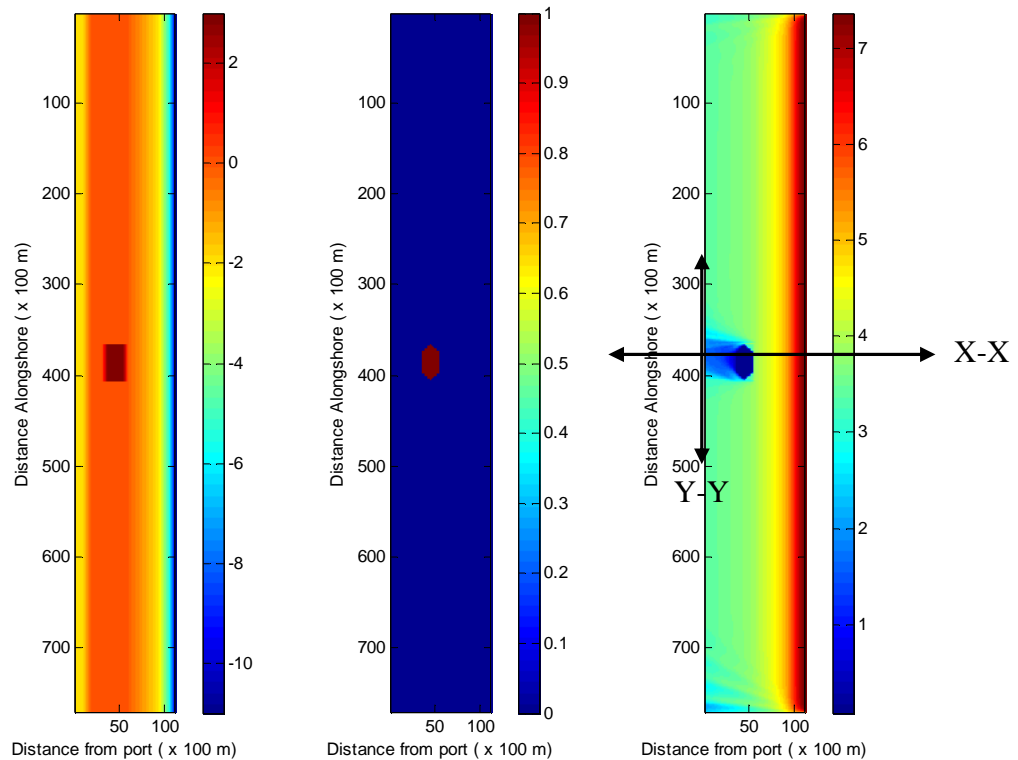


**Figure 45: Bathymetry grid (left), vegetation density grid (middle) and transmitted wave heights (right) for an island with a ‘high’ vegetation density and an event of a return period of 25 years. The two analysis sections X-X (cross-shore) and Y-Y (alongshore) are indicated on the transmitted wave heights grid.**

### 5.3.1. Effectiveness of Mangrove Vegetation

- The analysis of wave heights along Section X-X showed that the presence of vegetation has a considerable effect with regard to wave attenuation in the port for all three return periods. These results are shown in Figure 46 for a return period of 25 years. The same is observed in Figure XX and XX for return periods of 100 and 5 years. It was additionally observed that the island by itself also accounts for some wave attenuation though this is less than the effect of the vegetation patch.

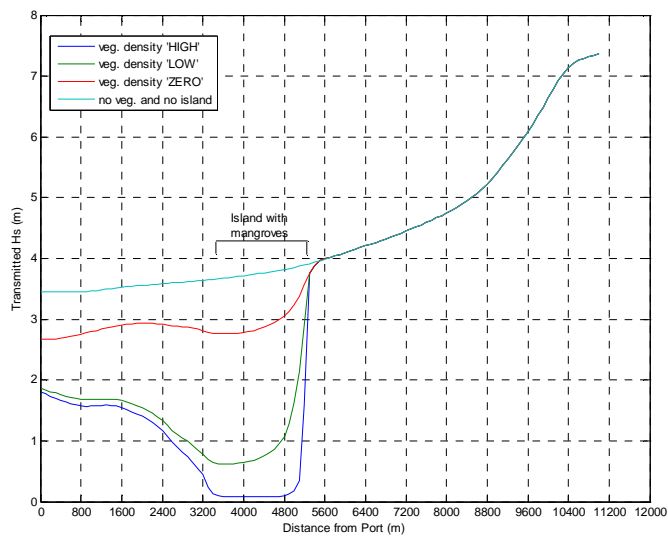


**Figure 46: Transmitted wave heights from offshore (right) along Section X-X (cross-shore) for different vegetation factors compared with the ‘no veg. and no island’ case for a 25 year event**

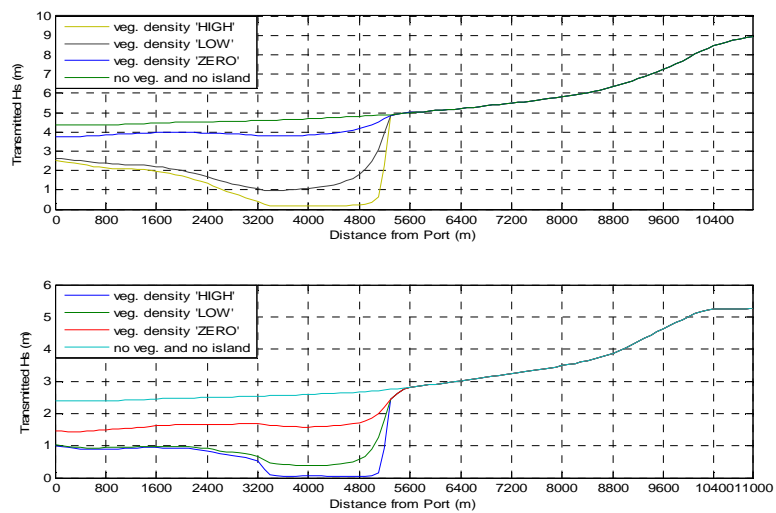


**Figure 47: Transmitted wave from offshore (right) along Section X-X (cross-shore) for different vegetation factors for return periods of 100 years (TOP) and 5 years (BOTTOM)**

2. It was seen from Figure 46 above that the vegetation patch is very effective in reducing wave heights at points immediately behind it with a difference of around 0.5 m being observed between low and high vegetation factor conditions.
3. A relatively sharp recovery of wave heights was seen beyond the vegetation patch with the sharpness increasing for increasing vegetation densities. This resulted in much higher wave heights at the port compared to points immediately behind the vegetation. For instance, if the mangroves had been 600 m from the port the wave heights would have been only 50% of the present values. Figure 48 below shows this effect in greater detail. The diamond shaped island geometry contributes to wave height recovery since it has a smaller shadow region compared to a rectangular island. It can therefore be concluded that the mangrove island has an effect on the port though this is limited by its geometry and its distance from the port.

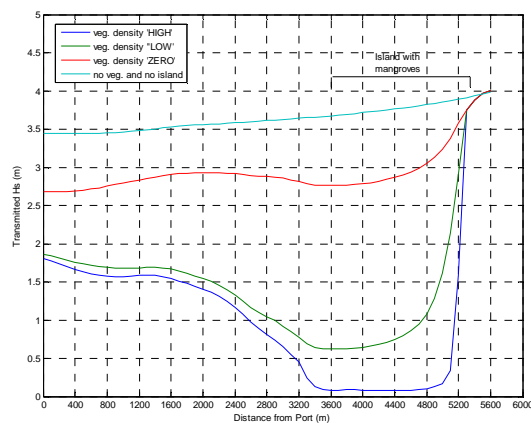


**Figure 48: Transmitted wave heights along Section X-X within the vegetation and between the vegetation and the port for a 25 year event**

4. Wave attenuation of nearly 60% was observed at the port due to the effect of the mangrove island. The attenuation within the island is however nearly 90%.
5. An analysis of the difference between transmitted wave heights was done for 'LOW' and 'HIGH' cases at different alongshore sections including Section Y-Y. Here a choice was made to use the difference in wave heights rather than the reduction factor since this was thought to highlight certain characteristics more clearly. Figure 49 below shows that the sensitivity to vegetation density variations reduces with increasing distance behind the mangroves. The difference in wave

attenuation between 'LOW' and 'HIGH' vegetation half-way between the island and port is only around 10 – 12 % of the difference within the island. The peaks in the mid-island case and the oscillations at Section Y-Y are thought to be model characteristics and are discussed in Points 2 and 3 of sub-section 5.3.2.

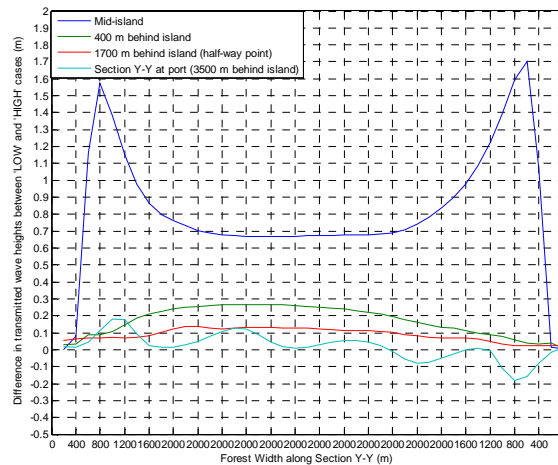


**Figure 49: Difference in transmitted wave heights between 'LOW' and 'HIGH' cases at different alongshore sections between the island and the port versus forest width at that point**

6. Simulations with variations in the angle of wave attack showed a shift in the region of lowest wave heights as expected. From Figure 50 below, along Section Y-Y, it can be seen that the optimum alongshore width of vegetation required to reduce the effect of waves between angles  $90^\circ$  and  $22.5^\circ$  to the coast is approximately 6 km. This is further studied in sub-section 5.4.1. The oscillations in the wave heights for all angles are a result of the exclusion of diffraction approximations from the computations. Point 2 of sub-section 5.3.2 elaborates on this effect.

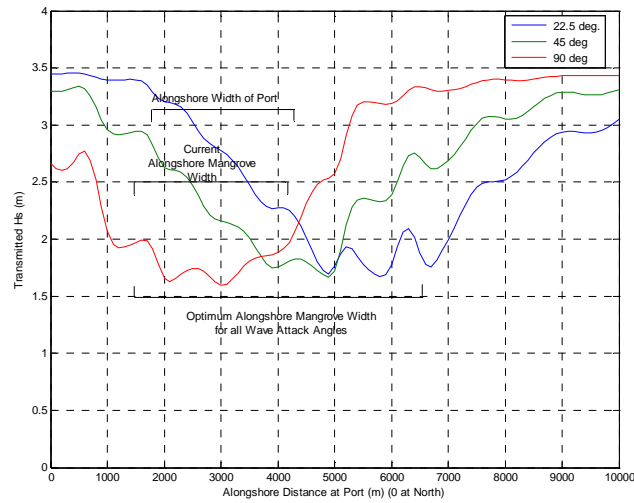


**Figure 50: Transmitted wave heights along Section Y-Y (alongshore) at the port for varying angles of wave attack and constant vegetation and hydraulic parameters corresponding to a 25 year event**

7. Wave data from the nearby port of Paradip indicate that the critical wave heights in Paradip port vary between 1.2 m under normal conditions and 2.5 m in the monsoon season (Iron Ore Handling Plant Tender Document, Paradip Port Trust, 2006). In this study, a 2.5 m wave height has a return period of more than 60 years under simulated conditions. If the vegetation were removed or destroyed the 2.5 m wave would occur at least once every 20 years posing the threat of a drastic reduction in the port's design life. The effect of the vegetation and its continued existence are therefore crucial for the design of the port. The effect of vegetation on the return periods for wave heights of 1.2 and 2.5 m is illustrated below in Figure 51.

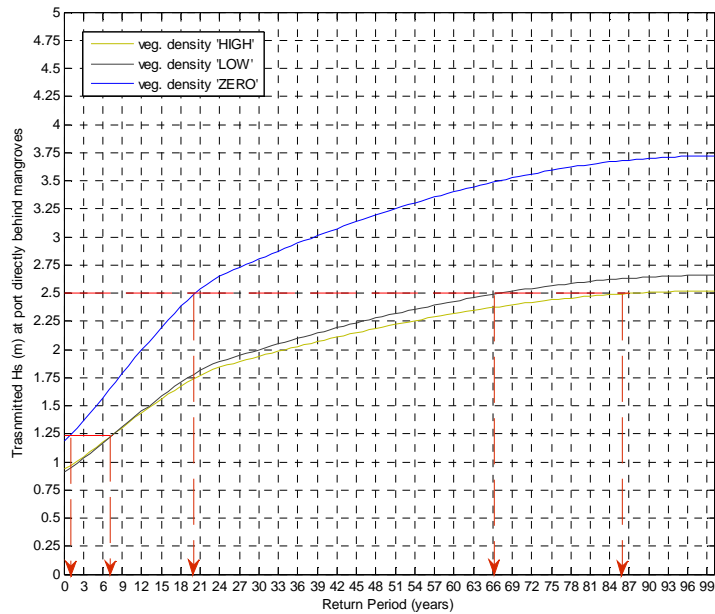


**Figure 51: Wave heights at the port at a point directly behind the mangroves versus return periods for different cases of vegetation**

8. It is also seen from Figure 51 that the effect at the port of a variation in vegetation density becomes appreciable only beyond a 20 year wave height.
9. Some simulations were carried out to establish the difference between the effect of the vegetation and the island. It is evident from Figure 52 below that the vegetation patch has a far greater effect on wave heights compared to the bathymetry in this situation. However the presence of vegetation in the absence of an island is considered unlikely.

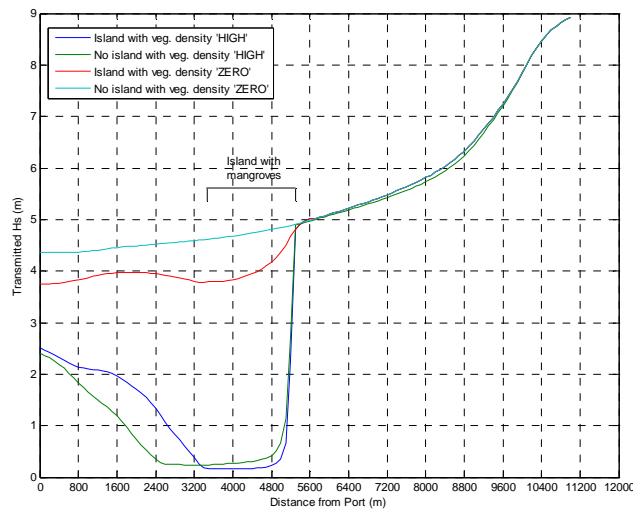


**Figure 52: Transmitted wave heights for cases of an island and no island both with vegetation of varying densities for a 25 year event**

10. Also interesting to note from Figure 52 is the extension of the vegetation effect beyond the actual vegetation for a flat bathymetry when the island is absent. This indicates the development of a shadow region behind the vegetation. The absence of the shadow region with the island could be due to the phenomenon of wave height recovery with a sudden increase in depth which dominates the shadow effect. Though the accuracy of the shadow effect is unsure, it is possible that a mangrove patch is more effective with a flat bathymetry beyond it than with a sudden increase in depth.

### **5.3.2. Model Characteristics**

1. The model shows an asymmetry in transmitted wave heights seen in Figure 53 below. It is felt that this asymmetry is partly a result of the errors caused due to the simplification of the island bathymetry described in section 5.1. Also, the model was instructed to use a default JONSWAP spectrum with a directional spreading of  $30^\circ$ . Long swell waves similar to those used in this typically have low values of directional spreading. This could cause errors in the island's shadow region due to SWAN's limited capability in dealing with such waves. In the case of a locally generated cyclone, the assumption of a  $30^\circ$  spreading would most probably be valid. Also, since this study did not look into the effects

immediately behind the island, it was assumed that these differences are not relevant here. However in the case of an offshore cyclone where the swell waves ‘overtake’ the cyclone the directional spreading may be considerably less and would have to be considered carefully.

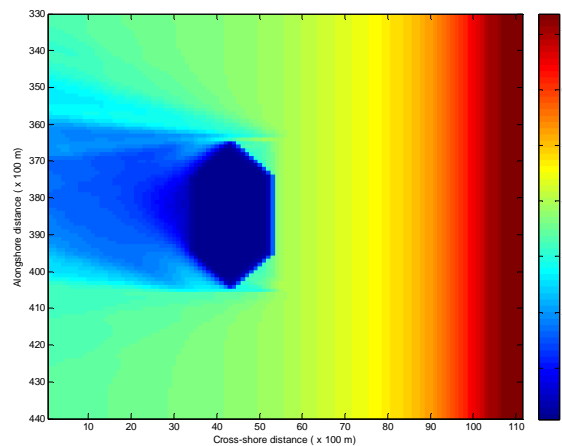


**Figure 53: Magnified view of transmitted wave heights around the mangrove island for a 25 year event and high vegetation factors**

2. The effect of neglecting diffraction was verified by analysing the wave heights along Section Y-Y at the port. From Figure 54 below it is seen that the inclusion of the diffraction approximations in SWAN results in a smoothing of the values and a partial reduction of the asymmetry in calculations. It is thought that the oscillations along Section Y-Y in Figure 49 are also due to the exclusion of diffraction approximations. The overall effect of this exclusion however was felt small enough, compared to the natural variations, to be ignored in this study.

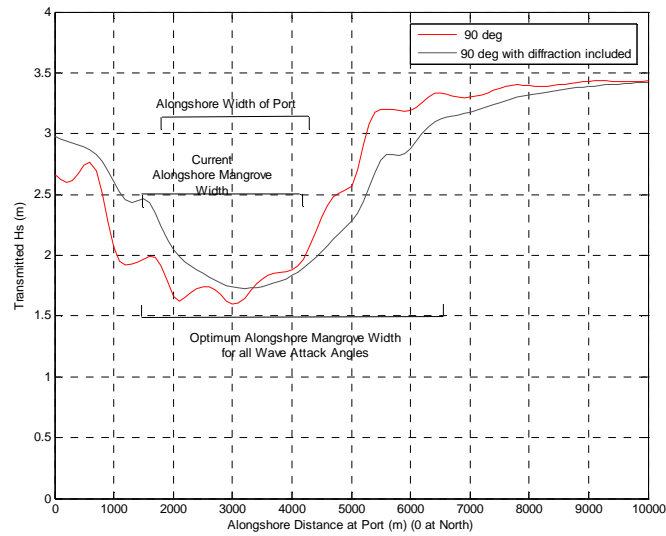


**Figure 54: Transmitted wave heights along Section Y-Y at the port with and without diffraction approximations for a 25 year event and high vegetation factors**

3. The two bends in the curve with diffraction in Figure 54 above are possibly due to edge effects in the model due to the sudden presence of mangrove vegetation in the cross-shore direction. Also, the peaks observed earlier in the mid-island case in Figure 49 are thought to be due to edge effects in the alongshore direction.
4. An aspect ratio of 1:7 is seen to be sufficient for studying wave heights along the central band while avoiding the effect of energy leakage.
5. It was concluded that the model currently has effective but limited capabilities with regard to modeling horizontal variation in vegetation.

## 5.4. Horizontal Variation Studies

Horizontal variations in the vegetation on Kanika Sands island could occur due to natural as well as artificial causes. While cyclonic events could cause a reduction of vegetation density and area over the short-term, the highly dynamic nature of the region could result in an increase in density and area or even a shift in position over the long term. On the other hand, controlled planting and other management strategies could be put in place to artificially enhance and maintain the vegetation in a desired pattern. An increase in density and area in the cross-shore direction, though possibly beneficial in other respects, was felt to be unimportant with regard to wave attenuation under the present conditions. However, variations like alongshore extensions and density reductions are of direct interest to the Dhamra Port. Some additional simulations were run that looked at possible effects of such variations in vegetation patterns across the horizontal plane. These were achieved by varying the values in the vegetation density file (refer section 5.1). Apart from providing an overall view of the effects of changes due to natural circumstances and management strategies, these simulations helped verify certain assumptions and conclusions drawn previously in the study. The details of the simulations performed and the conclusions drawn are given below. Apart from a change in the bathymetry for the first study all other input parameters were kept constant at the same values as in the rest of the case-study.

### ***5.4.1. Alongshore Extensions***

It was seen from sub-section 5.3.1 that the alongshore vegetation size is insufficient in case of wave attack from the north at angles greater than  $45^\circ$ . The Kanika Sands island has two arms on its northern and southern sides. However, these do not have vegetation except for a small area in the south. Initial results suggest that for optimum protection the size of the vegetation would need to be increased from 4 km to 6 km in the alongshore direction. Since the southern part of the island and the coast are relatively protected by the sand spit, wave attack from the north is felt to be more relevant. With these considerations, two cases were simulated – one with an extension of 1 km on the northern side (Case 1) and one with an extension of 2 km (Case 2). In both cases the extension was done for both bathymetry and vegetation for a cross-shore width of 500 m. This value

was chosen since it lies within the optimum range from sub-section 5.3.1. Figure 55 below shows the vegetation grids for the two cases.

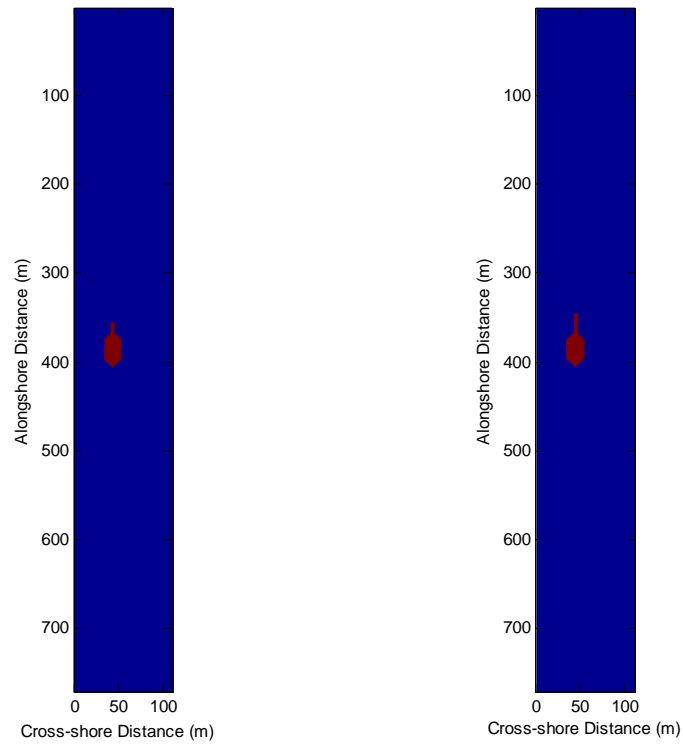


**Figure 55: Vegetation grids for Case 1 (Left) and Case 2 (Right)**

The results from the two simulations for an angle of 22.5 degrees are shown in Figure 56 below.

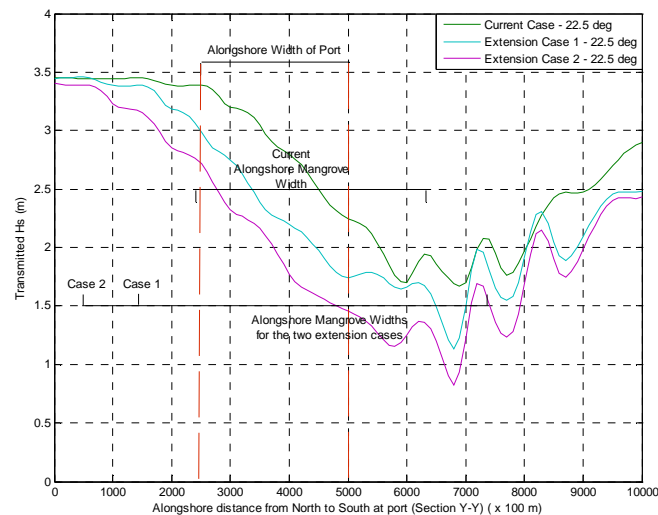


**Figure 56: Wave heights at port for original mangroves and the two extension cases at 22.5 deg wave attack angles for a 25 year event with the port region indicated**

It is seen from Figure 56 that Case 1 shows significant wave height reduction within the port. Case 2 shows even better attenuation with a wave height reduction of more than a metre from the current case. In both cases however the wave heights still remain in the range of 1.5 to 3 m. In conclusion, an extension of the island and vegetation on the northern side is highly beneficial to the port though additional protection measures may be needed. Further it would be worthwhile investigating a 2 km extension since this seems to give considerably better protection than a 1 km extension. The simulations only considered waves from the north since the southern side is currently relatively protected. The benefit of a southern arm under normal conditions is therefore questionable. In the absence of such protection however, especially in case of cyclones from the south with high storm surges a southern arm of vegetation could greatly enhance the safety of the port. The mismatch between the current mangrove width and the region of lowest wave height for the original case and the oscillations in wave heights are a result of the model characteristics discussed in sub-section 5.3.2.

### 5.4.2. Density Variations

While mangroves are a typically robust eco-system and can withstand extreme events, their capability to survive under extreme conditions is still limited. Extensive mangrove destruction has been observed under extreme situations such as storms, cyclones and tsunamis (UNEP – WCMC, 2006, Das S., 2007, Giesen W. et al., 2007). Since the case study region is very susceptible to cyclone attacks it is possible that such an event causes a reduction in the density of mangrove vegetation on the island, especially on the fringes. Like any natural system destroyed mangroves may take a while to regenerate. Under such conditions, it is possible that the reduced density at the fringes has an effect on the port behind. Simulations were therefore run to investigate the effect of such density reductions all around the island. The density reductions were simulated by specifying a lower number in the spatial density file in the model. Three cases were run - one with a density of 0.5 for a 200 m width (Case 1), one with a density of 0.5 for a 300 m width (Case 2) and a final one with a density of 0.1 for a 300 m width (Case 3). These cases were chosen as being illustrative of the possible reductions due to a cyclone. An example of the vegetation density file is shown in Figure 57 below. The three cases were run for a 25 year event with all other parameters being kept constant.

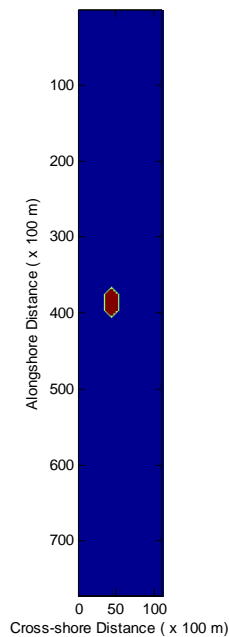
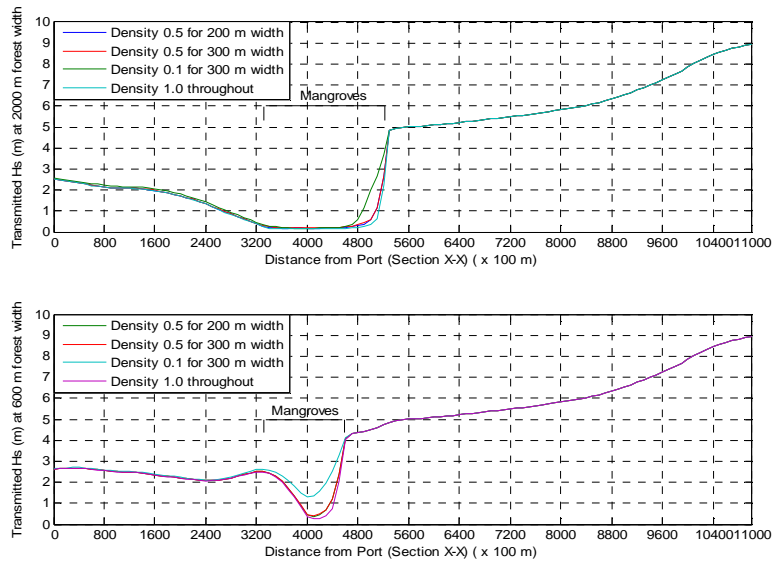


Figure 57: Vegetation density grid for the case with a value of 0.5 m for a 200 m width all around the island

The results from the three cases are illustrated below in Figure 58.



**Figure 58: Transmitted wave heights at 2000 m forest width (TOP) and 600 m forest width (BOTTOM) for the three density variation cases for a 25 year event**

The analyses were done across two sections – one at 2000 m forest width and one at 600 m forest width to compare the relative importance of the density reductions. As expected, the density reductions have a more pronounced effect at the 600 m forest width. Case 3, with a 300 m band of density 0.1, shows appreciable difference within and beyond the critical width at both sections. It is also seen that for Case 3 a width of more than 600 m is required for the wave attenuation to ‘catch up’ with that of the other cases. This is an important factor to be considered while planning sacrificial mangrove belts and for purposes of monitoring. However, in all the cases the effect is appreciable only up to approximately 400 m behind the vegetation. This is in line with the findings described in sub-section 5.3.1 that the effect of density reductions has a minimal effect at points far behind the island. This also validates to an extent the initial assumption of a uniform density throughout the vegetation patch.

### ***5.4.3. Vegetation Strip Plantations***

Given the conclusions of the existence of an optimum width investigations into the effectiveness of mangrove strips were thought worthwhile. While the Kanika Sands island is currently fully inhabited by mangrove vegetation, future strategies for similar

islands could look at a ‘ring of protection’ with mangrove strips. To include possible effects of density reduction which could be vital in case of such protection two simulations were performed. One was for a 300 m wide mangrove strip of density 0.1 (Case 1) and the second for a 300 m wide strip of density 1 (Case 2). In both cases there was no vegetation on the rest of the island. The value of 300 m was chosen as being the minimum of the optimum width range from sub-section 5.3.1. Based on point 10 from sub-section 5.3.1, an additional scenario with a 300 m strip of density 1 only on the eastern side and northern and southern tips was also performed (Case 3). The simulations were performed for the most extreme event in this study – the 100 year event with all other parameters constant. Figure 59 below shows the vegetation density file for Case 2.

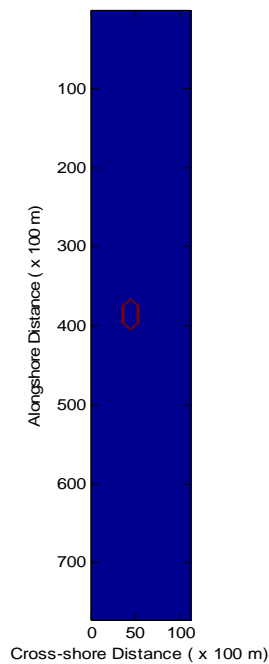


**Figure 59: Vegetation Density grid with a 300 m mangrove strip of density 1 (Case 2) all around and no mangrove in between for a 100 year event.**

The results of these cases compared to the normal case are shown in Figure 60 below.

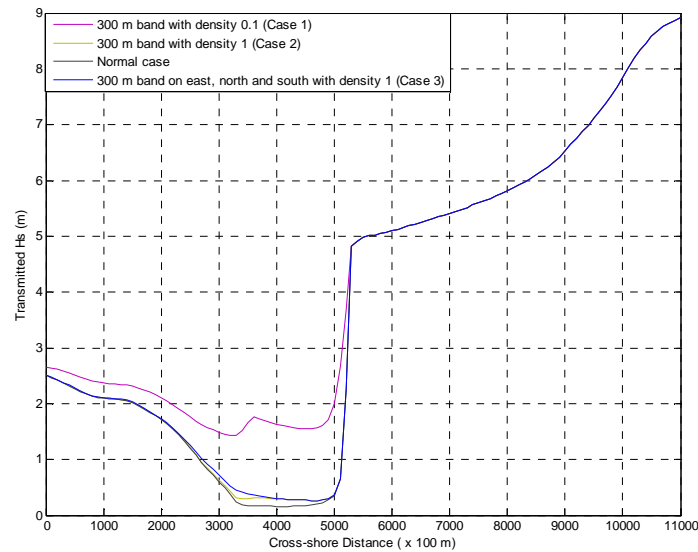


**Figure 60: Transmitted wave heights for three vegetation strip cases and the normal case for a 100 year event**

From Figure 60 it is seen that for a density of 1, a simple vegetation strip of 300 m has nearly the same effect as the normal scenario with vegetation throughout the island. The planting of vegetation strips therefore seems a far better solution in terms of wave attenuation as it gives the same effect with reduced costs and other difficulties. In such a case however very special attention has to be paid to monitoring and maintenance of the vegetation density. A decrease in vegetation density which is very possible in case of cyclones results in appreciably higher wave heights within the island and up to 800 m behind it with a smaller difference at the port. This is in contrast with the current situation, where the width of the forest is sufficient to negate the effect of a density reduction. Case 3 indicates that a vegetation strip may not be necessary on the western edge. Here a shadow region is seen up to the edge of the island similar to the findings from sub-section 5.3.1. Whether this effect is a good approximation of reality needs to be investigated further. Also, the destruction of the western vegetation strip in this case would leave the island and the port completely unprotected. This scenario therefore needs very careful investigation before application.

## 6 Conclusions

### 6.1. Process Summary and Assumptions

Wave attenuation in mangroves during extreme events was studied using a numerical model. Extreme event conditions of longer and higher waves and increased storm surge levels were approximated using available data and statistics for the region of Orissa, India. The case study site was chosen based on several factors. Mangrove vegetation characteristics for the site were established using data from nearby regions and making realistic assumptions. Several generic sensitivity analyses using a flat bathymetry and a rectangular vegetation patch were carried out to study the working and characteristics of the model under extreme conditions and to help select relevant scenarios for the case study. Finally, based on the generic model studies the case study was performed for the chosen site with reduced scenarios but more realistic bathymetry and vegetation parameter values. Additional simulations of possible horizontal variations were carried out within the case-study. Though the region of study is often affected by severe storm surges and wave heights it is felt that the extreme event conditions have possibly been overestimated. Also, the bathymetry used in the case study is an approximation of the real bathymetry. However, due to the high variability of the bathymetry in the region with large scale changes occurring within a decade under normal conditions and within a few weeks during extreme events the approximations made were felt to be sufficiently representative for the purposes of this study. The conclusions drawn from the study are summarised in the following sections.

### 6.2. Conclusions

#### *6.2.1. Mangroves and the Port*

It was concluded from the case study that the mangroves have a definite positive effect on the port in terms of wave attenuation. While the mangrove island's protective effect is limited by its distance from the coast it still causes a nearly 60% reduction in wave heights at the coast under the given conditions. Though the vegetation may not have a significant effect on daily operations its continued

existence is seen as crucial for ensuring the port's safety during its design life. The mangroves have a significant effect only at cross-shore widths greater than 300 to 400 m and an increase in width beyond 800 m does not make much of a difference to wave heights at the port. However the current alongshore width of the mangroves might be insufficient in case of waves approaching from the north at angles greater than  $45^{\circ}$ . The optimum width of the island for maximum protection solely in terms of wave attenuation under the given hydraulic and vegetation conditions therefore ranges from 300 to 800 m in the cross-shore direction with an along-shore length of around 6 km. These were verified with some horizontal variation simulations. Expansion to the north was thought more relevant given the present conditions. Such an island may be a cheap alternative to a conventional breakwater. Horizontal variation simulations also showed that density reductions on the island due to extreme events do not have much of an effect under present conditions. Further, the planting of 300 m wide mangrove strips seem a highly feasible and cost-effective substitute to foresting an entire region with mangroves. However, the required densities within the strips and their spacing would have to be studied carefully.

Due to the distance of the port from the mangroves and their sizeable width the effect of a change in vegetation density within the simulated range is negligible though there is a marked difference between the presence and absence of vegetation. Vegetation density variations have an appreciable effect only beyond a 20 year wave height and only up to a certain distance behind the island. From the generic analyses, vegetation height was seen to greatly influence wave attenuation. The vegetation heights used in this study ranged from 6 to 10 m roughly corresponding to a 15 – 20 year old forest. From the analyses it may also be concluded that the species *R. mucronata* and *S. alba* can offer effective protection against waves at the densities assumed in this study and may therefore be selected where suitable for purposes of artificial mangrove replenishment.

### ***6.2.2. Model and Vegetation Characteristics***

It was concluded that though the model is effective in approximating wave attenuation the lumping together of certain parameters limits its sensitivity to variations in vegetation

factors and heights. The model shows a predictable trend with regard to hydraulic and vegetation parameter variations. Very high wave attenuation of the order of 90% was observed within the mangroves even for extremely high waves and water levels. The increase in wave attenuation rates at the edge of the vegetation is worth investigating in detail. While this result seems to be in agreement with the findings of Vosse (2008) it is not clear how much of this behaviour is due to model characteristics and how much is representative of the actual situation. Detailed analyses revealed a trend in model sensitivity to hydraulic parameters with wave heights being the most important. Emergent vegetation with the canopy above water was observed to cause greater wave attenuation compared to submergent vegetation even for identical depth-averaged vegetation factors. The case study showed that wave height recovery beyond the mangroves is quite sharp with the rate of recovery increasing with an increase in vegetation density. The use of a flatter bathymetry in the case study was seen to cause an extension of the vegetation effect beyond the actual vegetation. Finally, the inclusion of diffraction approximations in the computations was seen to have little difference in the computed wave heights behind the island and vegetation.

## 7 Recommendations

### 7.1. Mangroves and the Port

The main objective of the study was to get an idea of the usefulness of a mangrove island to a port lying behind it. This was studied extensively in the case study and based on the findings some recommendations regarding the aspects that port and other interested authorities should consider are given below:

1. It is necessary for the port to preserve and if possible, increase the extent of mangroves on the island to ensure its survival until the end of its design life. It will also be necessary to ensure a minimum vegetation density while planning for events with return periods greater than around 20 years.
2. The recommended size of the mangrove patch for most effective wave attenuation is 300 to 800 m in the cross-shore direction and around 6 km in the alongshore direction under the conditions of this study. Since the alongshore length of the island currently seems insufficient, mangrove planting strategies could focus on expansion to the north with a minimum width being maintained throughout in the cross-shore direction.
3. A newly planted mangrove forest will need time to attain a height sufficient to afford protection. Also, younger mangrove vegetation with lesser densities and diameters will be more vulnerable to wave attack. Further, an increase in cross-shore forest width beyond 800 m does not have much of an effect on the port. Considering these factors, it is likely that along-shore expansion of the island would be easier and more relevant than cross-shore expansion with regard to wave attenuation.
4. 300 m wide mangrove strips seem to be just as effective as the entire vegetation patch in terms of wave attenuation at normal densities. These are also much more cost-effective and probably much easier to manage. However their effectiveness is dependent on the densities within the strips and possibly their spacing, both of which need to be given careful consideration.
5. At present the mangroves seem to be robust in terms of wave attenuation even with reduced densities at the fringes. However constant monitoring of the

condition of the island and the mangroves is essential due to the highly unstable nature of the morphology in the region and possible large – scale effects of extreme events and human activities.

6. Accurate determination of the vegetation species and characteristics on the island is necessary to verify the results of this study. It will also be useful in deciding the threshold parameters for the existence of the island and the health of the vegetation, especially with regard to port – related activities.

## 7.2. Numerical Model

The field of modeling wave attenuation in vegetation is still relatively new. The SWAN 40.55MOD model is considered reasonably effective in implementing the effect of mangrove vegetation on wave dissipation. During this study observations were made regarding possible future improvements to the model to help represent the actual situation better. Since the study did not go into the model in depth, most of the recommendations focus on the model implementation rather than the formulations. Some salient points in this regard are given below:

1. The present study neglected the effect of currents within the vegetation. Since in real life strong currents are often present within mangrove vegetations, even in extreme conditions, the inclusion of currents in the computations could help produce more accurate results. Also secondary processes such as circulation patterns behind the island need to be investigated in detail using models suited for the same.
2. It is possible that inertial forces play an important role in wave dissipation depending on the wave and vegetation conditions. The effect of neglecting inertial forces on mangrove vegetation needs to be investigated in detail.
3. The neglecting of the swaying motion may be accounted for in the root and stem layers by the rigidity of typical mangrove vegetation. However, special attention needs to be given to the canopy portion of mangroves which are not as rigid as the rest of the plant. It is very possible that the mangrove canopy is submerged under extreme conditions. It would therefore also be necessary in such cases to determine the exact nature of drag induced by the canopy. From this an accurate

- value or range of values for the drag coefficient in the canopy could be defined for use in the model.
4. It was felt that the results might be improved with the implementation of the Dalrymple formulation for each of the three mangrove layers before the depth-averaging of vegetation factors was carried out. However the extent of this improvement and its worth compared to the consequent increase in computation time would have to be investigated in detail.
  5. Literature studies indicate that a typical mangrove patch may show extensive height and density variations. While the model can currently calculate horizontal density variations in the form of relative factors, a single height distribution is assumed for all trees within the mangrove patch. The addition of the ability to incorporate horizontal vegetation height variations is therefore suggested. Though this may not contribute much to the understanding of wave dissipation processes it might improve results with regard to simulating real life scenarios.
  6. The peaks in reduction factors at the edge of the vegetation could be investigated further. The aspect of an increase in wave height recovery with increase in vegetation density is also worth investigating.
  7. Though SWAN does not calculate diffraction very precisely, the apparent smoothing of wave heights due to the inclusion of diffraction computations in this study is worth investigating.
  8. Some other characteristics, such as the low sensitivity to density variations at higher widths, the extension of the vegetation effect in case of a flatter bathymetry and the consistent increase in wave attenuation rates with an increase in vegetation factors need to be investigated further since it is not sure to what extent these effects are representative of reality.

### 7.3. Physical Modeling and Field Work

The SWAN 40.55MOD numerical model gives a fairly accurate representation of wave dissipation in mangroves. However, this model has been validated under normal hydraulic conditions only. This study, though limited in scope helped bring to light relevant issues and give some pointers on what needs to be done to improve current

understanding not only with regard to wave dissipation but in the broader field of flow within vegetation. These points are detailed below:

1. Field data would also be needed to establish a suitable range of drag coefficients for the canopy region of mangrove vegetations, especially under extreme conditions. Further physical tests on wave attenuation in mangroves may then be conducted using the measured drag coefficients.
2. It is suggested that wave measurement devices be set up before, within and after the mangrove vegetation to provide data, especially during extreme events to facilitate the studies described in point 1 and to facilitate the investigations of the peaks in reduction factors mentioned in Section 7.3. These devices could be of commercial value to the port as they would be handy in operations planning and also serve as a valuable record with regard to safety. While the devices within the mangroves and behind would be relatively protected, protection of the devices on the outside during extreme events will be difficult
3. It was seen in this study that *S. alba* and *R. mucronata* have more or less the same depth-averaged vegetation densities. Since the current model simulates horizontal density variations in terms of relative factors, it would be very convenient if field data could be used to parameterize vegetation properties of different species in terms of the controlling parameters in wave attenuation so they may be expressed as relative factors for similar numerical simulations.
4. It is possible that mangrove vegetation may behave differently under extreme conditions resulting in different processes or outcomes with regard to wave dissipation. For instance the damping effect of the canopy under extreme conditions is currently not well understood. Such effects may need to be investigated either on the field, or where possible, using satellite images and other techniques after an extreme event or even scaled down physical laboratory tests.
5. It is essential to establish the threshold parameters for mangrove existence with regard to high wave conditions using field data and physical tests since the current model assumes the existence of mangroves under any input conditions.
6. It is necessary to study the effect of extremely high vegetation densities with regard to wave attenuation. While the current model considers such vegetation similar to vegetation of lower densities, this may not be the case in real life where

the bulk of the volume of water may prefer to flow over the vegetation rather than through it at such high densities.

7. Though this study focuses on wave attenuation it is important to recognize the interdependency of this process with other complementary processes such as current flow patterns, sediment movement, wind movement, etc., all of which would need to be incorporated in any attempt to model the system in its entirety.
8. Finally, further research is needed to improve the effectiveness of mangrove management strategies for protecting ports and other coastal developments from cyclones and storms. For example, investigations could focus on the minimum cross-shore width needed, for events of different magnitudes, in case of mangrove belts intended as a sacrificial barrier.

#### 7.4. Detail and Accuracy

Due to the limited scope of this study approximations and assumptions were made where necessary to simplify the procedure and still obtain sufficiently accurate results. However improvements could be made in case more detailed and accurate results are required. Some possible improvements in these aspects for future studies of a similar nature are listed below.

1. The calculation of offshore cyclone and wave parameters could be improved upon in terms of the number of events used for the estimations. This is also true of the near-shore storm surge calculations used in this study. The highly empirical nature of the methods used bears consideration in case of more detailed studies of cyclones in the region as it is felt that this study overestimates the values of near-shore water levels.
2. Vegetation parameter values were based on observations of vegetation species and characteristics in nearby regions. Ideally however, field data would be the best way to obtain vegetation characteristics in a particular region. This is particularly important in the case of mangroves due to the high degree of natural variability and complexity in mangrove forests within a small region.
3. The bathymetries used in this study were simplified based on available hydrographic charts. A more realistic representation of the situation could benefit from the use of more accurate bathymetries.

## 8 References

1. Aggarwal D. & Lal M., 2000, Vulnerability of the Indian Coastline to Sea-Level Rise, [SURVAS] (internet) England: SURVAS (Published 17 October, 2002) Available at: <http://www.survas.mdx.ac.uk/pdfs/3dikshas.pdf> [Accessed: February 20, 2009]
2. Alam M Md., Hossain A Md. & Shafee S, SHORT COMMUNICATION - FREQUENCY OF BAY OF BENGAL CYCLONIC STORMS AND DEPRESSIONS CROSSING DIFFERENT COASTAL ZONES, 2003, *International Journal of Climatology*, 23: 1119-1125 (2003) Published online in Wiley InterScience ([www.wileyinterscience.com](http://www.wileyinterscience.com)). DOI: 10.1002/joc.927
3. Alongi D.M., 2002, Present state and future of the world's mangrove forests, *Environmental Conservation*, 29 (3) April 2002 pp 331-349
4. Alongi D.M., 2007, Mangrove Forests: Resilience, protection from tsunamis and responses to global climate change, *Estuarine, Coastal and Shelf Science*, 76 (2008) pp 1-13 (online)
5. Aluka Webpage, Ithaka Harbors Inc, 2006-2008 (online) Available at: <http://www.aluka.org/action/showCompilationPage?doi=10.5555/AL.AP.COMPILOTION.PLANT-NAME-SPECIES.SONNERATIA.ALBA&cookieSet=1> [Accessed March 11 2009]
6. Anon., Assessment of Mangrove in India (progress report of an ongoing study as of 2003) (n.d.), Forest Survey of India, Ministry of Environment and Forests, Government of India (online) Uttarakhand, India: Forest Survey of India (n.d.) Available at: [www.fsi.nic.in/fsi\\_projects/Assessment%20of%20Mangrove%20in%20India.pdf](http://www.fsi.nic.in/fsi_projects/Assessment%20of%20Mangrove%20in%20India.pdf) [Accessed February 24, 2009]
7. *Avicennia marina*, Protabase – Plant Resources of Tropical Africa (online) Available at: <http://database.prota.org/dbtw-wpd/exec/dbtwpub.dll> [Accessed February 14, 2009]
8. Azote – the green image agency, Copyright 2008 (online) Available at: <http://www.azote.se/index.asp?q=mangrove&id=5162&p=35&lang=eng> [Accessed March 11 2009]
9. Burger B., 2005, Wave Attenuation in Mangrove Forests, A Master's thesis publication, Delft University of Technology, Faculty of Civil Engineering and Geosciences, Section of Hydraulic Engineering, July 2005
10. Chittibabu P., et al., 2004, Mitigation of Flooding and Cyclone Hazard in Orissa, India, *Natural Hazards* 31(2), pp 455-485, Kluwer Academic Publishers, 2004.

11. Das S., 2007, Mangroves – A Natural Defense against Cyclones : An Investigation from Orissa, India, South Asian Network for Development and Environmental Economics (SANDEE) Policy Brief 24-07, September 2007 (online) Available at:  
<http://ideas.repec.org/p/ess/wpaper/id1296.html> [Accessed February 25<sup>th</sup> 2009]
12. De Vos W., 2004, Wave Attenuation in Mangrove Wetlands, Red River Delta, Vietnam, A Master's thesis publication, Delft University of Technology, Faculty of Civil Engineering and Geosciences, Section of Hydraulic Engineering, June 2004
13. Dube S.K., Chittibabu P., Rao A.D. & Sinha P.C., 2000, Extreme Sea Levels Associated with Severe Tropical Cyclones Hitting Orissa Coast of India, *Marine Geodesy* 23 (2000) pp 75-90 (online) Available at:  
[http://pdfserve.informaworld.com/657749\\_751308374\\_713833138.pdf](http://pdfserve.informaworld.com/657749_751308374_713833138.pdf) [Accessed February 12, 2009]
14. Duke N.C., Specific Profiles for Pacific Island Agroforestry, Ver. 2.1., *Rhizophora apiculata*, *R. mucronata*, *R. stylosa*, *R. x annamalai*, *R. x lamarckii*, April 2006, (online) Available at:  
<http://www.agroforestry.net/tti/Rhizophora-IWP.pdf> [Accessed 11 March 2009]
15. Flowers of India (n.d.) (online) Available at:  
<http://www.flowersofindia.net/catalog/slides/Sonneratia%20Mangrove.html> [Accessed March 11 2009]
16. Food and Agricultural Organisation of the United Nations, The World's Mangroves 1980 – 2005, FAO Forestry Paper 153 (2007)
17. Fritz H.M. & Blount C., 2007, Thematic Paper: Role of forests and trees in protecting coastal areas against cyclones, part IV of XII part FAO – RAP report titled Coastal Protection in the aftermath of the Indian Ocean tsunami: What role for forests and trees?, July 2007 (online) Available at:  
<http://www.fao.org/docrep/010/ag127e/ag127e00.htm> [Accessed March 3rd, 2009]
18. Giesen W., Wulffraat S., Zieren M. & Scholten S., Mangrove Guidebook for South East Asia, July 2007, Dharmasarn Co. Ltd., for FAO and Wetlands International
19. Hossain M.K. & Nizam M.Z.U., *Heritiera fomes* Buch.-Ham, 2003, Species Description, Tropical Tree Seeds Manual, The RNGR Team (online) Available at:  
<http://www.rngr.net/Publications/ttsm/Folder.2003-07-11.4726/PDF.2004-03-03.3400/view>  
[Accessed March 11 2009]
20. Hsu S.A., Martin M.F. Jr. & Blanchard B.W., 2000, An Evaluation of the USACE's Deepwater Wave Prediction Techniques under Hurricane Conditions During Georges in 1998, *Journal of Coastal Research*, 16(3) pp 823-829 (internet) LSU Earth Scan Laboratory (2009) Available at:  
<http://www.esl.lsu.edu/quicklinks/publications/pdfs/evaluationusace.pdf> [Accessed March 3, 2009]

21. Iron Ore Handling Plant (Office of Superintending Engineer), Paradip Port Trust, 2006, TENDER DOCUMENT for Design, Manufacture, Supply, Erection & Commissioning of One 3200 TPH slewing, luffing Bucket Wheel Reclaimer for Iron Ore Handling Plant (IOHP) Volume I, July 2006 (online) Available at:  
<http://www.paradiport.gov.in/tender/260.doc> [Accessed April 4 2009]
22. Johnston P. & Santillo D. The Dhamra-Chandbali Port Expansion Project, Orissa, India A Critique of the Environmental Assessment, May 2007, (online) Greenpeace International (n.d.) Available at:  
<http://www.greenpeace.org/raw/content/india/press/reports/critique-of-the-environmental.pdf>  
[Accessed February 8, 2009]
23. Kairo J.G., et al., Structural development and productivity of replanted mangrove plantations in Kenya, 2008, *Forest Ecology and Management* 255 (2008) pp: 2670 – 2677, (online)  
VLIZ – Integrated Marine Information Systems, Belgium (n.d.) Available at:  
<http://www.vliz.be/imis/imis.php?module=ref&refid=129598> [Accessed March 12 2009]
24. Lovelock C., 1993, Field Guide to the Mangroves of Queensland, Australian Institute of Marine Sciences, Queensland (1993) (online) Available at:  
<http://www.aims.gov.au/source/publications/marine-science-info/pdf/field-guide-to-the-mangroves-of-qld.pdf> [Accessed February 18, 2009]
25. Map Room, Delft University of Technology [Accessed February 2009]
26. Mascarenhas A., Oceanographic validity of buffer zones for the east coast of India: A hydrometeorological perspective, 2004, *Current Science* Vol. 86, No. 3, 10 February 2004 (online)  
Current Science Online, Indian Academy of Sciences, Available at:  
<http://www.ias.ac.in/currsci/feb102004/399.pdf> [Accessed February 20, 2009]
27. Mazda Y., Wolanski E. & Ridd P.E., The Role of Physical Processes in Mangrove Environments – Manual for the Preservation and utilization of mangrove ecosystems (pp: 15), 2007, TERRAPUB, Tokyo, Japan
28. Mishra P.K., Sahu J.R., & Upadhyay, V.P., Species Diversity in Bhitarkanika Mangrove ecosystem in Orissa, India, July 2005, *Lyonia A Journal of Ecology and Application* 8 (1), pp: 73 – 87 (online)  
Available at:  
<http://www.lyonia.org/downloadPDF.php?pdfID=142.387.1> [Accessed February 25 2009]
29. Mohanty P.K., Panda U.S., Pal S.R. & Mishra P., 2008, Monitoring and Management of Environmental Changes along the Orissa Coast, *Journal of Coastal Research* 24 (2B), March 2008 pp 13-27

30. Murthy T.S., Storm Surges in the Marginal Seas of the North Indian Ocean, January 2007, United Nations/International Strategy for Disaster Reduction (internet) Available at:  
<http://www.eird.org/encuentro/pdf/eng/doc15270/doc15270-contenido.pdf> [Accessed February 10, 2009]
31. Myrhaug D., Holmedal L.E. & Ong M.E., Nonlinear random wave-induced drag force on a vegetation field, 2009, *Coastal Engineering* 56 (2009) pp 371-376
32. National Academy of Sciences, Panel on Wave Action Effects Associated with Storm Surges, 1977, Methodology for Calculating Wave Action Effects Associated with Storm Surges, Washington D.C., 1977  
 (online) Available at:  
<http://books.google.nl/books?id=U5YrAAAAYAAJ&ots=sHDz3y3PeH&dq=Methodology%20for%20calculating%20wave%20action%20effects%20associated%20with%20storm%20surges&hl=en&pg=PP7>  
 [Accessed June 10 2009]
33. Pidwirny M., 2006, "Tropical Weather and Hurricanes", Fundamentals of Physical Geography, 2nd Edition (internet) Available at:  
<http://www.physicalgeography.net/fundamentals/7u.html> [Accessed March 2, 2009]
34. Rajesh G., Joseph K.J., Harikrishnan M. & Premkumar K., 2005, Observations on extreme meteorological and oceanographic parameters in Indian seas, 2005, Research Communications, *Current Science* 88 (8), 25 April 2005 (internet) *Current Science Online*, Indian Academy of Sciences, Available at:  
<http://www.ias.ac.in/currsci/apr252005/1279.pdf> [Accessed February 20, 2009]
35. Schiereck G.J. & Booij N., 1995, Wave Transmission in Mangrove Forests, INTERNATIONAL CONFERENCE ON COASTAL AND PORT ENGINEERING IN DEVELOPING COUNTRIES, 25/29 September 1995, RJ, Brazil
36. Selvam V. Environmental Classification of Mangrove Wetlands of India, *Current Science* 84(6), March 25, 2003 pp 757-765, *Current Science Online* (internet)  
 Bangalore, India: Current Science Online (25 March 2003) Available at:  
<http://www.ias.ac.in/currsci/mar252003/757.pdf> [Accessed February 15, 2009]
37. Sinha J & Mandal G.S., 1999, An Analytical Model of Over-Land Surface Windfield in Cyclone for the Indian Coastal Region, National Seminar on Wind Engineering-01, Indian Institute of Technology, Kharagpur, December 1999 (online) Available at:  
<http://www.rmsi.com/PDF/windfieldincycloneindiancoastal.pdf> [Accessed March 1, 2009]

38. Sun Q, Kobayashi K & Suzuki M, Intercellular space system in xylem rays of pneumatophores in *Sonneratia Alba* (Sonneratiaceae) and its possible functional significance, 2004, *IAWA Journal Volume 25* (4), pp: 141 – 154 (online) Available at:  
[bio.kuleuven.be/sys/iawa/PDF/IAWA%20J%2021-25/25%20\(2\)%202004/25\(2\)%20141-154.pdf](http://bio.kuleuven.be/sys/iawa/PDF/IAWA%20J%2021-25/25%20(2)%202004/25(2)%20141-154.pdf)  
[Accessed March 11 2009]
39. The SWAN team, SWAN User Manual, SWAN Cycle III version 40.72A, 2008, Delft University of Technology, Available at:  
<http://www.fluidmechanics.tudelft.nl/swan/index/htm>
40. Tomohiro Suzuki, PhD scholar, Department of Coastal Engineering, Civil Engineering, TU Delft, The Netherlands (Personal Communication)
41. UNEP-WCMC [2006], In the front line – Shoreline protection and other eco-system services from mangroves and coral reefs. UNEP-WCMC, Cambridge, UK, 33 pp
42. Vosse M., 2008, Wave Attenuation over Marshlands – Determination of marshland influences on New Orleans' flood protection, A Master's Thesis Publication, Royal Haskoning and University of Twente, Enschede, Netherlands, November 17<sup>th</sup> 2008
43. W.N.J. Ursem, Director, Botanische Tuin, T.U. Delft, The Netherlands (Personal Communication)
44. Young I.R., Parametric Hurricane Wave Prediction Model, 1988, *Journal of Waterway, Port, Coastal and Ocean Engineering* 114(5) September 1988 pp 637-652 (internet)  
Scitation, American Institute of Physics (2009) Available at:  
<http://scitation.aip.org/getpdf/servlet/GetPDFServlet?filetype=pdf&id=JWPED5000114000005000637000001&idtype=cvips&prog=normal> [Accessed February 23, 2009]

## 9 Appendices

### Appendix A: SWAN 40.55MOD Model Formulations

The detailed formulations in the SWAN 40.55MOD numerical model are given below (Tomohiro Suzuki, Personal Communication)

The energy conservation equation is described as follows.

$$\frac{\partial E c_g}{\partial x} = -\varepsilon_v \quad (8)$$

The definition for  $\varepsilon_v$  is given by:

$$\varepsilon_v = \int_{-h}^{-h+\alpha h} F u dz \quad (9)$$

The force  $F$ , acting on the vegetation per unit volume derived by Morison equation neglecting swaying motion and inertial force (Dalrymple et al., 1984), can be described as

$$F = \frac{1}{2} \rho C_D b_v u |u| \quad (10)$$

The solution of equation 10 is

$$\varepsilon_v = \frac{2}{3\pi} \rho C_D b_v N \left( \frac{gk}{2\sigma} \right)^3 \frac{\sinh^3 k\alpha h + 3 \sinh k\alpha h}{3k \cosh^3 kh} H^3 \quad (11)$$

According to Mendez and Losada (2004),

$$\langle \varepsilon_v \rangle = \frac{2}{3\pi} \rho \tilde{C}_D b_v N \left( \frac{gk}{2\sigma} \right)^3 \frac{\sinh^3 k\alpha h + 3 \sinh k\alpha h}{3k \cosh^3 kh} \frac{3\sqrt{\pi}}{4} H_{rms}^3 \quad (12)$$

$$\frac{\partial \left( \frac{1}{8} \rho g H_{rms}^2 c_g \right)}{\partial x} = - \frac{1}{2\sqrt{\pi}} \rho C_D b_v N \left( \frac{gk}{2\sigma} \right)^3 \frac{\sinh^3 k\alpha h + 3 \sinh k\alpha h}{3k \cosh^3 kh} H_{rms}^3 \quad (13)$$

This equation was implemented in SWAN.

$$\frac{\partial \left( \frac{1}{8} H_{rms}^2 c_g \right)}{\partial x} = - \frac{1}{2g\sqrt{\pi}} \tilde{C}_D b_v N \left( \frac{gk}{2\sigma} \right)^3 \frac{\sinh^3 k\alpha h + 3 \sinh k\alpha h}{3k \cosh^3 kh} H_{rms}^3 \quad (14)$$

where,

$$H_{rms} = 2\sqrt{2} \sqrt{\int_0^\infty \int_0^{2\pi} E(f, \theta) d\theta df} \quad (15)$$

$$\frac{\partial \left( \int_0^\infty \int_0^{2\pi} E(f, \theta) c_g(f) d\theta df \right)}{\partial x} \quad (16)$$

$$= - \int_0^\infty \int_0^{2\pi} \frac{8\sqrt{2}}{g\sqrt{\pi}} \tilde{C}_D b_v N \left( \frac{gk(f)}{2\sigma(f)} \right)^3 \frac{\sinh^3 k(f)\alpha h + 3 \sinh k(f)\alpha h}{3k \cosh^3 k(f)h} \sqrt{E(f, \theta)} E(f, \theta) d\theta df$$

$$S_{veg} = \int_0^\infty \int_0^{2\pi} \frac{8\sqrt{2}}{g\sqrt{\pi}} \tilde{C}_D b_v N \left( \frac{gk(f)}{2\sigma(f)} \right)^3 \frac{\sinh^3 k(f)\alpha h + 3 \sinh k(f)\alpha h}{3k \cosh^3 k(f)h} \sqrt{E(f, \theta)} E(f, \theta) d\theta df \quad (17)$$

$S_{veg}$  has to be solved by implicit.

$$S^n \equiv \int_0^\infty \int_0^{2\pi} \Phi^{n-1} E(f, \theta)^n d\theta df \quad (18)$$

In this case:

$$\Phi^{n-1} = \int_0^\infty \int_0^{2\pi} \frac{8\sqrt{2}}{g\sqrt{\pi}} \tilde{C}_D b_v N \left( \frac{gk(f)}{2\sigma(f)} \right)^3 \frac{\sinh^3 k(f)\alpha h + 3 \sinh k(f)\alpha h}{3k \cosh^3 k(f)h} \sqrt{E(f, \theta)} d\theta df$$

$$= \int_0^\infty \int_0^{2\pi} \frac{8\sqrt{2}}{g\sqrt{\pi}} \tilde{C}_D b_v N \left( \frac{gk(f)}{2\sigma(f)} \right)^3 \frac{\sinh^3 k(f)\alpha h + 3 \sinh k(f)\alpha h}{3k \cosh^3 k(f)h} \sqrt{\sigma(f) N(f, \theta)^{n-1}} d\theta df \quad (19)$$

where  $E(\sigma, \theta)^n$  is the frequency-direction spectrum in the current iteration level and  $E(\sigma, \theta)^{n-1}$  is the frequency-direction spectrum in the previous iteration level.

## Appendix B: Cyclone Parameter Estimation

The details of the three methods examined in sub-section 3.1.3 for estimation of cyclone parameters are given below. A sample worksheet is also shown to help clarify the process followed and the comparisons made.

### ***Method 1: USACE Recommendations***

This is an empirical method for the prediction of wave characteristics during extreme events such as hurricanes and cyclones, developed by the US Army Corps of Engineers and described in the Shore Protection Manual (1984). This method was further reviewed and discussed by Hsu, et al. (2000). While the USACE suggests the use of numerical models to calculate offshore conditions during a hurricane they also provide empirical relations for the approximation of maximum wave height and peak period for a slow-moving hurricane. Known values of the sustained wind speed,  $U_r$  were used in these formulae to calculate the values of  $U_{\max}$  and  $\Delta P$ . The procedure followed is as described below:

The measured sustained maximum wind speed,  $U_r$  was used to measure the maximum gradient wind speed,  $U_{\max}$  using the formula

$$U_r = 0.865 * U_{\max} + 0.5 * V_{fm} \quad (20)$$

The pressure drop,  $\Delta P$  ( $P_n - P_o$ ) was then calculated using the formula

$$U_{\max} = 0.447 * [14.5 * \sqrt{(P_n - P_o)} - R * (0.31f)] \quad (21)$$

### ***Method 2: From Chittibabu et al. (2004) and Kumar et al., (2003)***

The method proposed by Kumar et al. (2003) was chosen as the control method for this step since it has been calibrated specifically for tropical cyclones occurring in the Bay of Bengal region. Also, the input values for  $\Delta P$  were chosen as the previously measured or estimated values of  $\Delta P$  for the 16 selected events listed in Chittibabu et al. (2004). Using these values and the empirical relation developed by Kumar et al. (2003) for the southern Bay of Bengal the value of  $U_{\max}$  was estimated for each event.

$$U_{\max} = 4.298 * (P_n - P_o)^{0.527} * V_{fm}^{1.105E-3} * R^{-2.153E-5} \quad (22)$$

***Method 3: From the Wind-speed – Surface Pressure graph (Pidwirny, 2006)***

It is a common assumption that the wind speed,  $U_r$  in a cyclone varies linearly with the value of the central pressure,  $P_o$  - and therefore with the value of  $\Delta P$  since the peripheral pressure,  $P_n$  is more or less constant. This relationship described in the form of a graph shown in Figure 61 was used to determine the correlation between wind-speed and central pressure and to then calculate  $\Delta P$  values from the known values of  $U_r$  for the 16 events.

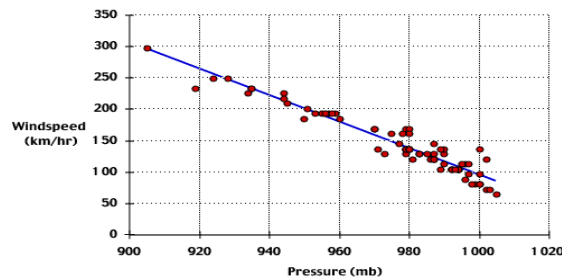


**Figure 61: Wind-speed Surface pressure correlation (from Pidwirny - Physicalgeography.net)**

# Offshore Cyclone Parameters – Sample Excel Worksheet

## Estimation of Parameters

(Assumptions: Radius of maximum wind, R = 45 km, velocity of forward movement, Vfm = 6 m/s)

### Method 1 - USACE Recommendations

Event	Date	Wind speed, Ur (knots)	Wind speed, Ur (m/s)	Delta-P (Pn - Po) (from USACE) (hPa)	Umax (m/s) (from USACE)	Correlation Delta- P	Correlation Umax
VSCS	Oct 71	100	51.4	74.7	56.0	0.86	0.79
CS	Oct 73	45	23.2	12.9	23.3		
SCS	June 82	55	28.3	20.4	29.2		
SCS	Oct 84	55	28.3	20.4	29.2		
CS	Sep 85	40.5	20.8	10.1	20.6		
SCS	Oct 85	55	28.3	20.4	29.2		
VSCS	Nov 95	70	36.0	34.7	38.2		
Tropical Storm (JTWC Classification)	Sep 97	54.5	28.1	20.0	29.0		
VSCS	Oct 99	82	42.2	48.8	45.3		
SC	Oct 99	140	72.0	151.6	79.8		
Deep Depression	June 06	33.5	17.2	6.4	16.4		
Deep Depression	Aug 07	33.5	17.2	6.4	16.4		
Deep Depression	Sep 08	33.5	17.2	6.4	16.4		

### Method 2 - From Chittibabu 2004 (Control) and Kumar et. al. 2003

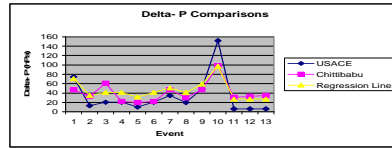
Event	Date	Delta P (from Chittibabu) (hPa)	Umax (from Kumar) (m/s)	Central Pressure Po (hPa)	R (km)	Wind speed Ur (check) (m/s)
VSCS	Oct 71	47	51.4	965.0	55.2	31.3
CS	Oct 73	33	27.2	979.0	55.2	26.5
SCS	June 82	61	37.6	951.0	52.7	35.5
SCS	Oct 84	22	22.0	990.0	51.9	22.0
CS	Sep 85	20	20.9	992.0	51.9	21.1
SCS	Oct 85	22	22.0	990.0	51.9	22.0
VSCS	Nov 95	47	32.8	965.0	55.2	31.3
Tropical Storm (JTWC Classification)	Sep 97	30	25.9	982.0	51.9	25.4
VSCS	Oct 99	47	32.8	965.0	55.2	31.3
SC	Oct 99	98	48.2	914.0	36	44.7
Deep Depression	June 06	31	26.3	981.0	51.9	25.8
Deep Depression	Aug 07	33	27.2	979.0	55.2	26.5
Deep Depression	Sep 08	35	28.0	977.0	55.2	27.3

### Method 3 - From Linear Regression Equation (graph from internet) and Kumar et. al. 2003

Event	Date	Wind speed, Ur (knots)	Wind speed, Ur (m/s)	Wind speed Ur (kmph)	Delta P (from regression line, Ur vs. Delta-P) (hPa)	Umax (from Kumar) (m/s)	Central Pressure Po (hPa)	R (km)	Correlation Delta- P	Correlation Umax
VSCS	Oct 71	100	51.4	185.2	70.8	40.7	941.2	52.7	0.81	0.76
CS	Oct 73	45	23.2	83.3	34.8	28.0	977.2	55.2		
SCS	June 82	55	28.3	101.9	41.4	30.6	970.6	55.2		
SCS	Oct 84	55	28.3	101.9	41.4	30.6	970.6	55.2		
CS	Sep 85	40.5	20.8	75.0	31.9	26.7	980.1	51.9		
SCS	Oct 85	55	28.3	101.9	41.4	30.6	970.6	55.2		
VSCS	Nov 95	70	36.0	129.6	51.2	34.3	960.8	55.2		
Tropical Storm (JTWC Classification)	Sep 97	54.5	28.1	101.0	41.0	30.5	971.0	55.2		
VSCS	Oct 99	82	42.2	151.9	59.0	36.9	953.0	52.7		
SC	Oct 99	140	72.0	259.3	97.0	48.0	915.0	36		
Deep Depression	June 06	33.5	17.2	62.0	27.3	24.6	984.7	51.9		
Deep Depression	Aug 07	33.5	17.2	62.0	27.3	24.6	984.7	51.9		
Deep Depression	Sep 08	33.5	17.2	62.0	27.3	24.6	984.7	51.9		

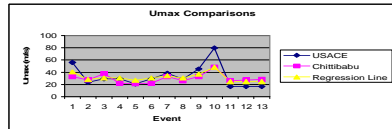
### Average Delta- P and Umax

Event	Date	Average Delta-P (hPa)	Average Umax (m/s)	Delta- P Correlation with Chittibabu	Umax Correlation with Kumar
VSCS	Oct 71	64	43	0.91358493	0.8647142
CS	Oct 73	27	26		
SCS	June 82	41	32		
SCS	Oct 84	28	27		
CS	Sep 85	21	23		
SCS	Oct 85	28	27		
VSCS	Nov 95	44	35		
Tropical Storm (JTWC Classification)	Sep 97	30	28		
VSCS	Oct 99	52	38		
SC	Oct 99	116	59		
Deep Depression	June 06	22	22		
Deep Depression	Aug 07	22	23		
Deep Depression	Sep 08	23	23		



### Average Delta- P and Umax without USACE

Event	Date	Average Delta-P (hPa)	Average Umax (m/s)	Delta- P Correlation with Chittibabu	Umax Correlation with Kumar
VSCS	Oct 71	59	37	0.954195309	0.9431303
CS	Oct 73	34	28		
SCS	June 82	51	34		
SCS	Oct 84	32	26		
CS	Sep 85	26	24		
SCS	Oct 85	32	26		
VSCS	Nov 95	49	34		
Tropical Storm (JTWC Classification)	Sep 97	36	28		
VSCS	Oct 99	53	35		
SC	Oct 99	98	48		
Deep Depression	June 06	29	25		
Deep Depression	Aug 07	30	26		
Deep Depression	Sep 08	31	26		



### Average Delta- P and Umax without Linear Line

Event	Date	Average Delta-P (hPa)	Average Umax (m/s)	Delta- P Correlation with Chittibabu	Umax Correlation with Kumar
VSCS	Oct 71	61	44	0.888443307	0.9363462
CS	Oct 73	23	25		
SCS	June 82	41	33		
SCS	Oct 84	21	26		
CS	Sep 85	15	21		
SCS	Oct 85	21	26		
VSCS	Nov 95	41	35		
Tropical Storm (JTWC Classification)	Sep 97	25	27		
VSCS	Oct 99	48	39		
SC	Oct 99	125	64		
Deep Depression	June 06	19	21		
Deep Depression	Aug 07	20	22		
Deep Depression	Sep 08	21	22		

## Appendix C: Offshore Wave Parameter Estimation

The five methods examined in sub-section 3.1.4 for determination of the final offshore wave parameters are described in detail below. A sample worksheet is also shown to help clarify the process followed and the comparisons made.

### ***Method 1: USACE Recommendations from Hsu, et al., (2000)***

The first method was the USACE recommendation for maximum significant wave height and peak period during a cyclone in the Shore Protection Manual 1984 as described in Hsu et al. (2000). This method makes use of the following empirical formulae for slow moving hurricanes:

$$H_o = 5.03e^{R_{\Delta P}/4700} \left[ 1 + \frac{0.29\alpha V_{fm}}{\sqrt{U_r}} \right] \quad (23)$$

$$T_p = 8.6e^{R_{\Delta P}/9400} \left[ 1 + \frac{0.145\alpha V_{fm}}{\sqrt{U_r}} \right] \quad (24)$$

where  $\alpha$  refers to the velocity coefficient (assumed as 1 for slow-moving hurricane)

### ***Method 2: Simplified Formulae from Hsu et al., (2000)***

Hsu et al. (2000) in addition to their validation of the USACE formulae for wave characteristics using Hurricane Georges also proposed a simplified relationship for wave heights and the use of the simplified USACE recommendation for wave periods. These are as follows:

$$H_o = 0.2 * (P_n - P_0) \quad (25)$$

and

$$T_p = 12\sqrt{H_o / g} \quad (26)$$

### ***Methods 3 and 4: From Kumar et al., (2003)***

Kumar et al. (2003) carried out a multiple regression analysis to obtain empirical expressions for maximum wave height and peak period for cyclones in the southern Bay of Bengal. The analysis was based on the parametric hurricane model proposed by Young (1988) and was verified for 11 selected events in the southern Bay of Bengal. These

expressions were deemed to be a good approximation of the cyclones near the Orissa coast due to the similarities in the characteristics of the cyclones studied.

$$H_o = 0.61 * (P_n - P_o)^{0.69} * V_{fm}^{5.43E-3} * R^{1.43E-5} \quad (27)$$

$$T_p = 4.125 * (P_n - P_o)^{0.288} * V_{fm}^{3.24E-3} * R^{1.63E-5} \quad (28)$$

Kumar et al. (2003) also proposed a simplified version of these formulae whose validity was checked for a total of 32 cyclones that occurred along the Indian coast between May 1961 and November 1982. Both these sets of formulae were used to calculate the maximum wave heights and peak periods for the 16 events being considered and were found to be in good agreement with each other.

$$H_o = 0.25U_{\max} \quad (29)$$

$$T_p = 4.5H_o^{0.48} \quad (30)$$

### ***Method 5: Young's Parametric Hurricane Prediction Model (Young, 1988)***

Ian Young of the University College, Australian Defence Force Academy, developed a parametric model to predict the offshore conditions for a hurricane given the values of the parameters  $V_{fm}$ ,  $U_{\max}$  and  $R$ . Based on a study of a synthetically generated database he proposed a three step method to determine the maximum wave height and peak period for a cyclone using the formula for a JONSWAP fetch-limited spectrum, with the additional improvement of the application of an equivalent fetch to account for the effect of the hurricane on the sea state. First the effective radius to maximum winds,  $R'$  is determined using the empirical equation

$$R' = 22.5 * 10^3 \log R - 70.8 * 10^3 \quad (31)$$

Next, the ratio  $F/R'$  and thus the equivalent fetch length,  $F$  are determined by substitution of  $V_{fm}$  and  $U_{\max}$  into the equation

$$\frac{F}{R'} = aV_{\max}^2 + bV_{\max}V_{fm} + cV_{fm}^2 + dV_{\max} + eV_{fm} + f \quad (32)$$

where,

$$a = -2.175 * 10^{-3}$$

$$b = 1.506 * 10^{-2}$$

$$c = -1.223 * 10^{-1}$$

$$d = 2.190 * 10^{-1}$$

$$e = 6.737 * 10^{-1} \text{ and}$$

$$f = 7.980 * 10^{-1}$$

The calculated values of  $U_{\max}$  and  $F$  are then substituted into the following equations to determine the values of  $H_o$  and  $T_p$

$$gH_o/U_{\max} = 0.0016 \left( gF/U_{\max}^2 \right)^{0.5} \quad (33)$$

$$gT_p/(2\pi * U_{\max}) = 0.045 \left( gF/U_{\max}^2 \right)^{0.33} \quad (34)$$

# Offshore Wave Parameters – Sample Excel Worksheet

## Estimation of Hs and Tp

(Assumptions:  $V_{fm} = 6 \text{ m/s}$ ; Peripheral Pressure,  $P_n = 1012 \text{ hPa}$ ;  $R$  taken from Bell;  $\alpha = 1$  (slow-moving); Delta- $P$  and  $U_{max}$  values - average values obtained above)

### Method 1 - USACE from Hsu et. al (2000)

Event	Date	Average Delta-P (hPa)	Central Pressure, $P_0$ ( $P_n - \Delta P$ ) (hPa)	R (Bell from Sirha, Mandal, 1999) (km)	Average $U_{max}$ (m/s)	Wind speed, $U_r$ (m/s)	Hs (max) (USACE) (m)	Tp (s)	Correlation (USACE vs control)
VSCS	Oct 71	59	953	52.7	37	51.4	12.1	18.7	0.915621424
CS	Oct 73	34	978	55.2	28	23.2	10.2	15.1	
SCS	June 82	51	961	55.2	34	28.3	12.2	18.3	
SCS	Oct 84	32	980	51.9	26	28.3	9.5	14.2	
CS	Sep 85	26	986	51.9	24	20.8	9.3	13.6	
SCS	Oct 85	32	980	51.9	26	28.3	9.5	14.2	
VSCS	Nov 95	49	963	55.2	34	36.0	11.5	17.5	
Tropical Storm (JTWC Classification)	Sep 97	36	976	55.2	28	28.1	10.1	15.2	
VSCS	Oct 99	53	959	52.7	35	42.2	11.6	17.7	
SC	Oct 99	98	914	36.0	48	72.0	12.8	20.0	
Deep Depression	June 06	29	983	51.9	25	17.2	9.8	14.3	
Deep Depression	Aug 07	30	982	51.9	26	17.2	10.0	14.5	
Deep Depression	Sep 08	31	981	51.9	26	17.2	10.1	14.7	

### Methods 2 and 3 - From Kumar et. al.

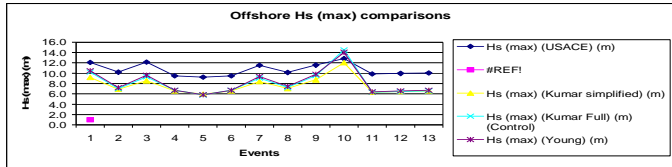
Event	Date	Average Delta-P (hPa)	Central Pressure, $P_0$ ( $P_n - \Delta P$ ) (hPa)	R (Bell from Sirha, Mandal, 1999) (km)	Average $U_{max}$ (m/s)	Hs (max) (Kumar simplified) (m)	Tp (Kumar simplified) (s)	Hs (max) (Kumar Full) (m)	Tp (Kumar Full) (s)	Correlation (Kumar simplified vs control)
VSCS	Oct 71	59	953	52.7	37	9.2	13.0	10.3	13.4	0.9993526
CS	Oct 73	34	978	55.2	28	6.9	11.4	7.0	11.4	
SCS	June 82	51	961	55.2	34	8.5	12.6	9.3	12.9	
SCS	Oct 84	32	980	51.9	26	6.6	11.1	6.7	11.2	
CS	Sep 85	26	986	51.9	24	5.9	10.6	5.8	10.6	
SCS	Oct 85	32	980	51.9	26	6.6	11.1	6.7	11.2	
VSCS	Nov 95	49	963	55.2	34	8.4	12.5	9.0	12.7	
Tropical Storm (JTWC Classification)	Sep 97	36	976	55.2	28	7.0	11.5	7.2	11.6	
VSCS	Oct 99	53	959	52.7	35	8.7	12.7	9.5	13.0	
SC	Oct 99	98	914	36.0	48	12.0	14.9	14.5	15.5	
Deep Depression	June 06	29	983	51.9	25	6.4	10.9	6.3	11.0	
Deep Depression	Aug 07	30	982	51.9	26	6.5	11.0	6.5	11.1	
Deep Depression	Sep 08	31	981	51.9	26	6.6	11.1	6.6	11.2	

### Method 4 - From Young

Event	Date	Average Delta-P (hPa)	Central Pressure, $P_0$ ( $P_n - \Delta P$ ) (hPa)	R (Bell from Sirha, Mandal, 1999) (km)	Average $U_{max}$ (m/s)	$R'$ (m)	F (m)	Hs (max) (Young) (m)	Tp (Young) (s)	Correlation (Young vs control)
VSCS	Oct 71	59	953	52.7	37	35441	314086	10.5	13.6	0.9967177
CS	Oct 73	34	978	55.2	28	35894	262516	7.2	11.6	
SCS	June 82	51	961	55.2	34	35894	303565	9.6	13.1	
SCS	Oct 84	32	980	51.9	26	35291	249391	6.7	11.2	
CS	Sep 85	26	986	51.9	24	35291	231674	5.8	10.6	
SCS	Oct 85	32	980	51.9	26	35291	249391	6.7	11.2	
VSCS	Nov 95	49	963	55.2	34	35894	300114	9.4	13.0	
Tropical Storm (JTWC Classification)	Sep 97	36	976	55.2	28	35894	266597	7.4	11.8	
VSCS	Oct 99	53	959	52.7	35	35441	303954	9.8	13.2	
SC	Oct 99	98	914	36.0	48	31717	326283	14.0	15.1	
Deep Depression	June 06	29	983	51.9	25	35291	243525	6.4	11.0	
Deep Depression	Aug 07	30	982	51.9	26	35291	246599	6.6	11.1	
Deep Depression	Sep 08	31	981	51.9	26	35291	249558	6.7	11.2	

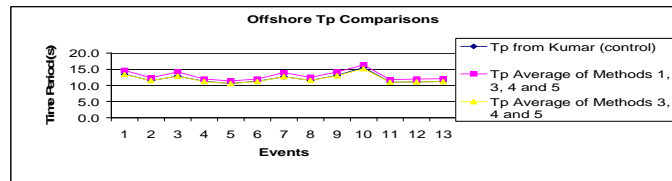
### Average Hs (max) and Tp

Event	Date	Average Hs (max) (m)	Average Tp (s)
VSCS	Oct 71	11	15
CS	Oct 73	8	12
SCS	June 82	10	14
SCS	Oct 84	7	12
CS	Sep 85	7	11
SCS	Oct 85	7	12
VSCS	Nov 95	10	14
Tropical Storm (JTWC Classification)	Sep 97	8	13
VSCS	Oct 99	10	14
SC	Oct 99	13	16
Deep Depression	June 06	7	12
Deep Depression	Aug 07	7	12
Deep Depression	Sep 08	7	12



### Average Hs (max) and Tp without USACE

Event	Date	Average Hs (max) (m)	Average Tp (s)	Hs Correlation with and without USACE	Tp Correlation with and without USACE
VSCS	Oct 71	10	13	0.998259636	0.996761878
CS	Oct 73	7	11		
SCS	June 82	9	13		
SCS	Oct 84	7	11		
CS	Sep 85	6	11		
SCS	Oct 85	7	11		
VSCS	Nov 95	9	13		
Tropical Storm (JTWC Classification)	Sep 97	7	12		
VSCS	Oct 99	9	13		
SC	Oct 99	14	15		
Deep Depression	June 06	6	11		
Deep Depression	Aug 07	6	11		
Deep Depression	Sep 08	7	11		



## Appendix D: Spreading Effect in SWAN

The SWAN 40.55MOD model, like other SWAN models assumes open boundaries on the two sides along the wave propagation direction. Due to this, there is an energy leakage along these boundaries that propagates into the model at the assumed directional spreading angle. This energy leakage results in an unnatural reduction in wave heights. To avoid this effect, it is suggested that the boundaries of the model grid be kept sufficiently far away from the area of interest (SWAN User Manual, SWAN Cycle III version 40.72A). Considering the characteristics of this study an aspect ratio of 1:7 was applied to the model grids for all the analyses as this was felt to provide sufficient accuracy across the central band of interest. The energy leakage effect in the grid used for the generic model analyses is illustrated in Figure 62 below.

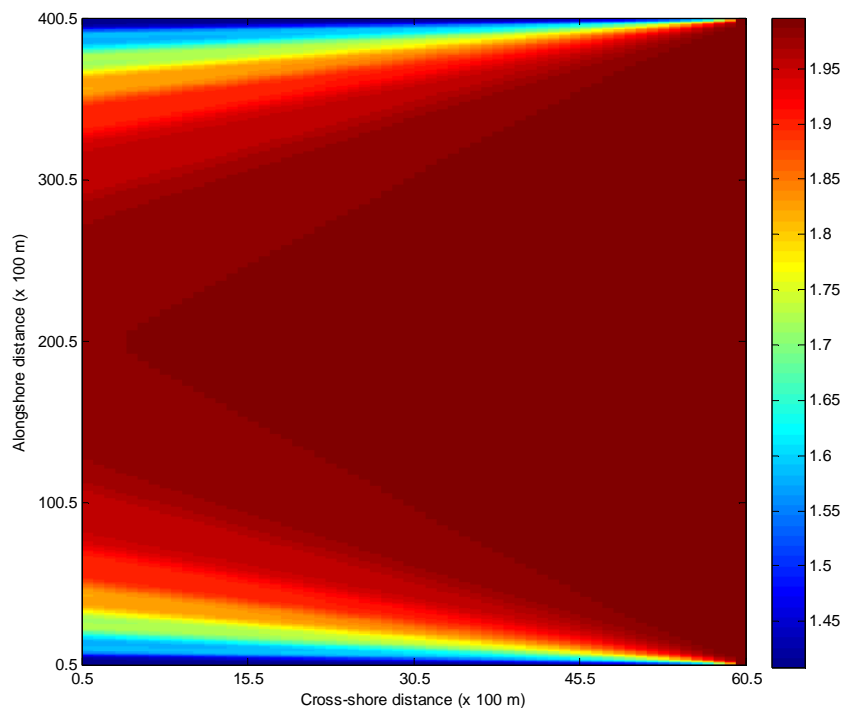


**Figure 62: Transmitted wave height chart for a flat bathymetry and no vegetation illustrating the energy leakage effect**

## Appendix E: SWAN Input File – Example

Figure 63 below shows a sample SWAN 40.55MOD input file from the case study.

```

$***** HEADING *****
$
PROJ 'Mangrove' '001'
$
$***** MODEL INPUT *****
SET 7.1
CGRID 0. 0. 0. 11000. 77000. 110 770 CIRCLE 32 .05 2 32
$
IMPGRID BOTTOM 0. 0. 0. 110 770 100. 100.
READIMP BOTTOM -1. 'bathyreal.dat' 1 0 FREE
$
IMPGRID MPLANTS 0. 0. 0. 110 770 100. 100.
READIMP MPLANTS 1. 'plantsreal.dat' 1 0 FREE
$
BOUN SHAPEPEC JONSWAP
BOUN SIDE E CCG CONSTANT PAR 5.28 12 180. 2
$
OFF QUAD
OFF WCAP
OFF WINDGROWTH
$
      height      FIX 1.0      FIX 1      bv*density*Cd
  VEGETATION  0.5      1.0      1      6.5 &
              5.0      1.0      1      0.6 &
              0.5      1.0      1      2
$
$ Upperlines(Line 22,23) shows this conditions)
$
      height(m)      stem diameter:bv(m)      density      Cd
$ First layer(r)  0.50      0.05      130      1.0
$ Second layer(s) 5.00      0.4      1.5      1.0
$ Third layer(c)  0.50      0.02      100      1.0
$
$***** MODEL OUTPUT *****
$
BLOCK 'COMPGRID' NOHEAD 'Hs1.mat' HSIGN
BLOCK 'COMPGRID' NOHEAD 'Hs2.dat' HSIGN
$
$***** COMPUTATIONS *****
$
TEST 1,0
COMPUTE
STOP

```

Figure 63: SWAN 40.55MOD input file for a case study scenario with high density plants and 25 year return period hydraulic conditions